APPLICATION OF THIN-FILM SOLID-PHASE DOSING TO MEASURE *IN VITRO* BIOTRANSFORMATION RATES OF ORGANIC CHEMICALS IN RAINBOW TROUT (*ONCORHYNCHUS MYKISS*)

by

Hsiao-Yi (Danny) Lee
Bachelor of Science, Simon Fraser University, 2005

PROJECT SUBMITTED IN PARTIAL FULFILLMENT OF
THE REQUIREMENTS FOR THE DEGREE OF

MASTER OF ENVIRONMENTAL TOXICOLOGY

In the
Biological Sciences Department

SIMON FRASER UNIVERSITY

Fall 2009

APPROVAL

Name: **Insert your name here**

Degree: **Insert your upcoming degree here**

Title of Thesis: **Insert your title here. Title page must be the same as this.**

Examining Committee:

Chair: **Name**
[Correct title – Consult your Grad Secretary/Assistant

_____

Name
Senior Supervisor
Correct title – Consult your Grad Secretary/Assistant

_____

Name
Supervisor
Correct title – Consult your Grad Secretary/Assistant

_____

Name
[Internal or External] Examiner
Correct title – Consult your Grad Secretary/Assistant
University or Company (if other than SFU)

Date Defended/Approved: _____

ABSTRACT

Methods for assessing the bioaccumulative potential of chemicals have been criticized for their inability to consider biotransformation in living organisms. This current study developed and tested an *in vitro* method, using liver S9 liver homogenates to determine biotransformation rates of very hydrophobic xenobiotics in rainbow trout (*Oncorhynchus mykiss*). The study compares two biotransformation assays, i.e. the solvent delivery method and a novel thin-film solid-phase dosing system. Biotransformation rate constants of benzo[a]pyrene (0.9087 min^{-1}; $logK_{ow}$ 6.04), chrysene (0.0796 min^{-1}; $logK_{ow}$: 5.81), and 9-methylanthracene (0.0011 min^{-1}; $logK_{ow}$: 5.07) determined by solid phase dosing were 44, 17, and 0.8-times higher than those measured using the solvent delivery method. The results suggest that the EVA dosing is a useful alternative to the solvent delivery method especially for chemicals of extreme hydrophobicity and for chemicals that are difficult to dissolve in aqueous media.

Keywords: biotransformation, solid-phase dosing, substrate depletion, trout liver S9

DEDICATION

I dedicate this work to my beloved parents, who have supported me no matter what happens.

ACKNOWLEDGEMENTS

The work in this M.E.T. project would not have been done possible without the support and collaborations of many colleagues, friends, and family members. I really appreciate Dr. Frank Gobas for his guidance throughout the entire research period. I have not only learned how to do a good scientific research but also learned to cope with challenges with a positive attitude from him. I am also very grateful of Dr. Chris Kennedy for his continual encouragement and insightful suggestions of my research. Thank you to Dr. Russell Nicholson for accepting to be on my examining committee and for his warm encouragement and support.

Special thanks to all the members of the Toxlab's Fugacity Club. Thank you to Victoria Otton and Yung Shan Lee for many insightful discussions and ideas. I am also very thankful of them for sharing much relevant experimental knowledge and techniques with me. I would also like to thank Janey Lam and Jennifer Trowell for their famous "Janey and Jennifer moments" to vastly improve the visual presentation of my speech. Many thanks to Juan Jose Alava and Justin Lo for providing useful suggestions and creating a positive learning environment all the time.

I also extend my thanks to all the colleagues that have spent this valuable M.E.T. period with me. A great thanks to Adebayo Adekola for continuously elevating my confidence level and providing sincere and powerful prayers. I am

also grateful of Ariel Blanc, Kirstin Webster, and Peter Kickham for their participation in my practice presentation and provided me with practical ways of improvement.

I have also greatly appreciated the support from the outstanding staffs from the Resource and Environmental Management and Biological Sciences departments. Thank you to graduate secretary, Marlene Nguyen, and department assistant, Barbara Sherman. Thank you to Laurence Lee for his generous help with my computer problems. I am also grateful of Bruce Leighton for his help in preparing rainbow trout for my experiment.

Finally, I would like to thank my parents as they are the chief reason that I am motivated to achieve something great in my life. I am very grateful of their never-ending love to me, and I am very thankful that they have supported my decisions and encouraged me in all aspects of my life.

TABLE OF CONTENTS

LIST OF FIGURES

LIST OF TABLES

GLOSSARY

A	peak area
B	bioaccumulation
BAF	bioaccumulation factor
BCF	bioconcentration factor
C	substrate concentration
C_0	initial substrate concentration
C_E	substrate concentration in the EVA film
$C_{E/M(i)}$	chemical concentration in either the EVA or medium phase at time i
$C_{E/M(i+1)}$	chemical concentration in either the EVA or medium phase at time i+1
CL_{int}	intrinsic clearance rate
C_M	substrate concentration in the trout liver S9 medium
CEPA	Canadian Environmental Protection Act
DCM	dichloromethane
DDT	dichlorodiphenyltrichloroethane
$\triangle C_{E/M}$	chemical concentration changes in either the EVA or medium phase in one time unit
DSL	Domestic Substances List
EVA	ethylene vinyl acetate
GC MS	gas chromatography mass spectrometer
i.s.	internal standard
iT	inherent toxicity
k_1	rate constant of chemical delivery from EVA to medium phase
k_2	rate constant of chemical delivery from medium to EVA phase
k_d	substrate depletion rate constant
K_M	Michaelis-Menten constant
k_{met}	biotransformation rate constant
Log K_{ow}	log octanol-water partition coefficient
M	chemical mass
OECD	Organization for Economic Cooperation and Development
P	persistence
PAHs	polycyclic aromatic hydrocarbons
PCBs	polychlorinated biphenyls
QSARs	Quantitative Structure Activity Relationships
REACH	Registration, Evaluation and Authorization of Chemicals
RRF	relative response factor
T	time
TCDD	tetrachlorodibenzo-*p*-dioxin

TSCA	Toxic Substances Control Act
UNEP	United Nations Stockholm Convention

1: INTRODUCTION

There is ample of evidence that certain commercial chemicals can be harmful to humans and the environment. For instance, dichlorodiphenyltrichloroethane (DDT), polychlorinated biphenyls (PCBs), pentachlorobenzene and xylenes are commercial chemicals that have long been consider to be harmful to humans and the environment. Recently, brominated flame retardants and certain perfluorinated chemicals are of concern (Ikonomou *et al*., 2002; Giesy and Kannan, 2001). These chemicals have the potential to be harmful to the environment and humans because of their continued presence and global distribution. Therefore, national and international chemical management programs, such as the United Nations Stockholm Convention (UNEP), the Canadian Environmental Protection Act (CEPA), the Registration, Evaluation and Authorization of Chemicals (REACH) in the European Union and the Toxic Substances Control Act (TSCA) in the United States, have developed methods to evaluate all chemicals in commerce and to identify potentially harmful substances. Because of their large number, chemical management includes an initial screening and categorization of all commercial chemicals for persistence (P), bioaccumulation (B), and inherent toxicity (iT). Chemicals that exhibit the characteristics of P or B and iT are then evaluated for their risk to the environment and human health in the second phase of the evaluation process. One of the larger challenges that chemicals evaluation programs are facing is

that the empirical data required for chemical evaluation are scarce. Currently, there are about 100,000 commercial chemicals that require evaluation, but relevant P, B, and T data are available for only 5% of these chemicals.

The bioaccumulation potential of chemicals is usually expressed in terms of the bioconcentration factor (BCF), bioaccumulation factor (BAF), or the log octanol-water partition coefficient (log K_{ow}). Bioconcentration is the process in which the chemical concentration in an aquatic organism exceeds that in water at steady state as a result of exposure to waterborne chemical (it does not include dietary exposure). Bioaccumulation is the process by which the chemical concentration in an aquatic organism achieves a level that exceeds that in the water at steady state as a result of chemical uptake through all possible routes of chemical exposure (e.g., diet, dermal, and respiratory). Log K_{ow} describes how a chemical thermodynamically distributes between the lipids of biological organisms and water as octanol is generally considered to be a reasonable surrogate phase for lipids in biological organisms (e.g., MacKay 1982). National and international chemical management programs have developed criteria based on those three bioaccumulation measures to evaluate and assess the bioaccumulation potential of chemicals. For example, a chemical is considered bioaccumulative according to the CEPA if the BCF and/or BAF are greater than 5,000 L/kg ww or the K_{ow} value is greater than 100,000 (Government of Canada 1999). Similarly, in the Stockholm Convention, a chemical is considered bioaccumulative if it has a BCF greater than 5,000 L/kg ww and/or K_{ow} value greater than 100,000 (UNEP 2001). Under the REACH regulatory framework for

chemicals, a chemical is considered “bioaccumulative” and “very bioaccumulative” if it has a BCF greater than 2,000 and 5,000, respectively (European Commission 2001). According to TSCA, a chemical is considered “bioaccumulative” and “very bioaccumulative” if it has a BCF between 1,000 to 5,000 and greater than 5,000, respectively (USEPA 1976).

Due to the lack of empirical BCFs for many chemicals, it is important to determine the bioaccumulation potential of chemicals in other ways. BAFs are typically measured from chemical concentration in field-collected animals. However, as Nichols *et al*. (2007) pointed out, the costs associated with measuring environmental contaminants in field-collected animals can vary and may be substantial. BCF data can be obtained experimentally using an *in vivo* bioconcentration test (OECD 305 E; OECD 1996). There are three major drawbacks to the application of bioconcentration testing to assess the bioaccumulation capacity of commercial chemicals. They are the lengths of time required to complete the tests, the large number of animals that are required to complete the tests, and the monetary costs of the testing. In a pilot exercise, it was estimated to simply collect the existing environmental toxicity and fate data of the 1,240 chemicals, which were identified by computational modelling as potentially bioaccumulative (Environment Canada 2006), would take 82 work-years of effort (Weisbrod *et al.* 2007). Additionally, the use of a large number of animals to generate empirical data for thousands of chemicals is discouraged in certain programs (i.e. REACH) and is not considered ethical by many people. Furthermore, a standard *in vivo* fish BCF test based on the standard

bioconcentration test protocol of the OECD 305 E (OECD 1996) costs approximately $125,000 USD per chemical. K_{ow} values are generated in the laboratory. They are relatively cheap and easy to measure for many chemicals of interest. However, the ability to use K_{ow} value in the determination of the chemical bioaccumulation potential is limited as it merely reflects the passive chemical partitioning. There are several physiological processes in fish that are not represented by using K_{ow} alone. These include active uptake/loss of chemicals via gills, chemical loss via fecal egestion, and biotransformation. For example, 2,3,7,8-tetrachlorodibenzo-*p*-dioxin (TCDD) and 1,3,6,8-TCDD both have high and comparable K_{ow} values (log K_{ow} = 6.8), but the former is bioaccumulative in fish whereas the latter is not due to its rapid biotransformation (Hu and Bunce 1999).

Because K_{ow} values are not always good predictors of bioconcentration, bioaccumulation assessments often rely on computational models (Arnot and Gobas 2006) and Quantitative Structure Activity Relationships (QSARs; Veith *et al.* 1979). Some models only require the single input of log K_{ow} values, such as the models developed by Veith *et al*. (1979), and Mackay (1982), while others use multiple parameters like the models developed by Arnot and Gobas (2003, 2004). One of the common limitations in using a computational model is absence of information on biotransformation rates. Biotransformation can reduce the extent of bioaccumulation. Several of the bioaccumulation models do not incorporate a biotransformation rate constant (k_{met}), and in the ones that do (e.g., Arnot and Gobas 2003, 2004), do not contain methods to assess

biotransformation rates and their effect on the bioaccumulation factor. Arnot and Gobas (2003) demonstrated that fitting their model with quality empirical BCF data for a group of PAHs resulted in a simulated k_{met} value of 0.05 d^{-1}, which was comparable to values in the literature. This suggests that the inclusion of the metabolic transformation information in computational modelling can reduce the incidence of overestimation of the BCF and produce more accurate estimates of the BCF. Therefore, it is important to develop rapid, cost-effective, and easily standardized methods to determine the biotransformation rate constants of organic chemicals, so they can be employed to improve the current practice of bioaccumulation assessment.

It has been suggested that *in vitro* hepatic metabolic transformation tests can provide effective and efficient measurements of fish metabolic potential (Nichols *et al*. 2007). These tests could be used to refine BCF computational models. The *in vitro* metabolism approach was developed in the 1930s mainly for academic purposes, and it took until the late 1980s for *in vitro* metabolism approaches to prove their worth, alongside *in vivo* studies, for modern drug discovery (Ekins *et al*. 2000). Methods for obtaining practical information on mammalian chemical metabolic transformation and extrapolating *in vitro* hepatic clearance data to the whole animals are well defined and widely accepted (Rane *et al*. 1977; Houston 1994; Houston and Carlile 1997). Therefore, recent research activities in the area of bioaccumulation have focused on the development and testing of several types of *in vitro* methods to measure the metabolic potential of xenobiotics in fish (e.g., Dyer *et al*. 2006; Han *et al*. 2007;

Han *et al*. 2009). These *in vitro* methods include the application of microsomes, liver S9 fractions, and isolated hepatocytes. The major advantages and limitations for various *in vitro* hepatic approaches have been discussed by Brandon *et al*. (2003).

The substrate depletion approach has been practiced in the pharmaceutical industry by Obach (1996, 1999) and Obach and Reed-Hagen (2002) to estimate the *in vitro* intrinsic clearance rates (CL_{int}, ml/h/mg) of drugs. More recently, by Han *et al*. (2007, 2009), applied the substrate depletion approach to assess the bioaccumulative potential of xenobiotics in fish. The substrate depletion approach is a practice, where the consumption of parent compound is monitored over time, to determine enzymatic parameters, such as the Michaelis-Menten constant (K_M) and k_{met}. One of the advantages of applying the substrate depletion approach is that the biotransformation rate can be determined at one substrate concentration, provided the concentration is far below the K_M (Nichols *et al*. 2006; Segel 1975). Another benefit of applying the substrate depletion approach is that the identity of metabolic products of a substrate need not be known. This is an important attribute that can streamline the process of measuring biotransformation rates for the B assessment/categorization as the metabolites of most of the commercial chemicals in fish are unknown and difficult to measure. Furthermore, under the assumption that all the enzymes responsible for the metabolism of the substrate are present in the incubation system, the biotransformation rate determined in

substrate depletion tests reflects all metabolic pathways contributing to the parent substrate's metabolism, which is more realistic.

The substrate depletion approach was applied in the present study using the hepatic S9 fraction of rainbow trout (*Oncorhynchus mykiss*) as the assay system to determine biotransformation rates of three high log K_{ow} polycyclic aromatic hydrocarbons (PAHs) which are ubiquitous in the environment. These substances are benzo[a]pyrene (log K_{ow}: 6.04), chrysene (log K_{ow}: 5.81), and 9-methylanthracene (log K_{ow}: 5.07). We chose to use S9 fractions due to its ease of preparation and the availability of long-term cryopreservation of S9 homogenates (Hodson *et al*. 1911). This preparation potentially supplies both cytosolic and microsomal phase I and II enzyme activities. The spiking of test chemicals is performed through a mechanical injection of a solution of the test chemical in an appropriate solvent into the incubation mixture. This procedure is referred to as the solvent delivery method. However, many potentially bioaccumulative contaminants are released into the environment gradually rather than in the form of a sudden large input. An alternate technique to administer the test chemical is through solid-phase dosing. This method has been applied successfully by Laak *et al*. (2005) to determine partition coefficients of hydrophobic chemicals in complex mixtures. In this study, I have applied both methods of chemical delivery in metabolic transformation assays. The objective of this study is to test both methods and their effect on biotransformation rates. This study shows that by applying the EVA dosing approach, it is possible to improve the measurement of the *in vitro* biotransformation rate constant of our reference chemicals over the

solvent delivery approach. The advantages and limitations of this approach for future applications are discussed.

2: THEORY

2.1 Solvent delivery method

Because the metabolic pathways of most environmental contaminants are not known, the biotransformation rate constants of reference chemicals were determined using the substrate depletion approach rather than by measuring the rate of product formation. In theory, if the dosing concentration is sufficiently low, the rate of substrate depletion follows first order enzyme kinetics. In other words, the biotransformation rate decreases with the decreasing concentration of the test substance over time. If the chemical biotransformation follows first order kinetics, a constant proportion of the chemical is metabolized per unit of time as described by

$$\frac{dC}{dt} = -k_d \bullet C \tag{1}$$

where C is the substrate concentration (ng/ml), t is time (e.g., minute), and k_d is the rate constant of substrate depletion. By rearranging dt and C, the equation becomes

$$\frac{1}{C} \bullet dC = -k_d \bullet dt \tag{2}$$

Integrating both sides, from t = 0 and its corresponding C = C_0 initial concentration to t = t and the corresponding C concentration, i.e.

$$\int_{C=C_0}^{C=C} \frac{1}{C} \bullet dC = \int_{t=0}^{t=t} -k_d \bullet dt \tag{3}$$

produces

$$\ln C = -k_d \bullet t + \ln C_0 \text{ (constant)} \quad (4)$$

The k_d value is determined from the decline of the natural logarithm of concentration of the test chemicals over time using linear regressions. The biotransformation rate constant of the substrate in trout liver S9 is determined here by subtracting the k_d values obtained from the active S9 and the heat-denatured S9, which is used as the negative control.

The advantage of the solvent delivery method is that it is a relatively simple procedure to obtain k_d values. In addition, the method has been used since the 1960s and has been well standardized. However, mixing high log K_{ow} organic chemicals in an aqueous incubation mixture is one major potential issue that can affect the effectiveness of this method. Laak *et al*. (2005), have pointed out that this chemical spiking method "often leads to unstable and variable concentrations and solutions containing not completely dissolved substances." This effect likely produces an underestimation of k_d values. The method was originally designed to test drugs, which have relatively low log K_{ow} values. Therefore, its applicability to assess the metabolic transformation potential of chemicals that are potentially bioaccumulative in fish may be limited. Also, the method only applies if the substrate concentration is far below its Michaelis-Menten constant, which is often unknown and requires extra effort to measure.

2.2 EVA dosing method

The ability of high log K_{ow} organic chemicals to passively partition between EVA and various environmental media has been demonstrated (Wilcockson and Gobas 2001; Vasiluk *et al*. 2006; Golding *et al.* 2007). In these studies, EVA is used to measure the activities and fugacities of high log K_{ow} organic chemicals in the environment. EVA's application in the reverse aspect, i.e. chemical dosing, has not yet been tested. The determination of the in vitro biotransformation rate of the test chemicals in trout liver S9 using the EVA dosing approach requires an understanding of the kinetics of the experimental set-up (Figure 1). The time-dependent kinetics of chemical partitioning between the EVA film and the liver S9 medium can be expressed as

$$\frac{dC_M}{dt} = k_1 \bullet C_E - (k_2 + k_d) \bullet C_M \quad (5)$$

and

$$\frac{dC_E}{dt} = k_2 \bullet C_M - k_1 \bullet C_E \quad (6)$$

where C_E is the substrate concentration in the EVA phase (ng/ml), t is time (minute), C_M is the substrate concentration in the liver S9 medium (ng/ml), k_1 is the rate constant of chemical delivery from the EVA to medium phase (minute^{-1}), k_2 is the rate constant of chemical delivery from the medium back to the EVA phase (minute^{-1}), and k_d is the rate constant of trout liver biotransformation in the medium phase (minute^{-1}).

The determination of the rate constants, k_1, k_2 and k_d, involves the application of the numerical integration method to chemical concentration-time profiles observed in EVA and medium phase of a control and test

$$C_{M(i+1)} = C_{M(i)} + \Delta C_M \tag{7}$$

and

$$C_{E(i+1)} = C_{E(i)} + \Delta C_E \tag{8}$$

where $C_{E(i+1)}$ and $C_{M(i+1)}$ are the chemical concentration (ng/ml) in the EVA and medium phase at time i+1, respectively, $C_{E(i)}$ and $C_{M(i)}$ are the chemical concentration (ng/ml) in the EVA and medium phase at time i, respectively, and $\triangle C_E$ and $\triangle C_M$ are the degree of chemical concentration changed (ng/ml) in the EVA and medium phase in one time unit, respectively. Conceptually, $\triangle C_E$ and $\triangle C_M$ are the same as dC_E/dt and dC_M/dt and can be substituted from equation 5 and 6 to give rise to

$$C_{M(i+1)} = C_{M(i)} + [k_1 \bullet C_{E(i)} - (k_2 + k_d) \bullet C_{M(i)}] \tag{9}$$

and

$$C_{E(i+1)} = C_{E(i)} + (k_2 \bullet C_{M(i)} - k_1 \bullet C_{E(i)}) \tag{10}$$

Therefore, two loops are created to numerically integrate the chemical concentration-time profiles in the respective EVA and medium phase over time, where each chemical concentration is derived from the previous chemical concentration one unit of time apart. Numerical simulations of the chemical concentration-time profiles from both the EVA (equation 10) and medium

(equation 9) phase are performed simultaneously by solver (Microsoft Excel), Initial (i.e. time 0) chemical concentration measured in the EVA and medium (i.e. 0) phase are required as starting values to begin the numerical simulations. In the first tier of the simulation, k_1 and k_2 are derived from the measured concentration-time profiles in the EVA and the medium of the controls (assuming k_d = 0). In the second tier of the simulation, k_d is determined from the concentration-time profiles in the test incubations while fixing the k_1 and k_2 values obtained from the control.

The advantage of applying the method of EVA dosing is in the way it releases test chemicals into the incubation mixture by passive diffusion. Because the test chemicals are released from the EVA phase by passive diffusion, they occur in the medium in a freely dissolved form. In addition, chemical concentrations are relatively low throughout the incubation period, and this avoids the possibility of enzyme saturation. For chemicals that exhibit high k_1 values, the determination of k_d can be done by fitting only the concentrations in the EVA phase of the assay. In this case, k_d is the rate limiting step in the process of chemical dosing and biotransformation. This greatly enhances the applicability of the method for the bioaccumulation assessment, as chemical extractions are done relatively easily with little error in the EVA phase. For chemicals that exhibit lower k_1 values (i.e. relatively higher log K_{ow} value substances), the determination of the k_d values can be done by fitting the chemical concentrations in the medium phase of the assay. However, errors in k_d values derived from concentration measurements in the medium, liver S9

homogenate, can be greater than those derived from concentration in the EVA because of the difficulty of extracting a liver S9 homogenate compared to EVA. As long as k_1 values are sufficiently large (i.e. relatively large k_1/k_d ratio), k_d values can be derived from the concentration in the EVA. The limitation of the EVA dosing method occurs when one intends to derive a k_d for a highly metabolizing chemical with a small k_1 value. Essentially, the chemicals cannot be delivered fast enough from the EVA to the medium phase to sustain the rate of biotransformation, so the k_d determined is an underestimate.

3: METHODS

3.1 Materials

Benzo[a]pyrene, chrysene, chrysene-d12, and 9-methylanthracene were obtained from Sigma-Aldrich (St. Louis, MO, USA) with purities of 98% or higher. EVA was obtained from DuPont (Wilmington, DE, USA). Monopotassium phosphate and potassium hydroxide were obtained from Caledon (Georgetown, ON, Canada). Magnesium chloride, glucose-6-phosphate, NADP, and glucose-6-phophate-dehydrogenase were obtained from Sigma-Aldrich. Potassium chloride was obtained from EMD (Darmstadt, HE, Germany). Dipotassium phosphate was obtained from Anachemia (Montreal, QC, Canada). Analytical grade dichloromethane (DCM) was obtained from Sigma-Aldrich. The stock solutions of 9-methylanthracene, chrysene, and benzo[a]pyrene were prepared in toluene (Caledon) at the following concentrations: 0.8487, 0.6334, and 0.8442 g/L, respectively. This corresponded to concentration of 104.2 µM for each test chemical. The chrysene-d12 internal standard working solution, 2.5 µg/ml, was prepared in hexane (EMD), and the external standards consisted of 50.07, 50.04, 49.81, and 49.11 µg/ml 9-methylanthracene, chrysene, benzo[a]pyrene, and chrysene-d12, respectively, in hexane.

3.2 Fish

Nine male rainbow trout (*Oncorhynchus mykiss*, approximately 1000 g each) were purchased from Miracle Springs (Mission, BC, Canada). The fish

were held in tanks with a continuous dechlorinated water flow-through system for at least two weeks under a 16:8-h light:dark cycle fed with 3.00 mm EWOS Pacific pellets (Surrey, BC, Canada) once daily. Water temperatures on the three sampling dates (July 16th, 17th, and 18th, 2008) were consistently 13.5 ^{o}C, and the degree of temperature fluctuation was within ± 2 ^{o}C for the 10 days prior to the removal of livers for the preparation of trout liver S9.

3.3 Preparation of trout liver S9

The procedures were adopted from Han *et al*. 2008 with some modifications. Three fish were humanely euthanized by anesthetic overdose using a solution of 0.3 g/L MS222 and 0.3 g/L sodium bicarbonate in dechlorinated water. The livers were immediately excised and rinsed in 4^{o}C 1.15% KCl solution. The livers were minced on an ice-cold Kimax pyrex glass Petri dish cover (approximate diameter of 100 mm) with a razor blade. Subsequently, they were homogenized in one volume of homogenization buffer (0.2 M phosphate buffer containing 1.15% KCl, at a pH of 7.4) using a Potter-Elvehjem tissue homogeniser with Teflon tipped pestle (Kimble tissue grind comp, size 22; Vineland, NJ, USA) and glass mortar (Kimble tissue grind tube, size 24; Vineland, NJ, USA) on ice. The speed of VWR Canlab homogenizer (West Chester, PA, USA) was set at approximately 1000 r.p.m., and the entire homogenizing process involved approximately fifteen passes. Because of the small size of livers in trout (i.e. generally less than 1% of body weight), livers from 3 fish were combined into a single sample to provide sufficient S9 volumes for testing. The homogenates were pooled in several 50 ml-Oak Ridge centrifuge

tubes (Nalgene Labware; Rochester, NY, USA), balanced, capped, and centrifuged (Hermle Model Z 360 K; Wehingen, BW, Germany) at 9,000 g for 20 minutes at 4 ^{o}C. One millilitre of the S9 homogenates were collected from the pool for protein analysis and the rest was transferred to multiple ice-cold 20ml glass scintillation vials with foil-lined caps (VWR Canlab). All S9 samples were immediately stored in a freezer (Sanyo V.I.P. series -86 ^{o}C; Moriguchi, Osaka, Japan) at -80 ^{o}C until the day of the experiment.

3.4 Liver S9 incubation using the solvent delivery approach

The active rainbow trout liver S9 incubation mixtures contained 0.1 ml NADPH regenerating system (8 µmol of glucose-6-phosphate, 0.8 µmol of NADP, 4 µmol of $MgCl_2$, and 1.6 units of glucose-6-phosphate dehydrogenase), 0.2 ml phosphate buffer (0.2 M at pH 7.4), and 0.2 ml defrosted S9 fraction. Incubation mixtures containing 0.3 ml of the same phosphate buffer and 0.2 ml heat-denatured trout liver S9 (80 ^{o}C for 5 minutes followed by cooling on ice) served as negative controls. Each incubation mixture was introduced in a 2 ml amber autosampler vial (Agilent; Mississauga, ON, Canada), capped with a screw cap with a Teflon/rubber/Teflon septum, and preincubated in a 13.5 ^{o}C water bath for 3 minutes. The reaction was initiated by adding 2.4 µL of a solution of 104.2 µM of benzo[a]pyrene, chrysene, and 9-methylanthracene in acetonitrile-190 (Caledon). The final acetonitrile concentration in the incubation mixture was less than 0.5% (v/v). The reaction was carried out in a Grant OLS 200 water bath with CS 200G refrigerated immersion cooler (Figure 2), at 13.5 ^{o}C. Vials were rolled at a speed of 60 r.p.m., approximately, throughout the incubation, and reactions

were terminated at time intervals (0, 15, 30, 60, 90, 120, 180, 240, 300, and 360 min) by adding 1 ml of ice-cold hexane. The vials were inverted multiple times and then placed on ice for 10 minutes to ensure the reaction was terminated. Chrysene-d12 internal standard (20 µL, final concentration 2.5 µg/ml) was added to each vial, followed by a 90-second vigorous shaking (SIP® vortex mixer, Baxter Scientific Products, USA) at setting #6 and then a 10-minute centrifugation (Centra CL2 benchtop centrifuge, Thermo IEC, USA) at 1,300 g to separate the two phases. The hexane supernatant (approximately 0.6 ml) was transferred to clean 2 ml amber autosampler vial (Agilent) and analyzed by GC MS.

3.5 Liver S9 incubation using the EVA dosing approach

In the application of the EVA dosing method, k_d is derived from concentration measured in an active S9 incubation mixture (i.e. a test) while fixing the k_1 and k_2 values derived from concentration measured in an inactive S9 incubation mixture (i.e. a control). Therefore, it is essential to choose a control that resembles the chemical kinetics in the test system to obtained an accurate measurement of k_d. Heat-denatured liver S9 homogenate was used in the solvent delivery method of the current study as a negative control. Because chemicals were mechanically introduced into an incubation mixture in the solvent delivery method, a change in the texture of liver S9 (i.e. becomes a greyish gel) due to heating did not affect the ability of heat-denatured liver S9 homogenate to serve as a control as long as there was no biotransformation activity. However, a change in liver S9 texture was likely associated with a change in the exchange kinetics (i.e. k_1 and k_2) of the test chemical between the EVA and medium phase.

The chemical dynamics in a heat-denatured liver S9 incubation may be different from that in an active liver S9 incubation medium. Deriving a k_d from an active liver S9 incubation medium based on the exchange kinetics measured from a heat-treated liver S9 incubation medium might introduce substantial error. Therefore, a no-cofactor liver S9 homogenates, preincubated 24 hours prior to the experiment (to "wear out" enzyme activities) was used in addition to a heat-denatured control in the current study.

All procedures and equipment were identical to those used in the conventional incubation except for the following modifications. An additional set of controls were introduced in the incubation procedure, in which the liver S9 sample was kept in a 13.5 ^{o}C water bath for 24 hours prior to incubation to eliminate enzyme activities without having to heat treat the liver homogenate. The composition of the incubation mixture included 0.2 ml time-treated liver S9 and 0.3 ml phosphate buffer, and it was denominated as a "no-cofactor control." Instead of directly introducing test compounds into the incubation mixture, the test chemicals were first dissolved in 0.1347 g/L EVA solution predissolved in DCM at concentrations of 20.02 μM for chrysene and 9-methylanthracene, and 50.05μM for benzo[a]pyrene. 25 μL of the solution of the EVA and test chemicals was injected into a 2 ml amber silanized autosampler vial (Agilent) and manually rolled for 60 seconds in a fume hood to produce a thin EVA film (approximately 4 nm). The vial was left in the fume hood for an additional 120 seconds to ensure the complete evaporation of DCM before it was capped. The EVA film appeared to be uniformly applied, based on the even distribution of Sudan IV dye added to

a separate EVA solution and coated in an identical manner. The components of the incubation mixture were equivalent to the conventional chemical spiking method but reactions were initiated by the addition of 0.2 ml liver S9 homogenate. Test incubations were terminated after 0, 10, 20, 40, 60, 90, 120, 180, 240, 300, and 360 min, and control incubations were terminated after 0, 10, 40, 60, 90, 180, 300, and 360 min by removing 0.4ml of the incubation mixture using a Gilson pipette (Mandel; Guelph, ON, Canada) and transferring it to a 2 ml vial containing 1 ml of ice-cold hexane with 20 µL of chrysene-d12 internal standard. The residual 0.1ml of the incubation mixture was discarded as waste (chemical concentration determined in the incubation mixture were multiplied by 1.25 to compensate for the 0.1 ml loss). The EVA film was rinsed four times with 1 ml deionized water. The vial was then gently tapped upside-down on a piece of tissue paper to remove excess water. The extracting/analyzing steps for handling the 0.4 ml incubation mixture followed those used in the conventional chemical spiking method. To extract the EVA films, 1 ml of hexane and 20 µL of chrysene-d12 internal standard were added to the EVA-coated vials. After 60 seconds of vigorous vortexing (SIP® vortex mixer, Baxter Scientific Products, USA) on setting #6, followed by 10 min of 1,300 g centrifugation (Centra CL2 benchtop centrifuge, Thermo IEC; Waltham, MA, USA), the hexane supernatant was transferred to a clean 2 ml amber autosampler vial (Agilent) and analyzed by GC MS.

3.6 Determination of extraction efficiency

It is a common practice to use heat-treated subcellular liver fraction or isolated hepatocytes as a negative control in metabolism studies (e.g., Han *et al*. 2007, 2009; Shappell *et al*. 2003; Minato *et al*. 1999; Kim *et al*. 1996; Parnham *et al*. 2005). In a metabolism study, a heat-denatured control assumes that the presence of metabolic activities is the only experimental factor that is different between a control and a test. Therefore, the biotransformation rate of a test chemical can be determined from the difference in measured rate constants of substrate depletion, k_d, of the test and the control. However, it is suspected that the assumption may not be valid because there is one important experimental factor, i.e. the difference in substrate extraction efficiencies between a heat-denatured liver S9 medium and an active liver S9 medium, is overlooked.

Procedures and equipment used to evaluate extraction efficiencies of test chemicals in a regular liver S9 medium adopted those used in the conventional incubation with the following modifications. Test chemicals (2.4 µL, final concentration 104.2 µM in acetonitrile-190) were manually injected into the incubation mixtures under the same condition as the no-cofactor control. The incubation was terminated after 0, 10, 20, and 60 min by adding 1 ml of ice-cold hexane. After shaking on the vortex mixer and centrifugation, 0.6 ml of the supernatant was transferred to clean 2 ml amber autosampler vials and 20 µL of the chrysene-d12 internal standard was added. The samples were then analysed by GCMS. Test chemicals (2.4 µL, final concentration 104.2 µM in acetonitrile-190) introduced into 1 ml of hexane served as the standard of 100%

extraction efficiency. The extraction efficiencies of each test chemical of the four time intervals (i.e. 0, 10, 20, and 60 min) were calculated by dividing to the standard value, and they were used to correct the experimental data obtained from extractions of the active and inactive (no-cofactor) S9 medium. For those experimental data collected right at 0, 10, 20, and 60 min, the values were corrected by the four corresponded extraction efficiencies. For the experimental data collected at 15 min, the values were corrected by the corresponded extraction efficiency averaged of time 10 and 20 min. For the experimental data collected beyond 20 min (i.e. 30, 40, 90, 120, 180, 240, 300, and 360 min), the values were corrected by the corresponded extraction efficiency averaged of time 20 and 60 min.

The decline of the natural logarithm of concentration of the test chemical over time (i.e. the “slope”) in every heat-denatured liver S9 incubation medium of the solvent delivery method was assumed to be caused by a decrease in extraction efficiency over time. In addition, these slopes were pooled and then averaged to establish the averaged time-coursed extraction efficiency for chemicals incubated in the heat-denatured liver S9 medium with ten time intervals: 0, 15, 30, 60, 90, 120, 180, 240, 300, and 360 min. It was used to correct for extraction efficiencies of the experimental data obtained in the medium phase of the EVA dosing method. For those experimental data collected right at some of these ten time intervals, the values were corrected by these corresponded extraction efficiencies. For the experimental data collected at the time intervals of 10 and 40 min, their values were corrected by the corresponded

extraction efficiencies averaged of time 0 and 15, and 30 and 60 min, respectively.

3.7 Determination of protein content

The Bradford protein assay (Bradford 1976) was used to determine the protein content of the trout liver S9 samples. A standard curve was made using bovine serum albumin (Sigma-Aldrich, St. Louis, MO, USA) at concentrations of 0, 20, 40, 60, 80, and 100 mg/mL. A Pharmacia LKB Ultrospec III UV/Vis spectrophotometer (Creve Coeur, MO, USA) was used to record the absorbance of the BSA standards and liver S9 samples at 595 nm wavelength. Each batch of liver S9 samples was examined in triplicate, and the mean value was used in the subsequent protein normalization process.

3.8 Sample analysis

The hexane extracts of the incubation mixture and the EVA coating were analysed for the test chemicals using an Agilent 6890 gas chromatograph (GC) attached to an Agilent 5973N mass spectrometer (MS), with a programmable cool on-column injection port, a 30m x 250µm x 0.25µm HP-5MS 5% phenyl methyl siloxane-coated column (Agilent), and a 5m x 530µm x 0.25µm fused-silica deactivated guard column (Agilent). The oven temperature program for the conventional experiment was 45 ^{o}C for 1.5 min, 15 ^{o}C/min to 150 ^{o}C, and finally 10 ^{o}C/min to 285 ^{o}C, which was held for 5 min. The injection port and ion source temperatures were 45 and 230 ^{o}C, respectively. The oven temperature program for the EVA experiment was 60 ^{o}C for 0.5 min, 25 ^{o}C/min to 200 ^{o}C and held for

0.5 min, and finally 20 ^{o}C/min to 300 ^{o}C, which was held for 4 min. The injection port and ion source temperatures were 60 and 230 ^{o}C, respectively. The carrier gas was helium at 1 mL/min flow rate. The ions selected for detection of 9-methylanthracene, chrysene, chrysene-d12, and benzo[a]pyrene were m/z 192, 228, 240, and 252, respectively. Those ions were selected based on the properties of high intensity with low interference. A sample of the extract, 1 µL, was injected into the column automatically by a 5-µL gas-tight glass syringe (Agilent). Peak areas were integrated and used to quantify the test chemicals using Chemstation (Hewlett Packard) software (Figure 3).

Introducing known amount of internal standard in each of the test vial was to account for the variability in GC MS responses, sample injection volume and volume of extraction solvent. At the beginning of sample analysis, linear standard curves of benzo[a]pyrene, chrysene, and 9-methylanthracene were constructed as functions of the ratio of the relative peak area of the test chemicals to the internal standard and chemical concentration, and they were displayed in figures 4, 5, and 6, respectively. Since the R^2 values for all three test chemicals were above 0.99, the relative response factor (RRF) approach was adopted as the application of this method was timesaving. The RRF was calculated as

$$RRF = (A_c / M_c) / (A_{i.s.} / M_{i.s.}) = (A_c \times M_{i.s.}) / (A_{i.s.} \times M_c) \quad (11)$$

where A is the peak area, M is the mass, and the subscripts c and i.s. represent the chemical and internal standard, respectively. Under the condition where the volume of each incubation mixture is constant, as it was in these experiments, the equation can be simplified to:

$$RRF = (A_c \times C_{i.s.}) / (A_{i.s.} \times C_c) \quad (12)$$

where the unsubscribed C is the concentration. The RRF of a specific chemical can be determined by measuring peak areas of the chemical and internal standard at known concentrations. A well established RRF curve is a straight line regardless of chemical concentrations (Figure 7). A test chemical with unknown concentration, thus, can be determined by rearranging equation (2) to

$$C_{c\,(unknown)} = (A_c \times C_{i.s.}) / (A_{i.s.} \times RRF) \quad (13)$$

RRF values were established at 50 ng/ml of the test chemicals and internal standard in hexane several times during each GCMS run. The standard was analysed once after running eight to eleven samples. The concentrations of the test chemicals from each of those eight to eleven samples were determined using the RRF values averaged from the two runs that bracketed the sample sequence.

3.9 Data analysis and statistical design

The detailed methodology used to determine the biotransformation rate constants of the three test chemicals from both the conventional chemical spiking method and EVA dosing method was described in the theory section above.

The livers of three male rainbow trout were pooled to compose one batch of liver S9, and there were three batches made (i.e. 9 fish were used in total). Each batch of liver S9 was tested in both solvent delivery and EVA dosing experiments. Each experiment was conducted in triplicate. k_d values of the three test chemicals were determined in three ways. Firstly, they were determined by

the solvent delivery method. Secondly, they were determined by chemical concentration measured from the EVA phase of the EVA dosing method. Lastly, they were determined by chemical concentration measured from the medium phase of the EVA dosing method. Linear regression, from the Microsoft Excel, was used to test for statistical significance between the slopes of test and control (i.e. zero) in the solvent delivery method. Statistical analysis software, JMP 7, was used to perform the following tests. Student's t-test was used to test for statistical significance of the mean k_d values of a test chemical determined from the solvent delivery method and the medium phase of the EVA dosing method. The test was also used to test for statistical significance of the mean k_1 and k_2 values of a test chemical determined in the two phases of the EVA dosing method. A Bartlett test was used to test for statistical significance of the variances of samples. Depending on the statistical significance of the variances of samples, a Welch ANOVA or ANOVA, in conjunction with Tukey's test, was used to test for statistical significance of the mean k_d values among the three test chemicals determined from each dosing method.

4: RESULTS AND DISCUSSION

4.1 Protein content of trout liver S9 samples

The mean protein contents of the first, second, and third replicate/batch of the trout liver S9 samples were determined to be 54.4 ± 6.3, 57.6 ± 3.9, and 63.9 ± 3.7 mg protein/ml S9. These concentrations were within the linear range of the standard curve. The standard curve was measured using protein concentration of 0, 20, 40, 60, 80, and 100 mg protein/ml S9 and had a R^2 of 0.9958 (Figure 8).

4.2 The solvent delivery method

4.2.1 Extraction efficiencies of the test chemicals in the solvent delivery method

Figures 9 to 11 show that extraction efficiencies of benzo[a]pyrene, chrysene, and 9-methylanthracene drop over the initial 10 min of incubation and reach plateaus between 20 to 60 min. Figure 12 shows that the magnitude of the reduction in extraction efficiency over time differ among the three test chemicals with the greater drop in extraction efficiency for the higher log K_{ow} chemicals. Benzo[a]pyrene, with the greatest log K_{ow} value (i.e. 6.04), shows a drop in the extraction efficiency of about 60% over the first 20 min. Chrysene (log K_{ow} value of 5.81) and 9-methylanthracene (log K_{ow} value of 5.07) show a drop in the extraction efficiency of around 40 and 30%, respectively, over the first 20 min. The extraction efficiencies of the three test chemicals at the four incubation time points of the three test replicates are summarized in table 1. Substrate

concentrations of the three chemicals in the test are corrected for extraction efficiency.

The k_d values of the three test chemicals from three replicates of the control are generally small, ranging from 0.0004 ± 0.0004 to 0.0015 ± 0.0003 min^{-1} and are not significantly different from zero (i.e. p-values ranged from 0.998 to 0.883). In addition, an analysis of variance shows that ANOVA reveals that the mean k_d values of the three test chemicals in the control are not significantly different at the 95% confidence level (p = 0.38; Figure 13).

4.2.2 k_d values of the test chemicals determined by the solvent delivery method

Figure 14 to 16 illustrate the test chemical concentrations in the incubation medium as a function of incubation time in the test and control for the three test chemicals. The decline of the natural logarithm of concentration of the test chemicals over time (i.e. the “slope”) is calculated using linear regressions. Only those chemical concentrations measured in the incubation medium that are within the initial ln-linearity region are used to determine the slope.

The steepest decline in concentration throughout the duration of incubation over time is observed for benzo[a]pyrene followed by chrysene, and then 9-methylanthracene. Regression analysis shows that the slopes of benzo[a]pyrene in replicate number one, two, and three of the test are significantly different from zero with p-values of 0.043, 0.017, and 0.008, respectively. Therefore, the test shows significant rates of depletion of benzo[a]pyrene characterized by k_d values of 0.0113 ± 0.0039, 0.0232 ± 0.0049,

and 0.0279 ± 0.0044 min^{-1} for the three replicates (Table 2). Similarly, regression analysis shows the slopes of chrysene and 9-methylanthracene in the test are also significantly different from zero with p-values of 4.79E 10^{-6}, 0.0021, and 3.04E 10^{-6} for chrysene, and 1.72E 10^{-04}, 0.0048, and 1.69E 10^{-04} for 9-methylanthracene in replicate number one, two, and three, respectively. The corresponding k_d values of chrysene are 0.0030 ± 0.0003, 0.0024 ± 0.0005, and 0.0086 ± 0.0005 min^{-1}, and they are 0.0014 ± 0.0002, 0.0007 ± 0.0002, and 0.0020 ± 0.0003 min^{-1} for 9-methylanthracene (Table 2). The mean k_d values and standard deviations of benzo[a]pyrene, chrysene, and 9-methylanthracene are 0.0208 ± 0.0086, 0.0047 ± 0.0034, and 0.0014 ± 0.0007 min^{-1}, respectively (table 2). Bartlett test shows that the variances of the k_d values of the three test chemicals are significantly different (p = 0.034). A Welch ANOVA (p = 0.080) reveals that the mean k_d values of the three test chemicals are not significantly different from each other at the 95% confidence level (Figure 17).

4.2.3 Factors controlling k_d

In the current experimental setup, the absence of the phase II cofactors can result in an accumulation of phase I hydroxylated metabolites. As the structures of these metabolites resemble those of their parent compounds, they can compete with the parent compounds for the same P450 enzyme site, namely CYP1A1, which is the principle CYP450 enzyme involved in the metabolism of PAH in fish (Hankinson 1995; Ryan *et al*. 1982; Wilson *et al*. 1984) although other P450 enzymes (e.g., CYP1B1) might also contribute (Savas *et al*. 1993). This phenomenon is known as end-product inhibition. Much effort has been

devoted to studying of end-product inhibition of benzo[a]pyrene. For instance, it has been reported that at least 79% of the metabolites of benzo[a]pyrene produced in rat microsomes show competitive inhibition of the parent compound in the phase I hydroxylation process (Shen *et al*. 1979; Keller and Jefcoate 1984; Keller *et al*. 1987). However, It has been shown that fish and rat liver enzymes differed greatly in terms of the overall substrate specificity and regioselectivity for metabolism of PAHs (Pangrekar *et al*. 2003; Sikka *et al*. 1990; Varanasi *et al*. 1986; Tuan *et al*. 1999).

Another factor that can affect the k_d values determination is the gradual decline in analyte concentration during substrate depletion. Throughout the incubation period, chemical concentration can reach the method detection limit. This can interfere with the correct measurement of the concentration decline over time. Nath and Atkins (2006) suggested that the apparent first-order rate constant of a substrate depletion experiment "should only be [determined] from time points where no more than 10% of the substrate has been consumed." However, because of analytical reasons, the application of the substrate depletion approach requires at least 20% of the substrate being metabolized within the incubation period (Jones *et al*. 2005). Consequently, the attempt to conform to such a standard was held back in this study. I therefore used concentration over the entire initial incubation period to derive the k_d, which was akin to Obach and Reed-Hagen's (2002).

4.2.4 Comparison to the literature values

Benzo[a]pyrene was selected as a test chemical because its metabolic potential in fish is well characterized (Han *et al*. 2007, 2009; Miranda *et al*. 2006; Kennedy and Tierney 2008; Maria *et al*. 2002; Kennedy *et al*. 1989, 1991; Kennedy and Walsh 1994). The research from this experiment could therefore be compared to the results of comparable measurements in the literature. Han *et al*. (2009), determined the mean clearance rate, CL_{int} (ml/h/mg) of benzo[a]pyrene in trout liver S9 to be 0.068 ml/h/mg protein (= 1.13E 10^{-3} ml/min/mg protein). The mean k_d, normalized to protein content, of benzo[a]pyrene determined in the current study is 0.0017 min^{-1}·mg $protein^{-1}$. After normalizing to the volume of incubation (i.e. 0.5 ml), this rate can be converted to a clearance rate, CL_{int} of 0.89 E 10^{-3} ml/min/mg protein, which is comparable to the CL_{int} reported in Han *et al*.'s study (2009).

Carpenter *et al*. (1990) reported several measurements of the Michaelis-Menten constant, K_M, ranging from 33 to 125 µM in rainbow trout microsomes under various acclimation and incubation temperatures. Although Obach and Reed-Hagen (2002) showed that there is substantial variability in K_M values reported in the scientific literature, it is encouraging that the concentration of benzo[a]pyrene used in both the current and Han *et al*.'s (2009) (i.e. 0.5 and 2 µM, respectively) were both considerably lower than reported K_M values. This implies that experiments were conducted at sufficiently low substrate concentrations to satisfy the assumption of first order reaction conditions.

It is of interest that there is a wide range of k_d values or CL_{int} values determined for benzo[a]pyrene in fish. Pedersen *et al.* (1976) have reported a greater than 50-fold difference in liver microsomal benzo[a]pyrene-hydroxylase activity among six trout strains examined. In addition, biotransformation rates can be affected by a range of external factors, such as pre-exposure to xenobiotics, and water quality parameters such as temperature and salinity (Johnston *et al*. 1999; Seubert and Kennedy 1997). Diet can have effects on depletion and intrinsic clearance rates of chemicals. It has been reported that glutathione-S-transferase activity was attenuated 34% compared to the control within 6 weeks of fasting for rainbow trout (Gourley and Kennedy 2009). It has also been reported that an increase in dietary fat intake in rats can lead to an increase in the proportion of total polyunsaturated fatty acids in the mucosal endoplasmic reticulum which can alter the configuration of active enzymes in the membranes, possibly elevating biotransformation rates of benzo[a]pyrene (Wills 1983). In the case of PAHs, prior exposure of animals to CYP1A1 inducers, which include PAHs themselves (e.g., benzo[a]pyrene; Sandvic *et al*. 1997), will increase their *in vitro* rates of biotransformation. Therefore, caution should be taken when considering experimental biotransformation rates in an environmental management schemes as in real-world situations, animals are likely to be exposed to a variety xenobiotics that may induce or inhibit CYP450 activity.

4.3 The EVA dosing method

4.3.1 Extraction efficiencies of the test chemicals in the EVA dosing method

Figure 18 to 20 shows that the time-coursed extraction efficiency of each test chemical in the heat-denatured liver S9 incubation mixture. ANOVA revealed that the mean extraction efficiencies of the three test chemicals in the heat-denatured liver S9 incubation mixture were not significantly different from each other ($p = 0.38$). Figure 21 shows the combined extraction efficiency of the three test chemicals from the heat-denatured liver homogenate dropped of about 10% over the initial 180 minutes of the incubation period. After 180 minutes, the extraction efficiency remained constant.

4.3.2 Comparison of the dynamics of the three chemicals using the no-cofactor and heat-denatured controls

Figure 22 to 24 show the measured and fitted chemical concentration of benzo[a]pyrene, chrysene, and 9-methylanthracene in the EVA phase of experiments using the no-cofactor control. The concentration-time profiles of the three test chemicals in the control were similar to those observed in the active S9. Generally, the concentration of the three test chemicals declined initially and remained constant towards the end of the incubation period in both the control and the active S9. Figure 25 to 27 show measured and fitted chemical concentration of the three test chemicals in the medium phase of experiments using the no-cofactor control. The concentration-time profiles of 9-methylanthracene in the control were similar to that observed in the active S9 medium. However, the situation was different for benzo[a]pyrene and chrysene.

As opposed to the concentration of 9-methylanthracene rapidly increased and gradually declined in the active S9 medium, the concentration of benzo[a]pyrene and chrysene increased for a short period followed by a rapid decline in the active S9 medium.

Figure 28 to 30 show measured and fitted chemical concentration of benzo[a]pyrene, chrysene, and 9-methylanthracene in the EVA and medium phase of experiments using the heat-denatured control. The general concentration-time profiles of the three test chemicals in the incubation system using the heat-denatured control and no-cofactor control were similar except for the following differences. The concentration-time profiles of benzo[a]pyrene and chrysene in the control were not similar to that observed in the active S9 in the EVA phase. Figure 28 and 29 show there are obvious divergences between the concentration-time profiles in the control than those observed in the active S9 for benzo[a]pyrene and chrysene in the EVA phase. In addition, the concentration-time profiles of 9-methylanthracene in the control were not similar to that observed in the active S9 in the medium phase. Figure 30 shows the concentration of 9-methylanthracene in the active S9 incubation medium elevates and exceeds that observed in the control.

The heat-denatured control did not appear to provide a representative/comparable incubation environment to that of the active S9. More specifically, some of the exchange kinetics derived from the incubation system using the heat-denatured control were incomparable to those of the no-cofactor control. The mean k_1 of benzo[a]pyrene, chrysene, and 9-methylanthracene

derived from the concentration in the no-cofactor control were significantly greater from those derived from the concentration in the heat-denatured control in the EVA phase with p-values of 0.006, 0.042, and 0.009, respectively, by a Student's t-test. Due to the small sample size and larger sample variances, only the mean k_1 of benzo[a]pyrene derived from the concentration in the no-cofactor control was significantly greater ($p = 0.045$) from that derived from the concentration in the heat-denatured control in the medium phase by a Student's t-test. The mean k_2 of the three test chemicals derived from the concentration in the no-cofactor control were not significantly different ($p > 0.05$) from those derived from the concentration in the heat-denatured control in both the EVA and medium phase by a Student's t-test. Figure 28 to 30 show that the majority of the k_d values of the three test chemicals derived from the concentration measured in the active S9 in the EVA phase exceed that of the corresponded k_1 values. This is unreasonable as a k_d cannot exceed a k_1 in the EVA phase under normal circumstances as k_d is limited by how fast a chemical is being delivered from the EVA (i.e. k_1). Figure 30 shows that the concentration of 9-methylanthracene in the active S9 medium exceeds that in the heat-denatured control medium. This is also unreasonable, and it indicates the heat-denatured control medium is incomparable to the active S9 medium. The exchange kinetics and k_d values of the three test chemicals determined in EVA and medium in both the heat-denatured control and no-cofactor experiments are summarized in table 4 and 3, respectively. Based on these lines of evidence, I conclude that it is necessary to apply the no-cofactor control in the EVA dosing method to produce meaningful

results. Only results obtained from incubations using no-cofactor controls will be used in the following discussion.

4.3.3 k_d values determined from concentration in the EVA and the incubation medium phase in the EVA dosing experiment

The k_d values of the three test chemicals determined from the concentration in EVA phase of the EVA dosing method are given in table 3, and in figures 22 to 24. A Bartlett test showed that the variance of the k_d values of the three test chemicals are not significantly different ($p = 0.58$). ANOVA revealed that the mean substrate depletion rate constants of the three test chemicals were not significantly different from each other at the 95% confidence level ($p = 0.37$, Figure 33).

The k_d values were also calculated from the observed chemical kinetics in the medium phase. Figures 25 to 27 show that the k_d values determined in the three independent experiments. The data are summarized in table 3. A Bartlett test showed that the variances of the k_d values of the three chemicals were significantly different from each other ($p < 0.0001$). The combination of Welch ANOVA ($p = 0.023$) and Tukey's test revealed the mean k_d of benzo[a]pyrene was significantly ($p < 0.05$) larger than that of the other two chemicals (Figure 34). The mean k_d values of chrysene and 9-methylanthracene, on the other hand, were not statistically significantly different from each other at the 95%confidence level (Figure 34).

The k_d values obtained using the EVA dosing method where determined as the best estimates (i.e. method of least squares) using the solver function of

Microsoft Excel. A limitation in the application of solver is that it does not provide confidence intervals of the fitted values. Therefore, the k_d values of the three chemicals determined from the test of each experimental replicate by solver could not be formally used to determine the statistical significance of the test. However, from the figure it is obvious that the concentration difference in the test and the control are highly significant. Development of a method that is able to provide statistical comparisons between the values fitted for the test and control is needed in the future.

4.3.4 Exchange kinetics, k_1 and k_2, determined from the EVA and S9 phases using the EVA dosing method

The EVA-medium exchange kinetics, k_1 and k_2, were different among the three test chemicals. Figure 31 shows that the mean k_1 of the three test chemicals determined from both the EVA and medium drops as the log K_{ow} of the chemical increases. Figure 32 shows that the mean k_2 of the three test chemicals do not display a similar correlation but are approximately the same. Figures 31 and 32 also show that the degree of variation in k_1 and k_2 is smaller when determined from the concentration in the EVA than when determined from the concentration in the medium. Table 3 summarizes these observations and shows that the mean k_1 of 9-methylanthracene, chrysene, and benzo[a]pyrene are 0.2147 ± 0.0110, 0.0195 ± 0.0025, and 0.0137 ± 0.0030 min^{-1}, respectively, when determined from the concentration in the EVA phase, and are 0.3275 ± 0.3445, 0.0187 ± 0.0049, and 0.0101 ± 0.0048 min^{-1}, respectively, when measured in the medium phase. The same table also shows the mean k_2 values of

benzo[a]pyrene, chrysene, and 9-methylanthracene are 0.0084 ± 0.0022, 0.0085 ± 0.0060, and 0.0062 ± 0.0013 min^{-1}, respectively, when determined from the concentration in the EVA, and are 0.0134 ± 0.0154, 0.0153 ± 0.0137, and 0.0495 ± 0.0611 min^{-1}, respectively, when determined in the medium. Student's t-test shows the mean k_1 of benzo[a]pyrene, chrysene, and 9-methylanthracene determined from the concentration measured in the EVA are not significantly different ($p > 0.05$) from those determined in the medium. This is also the case for the mean k_2 of the three test chemicals.

4.3.5 Discussion of relevant issues affecting the k_d determined by the EVA dosing method

The relationship between the parameters k_1 and k_d is critical in the application of the EVA dosing approach. As described earlier in the Theory section, a substance with a low log K_{ow} value (and correspondingly larger k_1 value) is likely to have a higher k_1/k_d ratio, and k_d is the rate limiting step. Under this condition, deriving the k_d from the concentration in the EVA phase of the EVA dosing method may be adequate. Using the k_1 and k_d values derived from the concentration in the medium, the mean k_1/k_d ratio of 9-methylanthracene is approximately 298, which is the largest of the three test chemicals. The associated mean k_d of 9-methylanthracene derived from the concentration in the EVA is not significantly different from the value derived from the medium of the EVA dosing method ($p = 0.644$, Student's t-test, $\alpha = 0.05$). By contrast, the mean k_1/k_d ratio of chrysene is 0.235. However, the mean k_d of chrysene determined from the concentration in the EVA phase was considerably smaller than that

derived from the concentration in the medium phase ($p = 0.011$, Student's t-test, $\alpha = 0.05$). If the k_1/k_d ratio is small, the chemicals is not being delivered fast enough from the EVA to the medium phase, and, an underestimate of k_d is derived. In such a case, the medium is more sensitive in capturing the chemical dynamics of the incubation system, and provides a more accurate measurement of k_d. The mean k_d of benzo[a]pyrene determined from the current study is close to the scenario described for chrysene. It has the smallest k_1/k_d ratio of 0.011 of all test chemicals, and figure 25 shows that its chemical concentration measured in the medium are at or below the limit of detection. However, if the mean k_d of benzo[a]pyrene were derived from the concentration in the medium which were all below the limit of detection, it would be an underestimate of the real value. If the k_1/k_d ratio is small, as in this case, for example, for the mean k_d of benzo[a]pyrene derived from the chemical concentration in the EVA phase can be different from that derived from the concentration in the medium phase ($p = 0.049$, Student's t-test, $\alpha = 0.05$). It is important for the application of thin-film dosing to find means to increase k_1. Increasing the k_1/k_d ratio allows a wider range of chemicals, especially the ones with high log K_{ow}, to be tested. Some potential improvements that can be made to achieve this include increasing the EVA dosing surface area (e.g., coat EVA film in a larger vial) or decreasing the thickness of EVA film (e.g., decrease EVA concentration). In addition, it is probably worthwhile to quantify two limits of the k_1/k_d ratio. Figure 35 shows a first limit for the derivation of a k_d by making concentration measurements in the EVA or the medium phases, and the second limit directs the derivation of a k_d of

a substance be done in the medium or exerts a warning that the k_d is prone to underestimation. 9-methylanthracene has the k_1/k_d ratio of 298, which is likely above the first k_1/k_d ratio limit, so the k_d can be measured from the concentration in the EVA phase. Chrysene and benzo[a]pyrene have the k_1/k_d ratios of 0.235 and 0.011, respectively, which are likely between the first and second k_1/k_d ratio limits, so the respected k_d has to be measured from the concentration in the medium phase in order to avoid obtaining underestimated k_d values from that of the EVA phase. For chemicals that have the k_1/k_d ratios below the second limit, the k_d values derived from the concentration in the medium phase are also subject to underestimation.

Because k_1 is a function of incubation temperature, another limitation of the application of the EVA dosing method is encountered when the determination of k_d of a particular chemical is in ectotherm that resides in a cool environment (e.g., <10 ^oC). It is common to set the incubation temperature to the temperature that the organism has been acclimated (Fitzsimmons *et al.*, 2007). A lower incubation temperature is associated with a lower k_1. A lower k_1/k_d ratio limits the ability of the concentration in EVA to detect reaction rates.

The mean k_d values of benzo[a]pyrene and chrysene determined from concentration in the medium of the EVA dosing experiment appear to be more accurate than the mean k_d values determined from concentration in the EVA because of their small k_1/k_d ratios. The mean k_d values of 9-methylanthracene determined from concentration in the EVA and medium phase are not

significantly different and are both likely to be accurate as 9-methylanthracene has a high k_1/k_d ratio.

4.3.6 Comparisons of k_d values to literature values

The mean k_d, normalized to protein content, of benzo[a]pyrene determined from the concentration in the medium phase of the EVA dosing experiment is 0.0775 1/min/mg protein. After normalizing to the volume of incubation (i.e. 0.5 ml), this rate can be converted to a clearance rate, CL_{int} of 38.74 E 10^{-3} ml/min/mg protein, which is approximately 34-times higher than that reported in Han *et al*.'s study, 2009 (i.e. CL_{int} of 1.13E 10^{-3} ml/min/mg protein).

4.3.7 Inter-methodological k_d values comparisons

Figure 36 displays the mean k_d values of benzo[a]pyrene, chrysene, and 9-methylanthracene determined by the EVA dosing method (from medium) and the solvent delivery method. Student's t-test revealed the mean k_d of benzo[a]pyrene and chrysene determined from medium of the EVA dosing method were significantly greater than that determined by the solvent delivery method at α = 0.05 with p-values of 0.050 and 0.011, respectively. The mean k_d of 9-methylanthracene determined from the concentration in the medium of the EVA dosing experiment is not significantly different from that determined by the solvent delivery method (p = 0.619).

The mean k_d of benzo[a]pyrene of 0.0208 min^{-1} determined in the current study by using the solvent delivery method is higher than the only comparable literature value of 0.0023 min^{-1} (i.e. Han *et al*., 2009). However, it is significantly

lower than that derived from concentration in the medium of the EVA dosing method. Similarly, the mean k_d of chrysene derived from concentration in the medium of the EVA dosing method is significantly higher than that determined by the solvent delivery method. Furthermore, figures 25 and 26 show that simulated curves of the chemical dynamics for benzo[a]pyrene and chrysene in medium of the EVA dosing method, constructed using k_d values derived from the solvent delivery method, are not in close agreement with the measured concentrations. This may be due to the differences in the amount of test chemicals presented in their free/unbound form in the incubation system. It is believed that only substances in their free form are available for biotransformation; ideally, k_d values should be derived only using this fraction, not the fraction bound non-specifically to protein or in crystals/aggregates. It has been postulated earlier (in the theory section) that mechanically introducing high log K_{ow} test chemicals into an aqueous incubation mixture (as the solvent delivery method does) is difficult and tantamount to mixing oil and water. It has been discovered that hydrophobic pharmaceutical compounds form immiscible crystals when added to aqueous solution (Lafferrere *et al*., 2004), and this property was exploited to generate nanometer-scale crystals in chemical engineering technology (Maeda *et al*., 2004). The EVA dosing method introduces test chemicals slowly and steadily into an incubation mixture over time as a result of passive diffusion. Therefore, test chemicals have more time to be dissolved in the incubation mixture, and may exhibit a larger fraction of the chemical in the free, unaggregated form than in the solvent delivery method, and thus produce higher values of k_d.

Theoretically, substances with higher log K_{ow} are more prone to the formation of crystals in an aqueous incubation mixture resulting in the formation of a smaller fraction of substances in their free form. Consequently, for metabolizable substances, the difference between k_d values measured in an EVA dosing system and a solvent delivery system can expected to be greater for substances with higher log K_{ow}. The data presented here support this as the difference in k_d values of benzo[a]pyrene (log K_{ow} value of 6.04) determined from the two dosing methods is approximately 44-fold, whereas the difference is only approximately 17-fold for chrysene (log K_{ow} value of 5.81) (Tables 2 and 3). This implies that the application of the solvent delivery method to estimate k_d of a substance is subject to underestimation due to the limited quantity of free chemical present in the incubation mixture. This is especially true for substances with high log K_{ow} and a sufficiently high metabolic potential. However, for substances with low K_{ow}, k_d values derived by the solvent delivery method may be as accurate as those derived by the EVA dosing method. 9-methylanthracene may fit this scenario as the data show that the k_d values determined by the solvent delivery method and derived from concentration in the medium of the EVA dosing approach are not significantly different ($p = 0.619$) in a Student's t-test. Future studies should focus on the comparison of k_d values determined from both the solvent delivery method and the EVA dosing method of chemicals with similar log K_{ow} values as 9-methylanthracene but with higher metabolic potentials to verify the postulation of different degrees of free chemical fractions between these dosing methods. Future study should also focus on comparing the k_d

values of the three test chemicals determined by the EVA dosing method to those determined *in vivo* to verify the degree of *in vitro-in vivo* correlations.

5: CONCLUSION

In conclusion, the results of the current study reveal some promising features of the application of the EVA dosing method for measuring biotransformation rates. It is necessary yet to establish how well a biotransformation rate constant derived from the EVA dosing method predicts the *in vivo* intrinsic clearance. It has been shown that the intrinsic clearance rates measured using liver microsomes or S9 is lower than that using hepatocytes (Han *et al*. 2009; Houston and Carlile 1997; Ito and Houston 2004; Jones and Houston 2004). However, the EVA dosing method has been shown here to produce significantly greater biotransformation rate constants than the solvent delivery method. Trout liver S9 possesses useful traits, such as the availability of long-term storage techniques, the presence of both phase I and II metabolic enzyme activities (if the appropriate cofactors are included). The ease of preparation, renders it one of the best *in vitro* systems to assess k_d values of commercial chemicals at the screening level. In the future, it may be possible to apply the EVA dosing approach to other *in vitro* media (e.g., supersomes, microsomal fractions, and isolated heptatocytes) and develop other applications. Theoretically, the experimental k_d values can vary considerably even between similar test setups. Therefore, regulators and managers that intend to interpret these values in their decision-making should be cautious. Future work is needed

to better understand the utility of trout liver S9 and the EVA dosing method in bioaccumulation assessment of xenobiotics.

TABLES

Table 1. Time-coursed extraction efficiencies of benzo[a]pyrene, chrysene, and 9-methylanthracene using hexane in trout liver S9 incubation mixtures of three S9 sample preparations.

Test Chemicals		Sample 1			Sample 2			Sample 3			Total Mean +/-SD
	Incubation Time (min)	1[a]	2[a]	Mean +/- SD	1	2	Mean +/- SD	1	2	Mean +/- SD	
Benzo[a]pyrene	0	0.983	0.912	**0.947 +/- 0.050**	0.969	1.032	**1.000 +/- 0.044**	0.997	0.958	**0.978 +/- 0.028**	**0.975 +/- 0.040**
	10	0.464	0.382	**0.423 +/- 0.058**	0.468	0.493	**0.480 +/- 0.018**	0.549	0.520	**0.535 +/- 0.021**	**0.479 +/- 0.058**
	20	0.355	0.352	**0.354 +/- 0.002**	0.483	0.329	**0.406 +/- 0.108**	0.389	0.457	**0.423 +/- 0.048**	**0.394 +/- 0.062**
	60	0.384	0.363	**0.373 +/- 0.015**	0.326	0.267	**0.296 +/- 0.042**	0.519	0.404	**0.461 +/- 0.081**	**0.377 +/- 0.085**
Chrysene	0	1.103	0.986	**1.044 +/- 0.083**	0.969	1.034	**1.002 +/- 0.046**	1.004	0.971	**0.987 +/- 0.023**	**1.011 +/- 0.051**
	10	0.605	0.648	**0.627 +/- 0.030**	0.664	0.638	**0.651 +/- 0.019**	0.709	0.626	**0.668 +/- 0.058**	**0.648 +/- 0.036**
	20	0.580	0.606	**0.593 +/- 0.019**	0.645	0.497	**0.571 +/- 0.104**	0.544	0.614	**0.579 +/- 0.050**	**0.581 +/- 0.053**
	60	0.644	0.623	**0.634 +/- 0.015**	0.501	0.435	**0.468 +/- 0.047**	0.668	0.552	**0.610 +/- 0.082**	**0.571 +/- 0.091**
9-methylanthracene	0	0.969	0.964	**0.966 +/- 0.003**	0.980	1.026	**1.003 +/- 0.032**	1.153	1.143	**1.148 +/- 0.007**	**1.039 +/- 0.087**
	10	0.797	0.739	**0.768 +/- 0.041**	0.835	0.837	**0.836 +/- 0.001**	0.725	0.723	**0.724 +/- 0.001**	**0.776 +/- 0.054**
	20	0.730	0.711	**0.721 +/- 0.014**	0.769	0.696	**0.732 +/- 0.052**	0.799	0.675	**0.737 +/- 0.088**	**0.730 +/- 0.047**
	60	0.737	0.699	**0.718 +/- 0.027**	0.793	0.676	**0.735 +/- 0.083**	0.923	0.742	**0.833 +/- 0.128**	**0.762 +/- 0.089**

SD = standard deviation.

[a] = replicate 1 and 2.

Table 2. Substrate depletion rate constants, k_ds (min^{-1}), of benzo[a]pyrene, chrysene, and 9-methylanthracene determined by the solvent delivery method using rainbow trout liver S9.

	Benzo[a]pyrene			Chrysene			9-methylanthracene		
Test replicate	1	2	3	1	2	3	1	2	3
k_d [a]	0.0113	0.0232	0.0279	0.0030	0.0024	0.0086	0.0014	0.0007	0.0020
Mean +/- SD	0.0208 +/- 0.0086			0.0047 +/- 0.0034			0.0014 +/- 0.0007		

SD = standard deviation.

[a] = substrate depletion rate constant (min^{-1}) determined by subtracting the slope of chemical depletion obtained from the active S9 and the heat-denatured S9 at the logarithmic scale.

Table 3. Substrate depletion and ethylene vinyl acetate (EVA) delivery/receiving rate constants (min^{-1}) for benzo[a]pyrene, chrysene, and 9-methylanthracene of both the EVA and medium phases in EVA dosing experiment using trout liver S9 with no-cofactor control.

		Benzo[a]pyrene			Chrysene			9-methylanthracene		
Test replicate		1	2	3	1	2	3	1	2	3
EVA phase	k_1[a]	0.0120	0.0172	0.0120	0.0211	0.0166	0.0209	0.2026	0.2241	0.2175
	Mean +/- SD	**0.0137 +/- 0.0030**			**0.0195 +/- 0.0025**			**0.2147 +/- 0.0110**		
	k_2[b]	0.0060	0.0104	0.0088	0.0036	0.0067	0.0151	0.0047	0.0069	0.0070
	Mean +/- SD	**0.0084 +/- 0.0022**			**0.0085 +/- 0.0060**			**0.0062 +/- 0.0013**		
	k_d[c]	-0.0009	0.0001	0.0028	0.0009	0.0024	0.0064	0.0007	0.0009	0.0029
	Mean +/- SD	**0.0007 +/- 0.0019**			**0.0032 +/- 0.0028**			**0.0015 +/- 0.0012**		
Medium phase	k_1[a]	0.0074	0.0073	0.0157	0.0152	0.0165	0.0243	0.1500	0.1080	0.7245
	Mean +/- SD	**0.0101 +/- 0.0048**			**0.0187 +/- 0.0049**			**0.3275 +/- 0.3445**		
	k_2[b]	0.0030	0.0061	0.0310	0.0064	0.0084	0.0311	0.0175	0.0110	0.1200
	Mean +/- SD	**0.0134 +/- 0.0154**			**0.0153 +/- 0.0137**			**0.0495 +/- 0.0611**		
	k_d[c]	0.2985	1.2446	1.1830	0.0582	0.0818	0.0989	0.0008	0.0003	0.0023
	Mean +/- SD	**0.9087 +/- 0.5293**			**0.0796 +/- 0.0204**			**0.0011 +/- 0.0010**		

SD = standard deviation.

[a] = EVA to trout liver S9 medium chemical delivery rate constant (min^{-1}).

[b] = trout liver S9 medium to EVA chemical delivery rate constant (min^{-1}).

[C] = substrate depletion rate constant (min^{-1}).

Table 4. Substrate depletion and ethylene vinyl acetate (EVA) delivery/receiving rate constants (min^{-1}) for benzo[a]pyrene, chrysene, and 9-methylanthracene of both the EVA and medium phases in EVA dosing experiment using trout liver S9 with heat-denatured control.

		Benzo[a]pyrene			Chrysene			9-methylanthracene		
Test replicate		1	2	3	1	2	3	1	2	3
EVA phase	k_1[a]	0.0034	0.0061	0.0011	0.0088	0.0160	0.0045	0.0934	0.1196	0.0492
	Mean +/- SD	**0.0035 +/- 0.0025**			**0.0098 +/- 0.0058**			**0.0874 +/- 0.0356**		
	k_2[b]	0.0048	0.0112	0.0032	0.0071	0.0238	0.0111	0.0042	0.0056	0.0041
	Mean +/- SD	**0.0064 +/- 0.0042**			**0.0140 +/- 0.0087**			**0.0046 +/- 0.0008**		
	k_d[c]	1.9918	0.0248	1.9957	2.0158	0.0192	1.9844	1.9025	0.0033	1.9467
	Mean +/- SD	**1.3374 +/- 1.1368**			**1.3398 +/- 1.1438**			**1.2842 +/- 1.1095**		
Medium phase	k_1[a]	0.0024	0.0023	0.0007	0.0471	0.0057	0.0020	0.3793	0.0957	0.348
	Mean +/- SD	**0.0018 +/- 0.0010**			**0.0183 +/- 0.0250**			**0.2743 +/- 0.1555**		
	k_2[b]	0.0108	0.0214	0.0145	0.1722	0.0365	0.0312	0.4921	0.1179	0.6520
	Mean +/- SD	**0.0156 +/- 0.0054**			**0.0800 +/- 0.0799**			**0.4207 +/- 0.2741**		
	k_d[c]	0.0992	0.4395	0.2116	0.0446	0.0150	-0.0009	-0.0058	-0.0050	-0.0049
	Mean +/- SD	**0.2501 +/- 0.1734**			**0.0196 +/- 0.0231**			**-0.0052 +/- 0.0005**		

SD = standard deviation.

[a] = EVA to trout liver S9 medium chemical delivery rate constant (min^{-1}).

[b] = trout liver S9 medium to EVA chemical delivery rate constant (min^{-1}).

[c] = substrate depletion rate constant (min^{-1}).

FIGURES

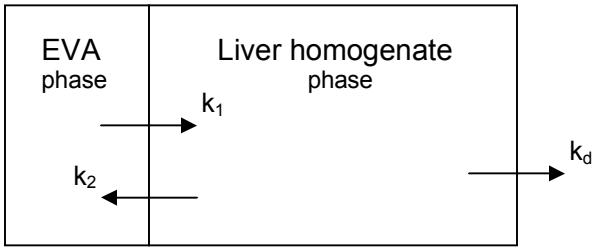

Figure 1. A conceptual diagram showing chemical partitioning between an ethylene vinyl acetate (EVA) phase and a S9 homogenate phase and biotransformation within the S9 liver homogenate medium, where k_1 is the rate constant of chemical delivery from the EVA to medium phase, k_2 is the rate constant of chemical delivery from the medium to EVA phase, and k_d is the rate constant of substrate depletion in the S9 homogenate.

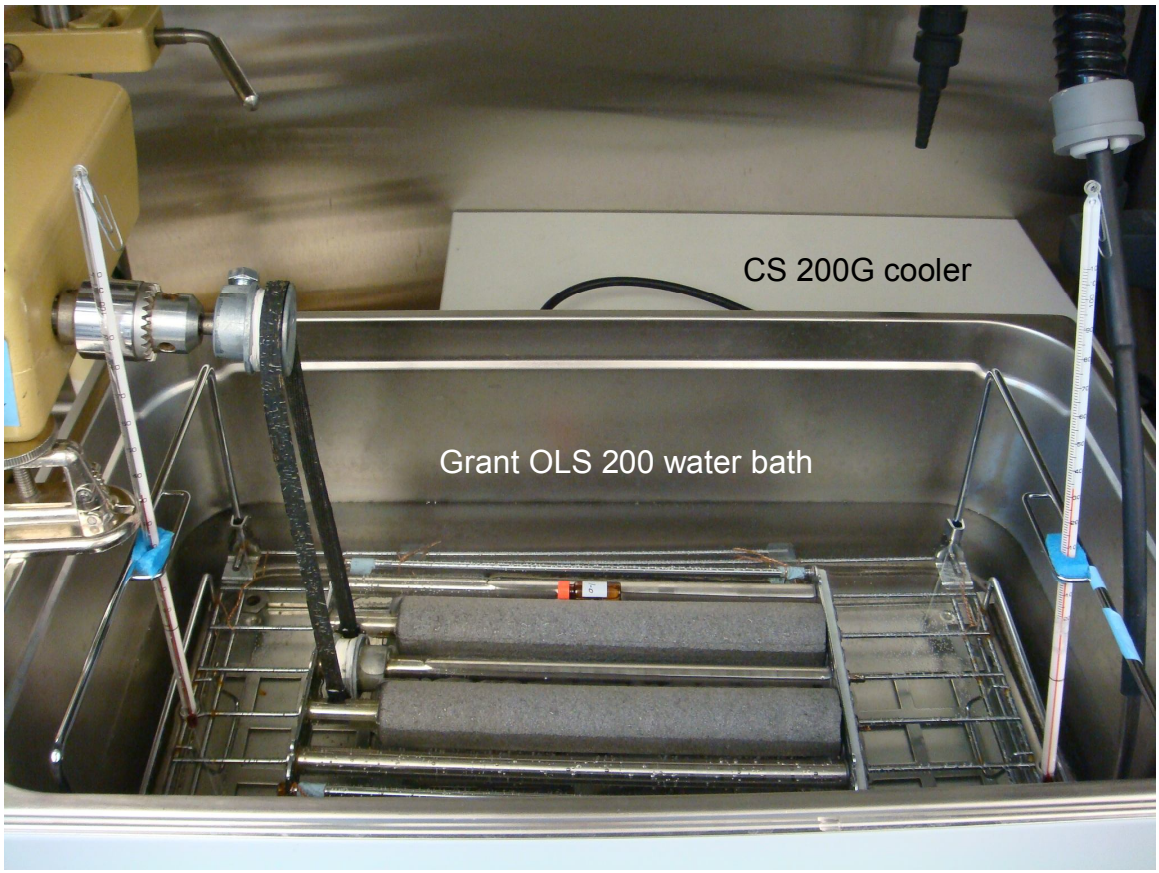

Figure 2. A photograph of the trout liver S9 incubation system setup. The system includes a temperature controlled Grant OLS 200 water bath and CS 200G refrigerate immersion cooler to control/maintain the incubation temperature at 13.5°C. Incubations are conducted in 2 ml amber Agilent autosampler vial placed in the middle of rolling rack spinning at a speed of approximately 60 r.p.m..

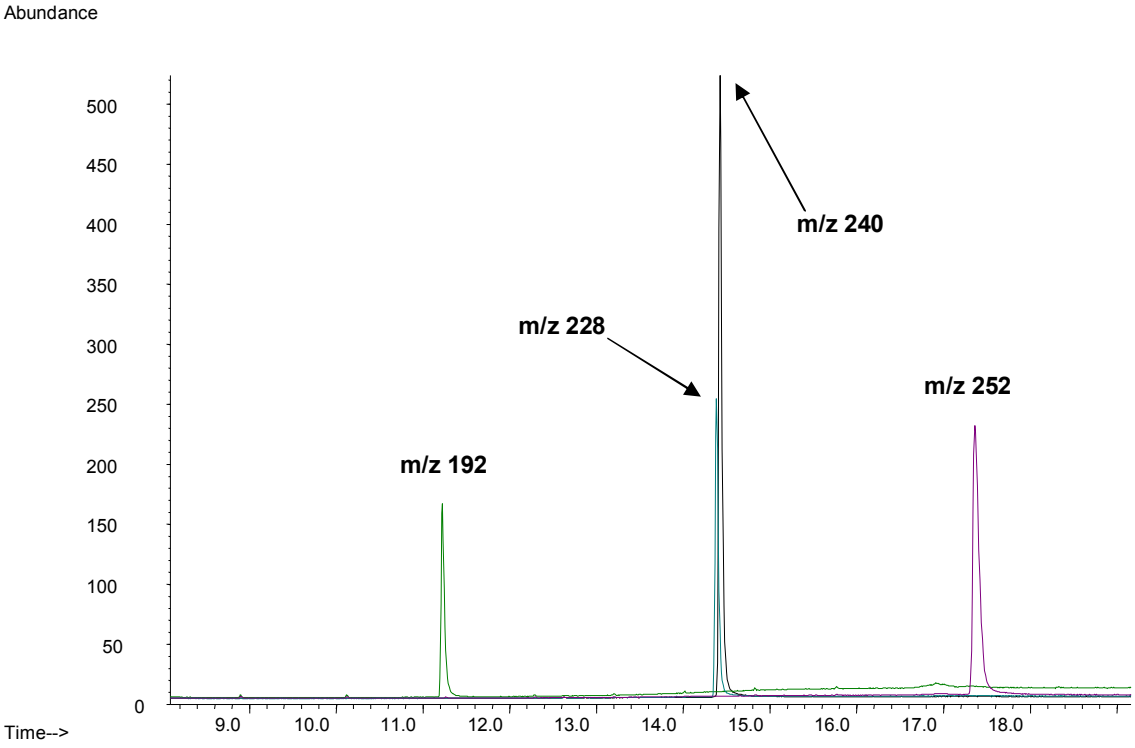

Figure 3. A typical GC MS chromatogram displaying intensities of 9-methylanthracene (m/z 192), chrysene (m/z 228), chrysene-d12 (m/z 240), and benzo[a]pyrene (m/z 252) as a function of the retention time (minute).

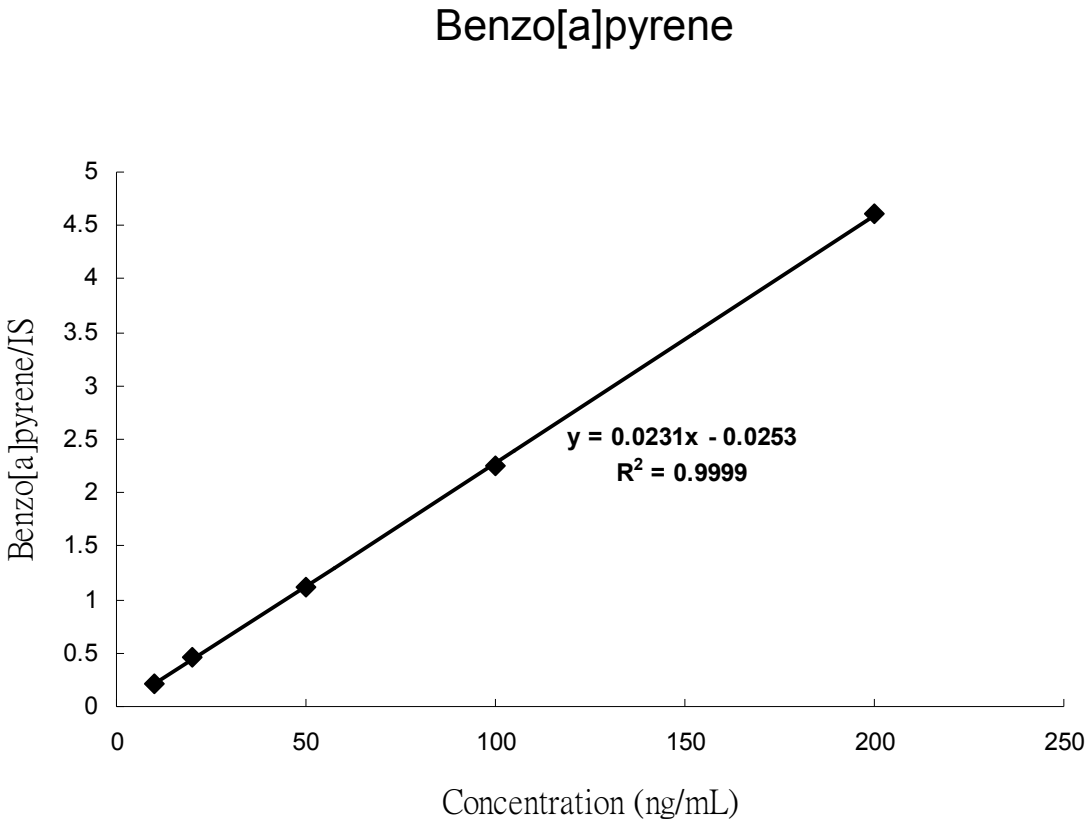

Figure 4. Standard curve showing the response (measured in terms of peak area) of benzo[a]pyrene relative to that of the internal standard (chrysene-d12) as a function of the benzo[a]pyrene concentration (ng/ml).

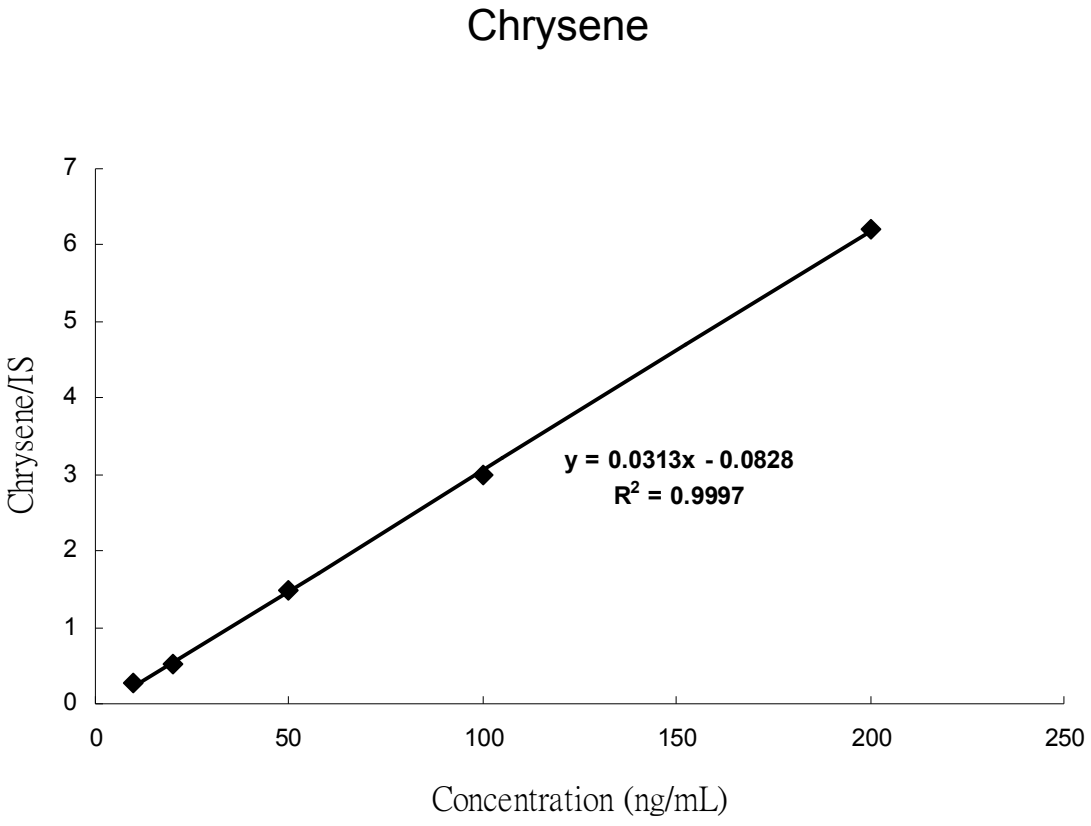

Figure 5. Standard curve showing the response (measured in terms of peak area) of chrysene relative to that of the internal standard (chrysene-d12) as a function of the chrysene concentration (ng/ml).

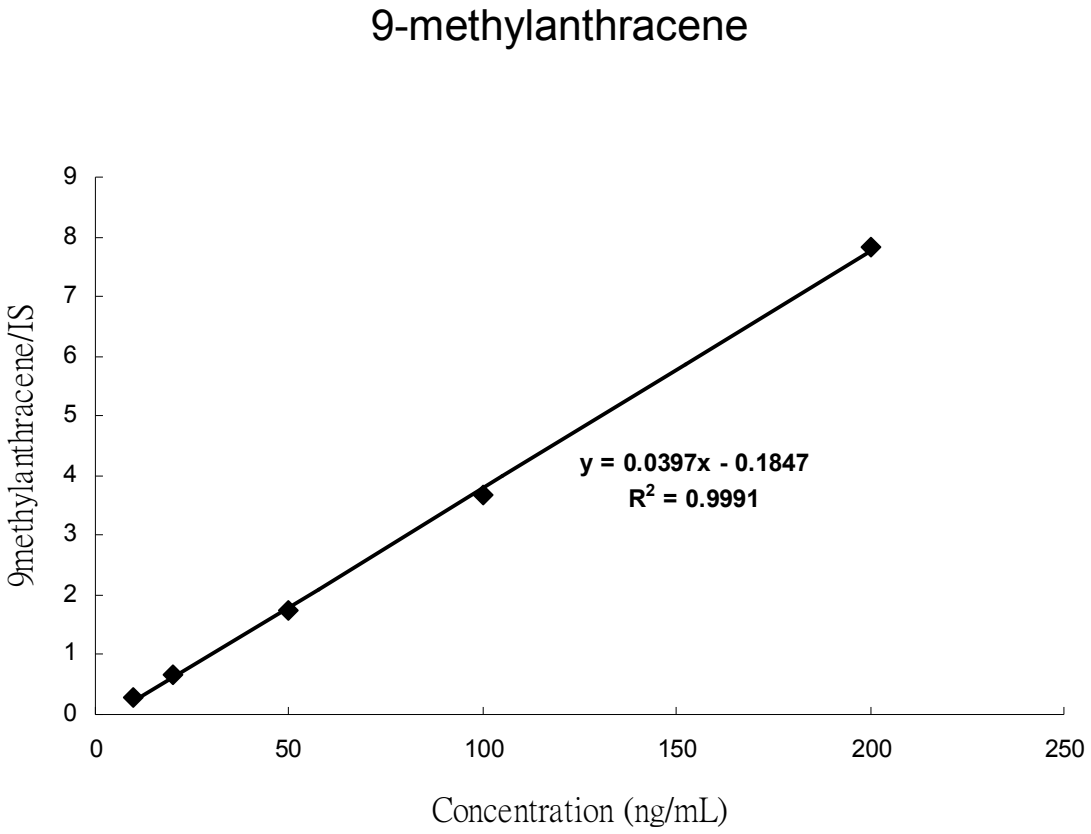

Figure 6. Standard curve showing the response (measured in terms of peak area) of 9-methylanthracene relative to that of the internal standard (chrysene-d12) as a function of the 9-methylanthracene concentration (ng/ml).

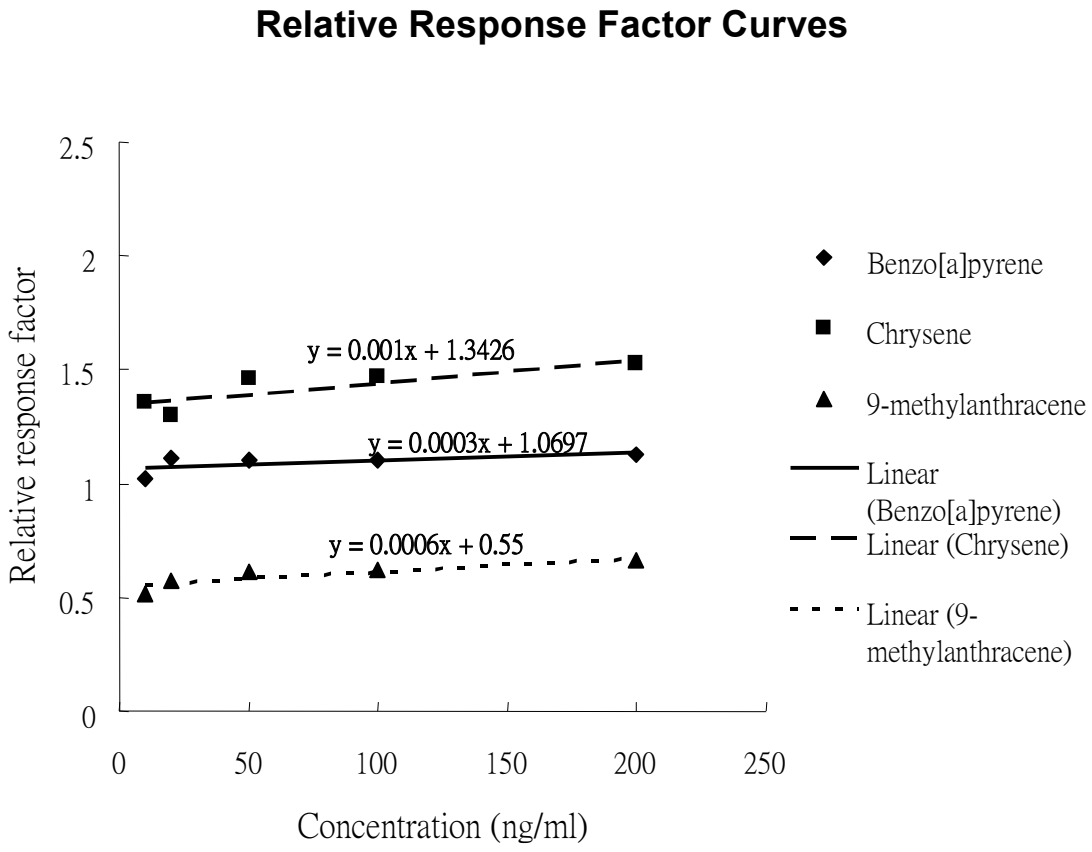

Figure 7. Relative response factors (RRF) as a function of the analyte concentration for benzo[a]pyrene, chrysene, and 9-methylanthracene.

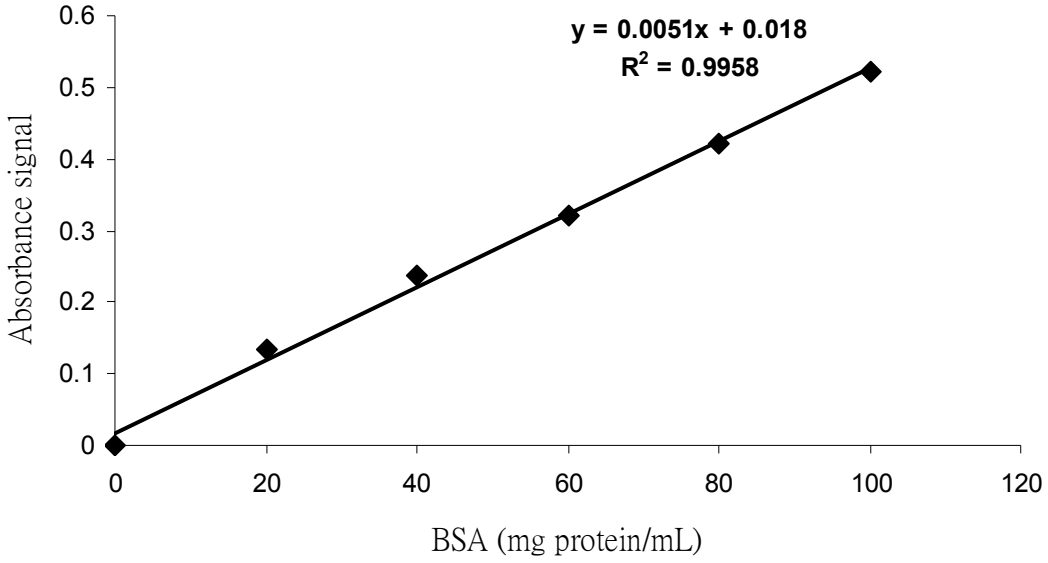

Figure 8. Standard curve showing the spectrophotometer response as a function of the concentration of bovine serum albumin used for protein contents analysis.

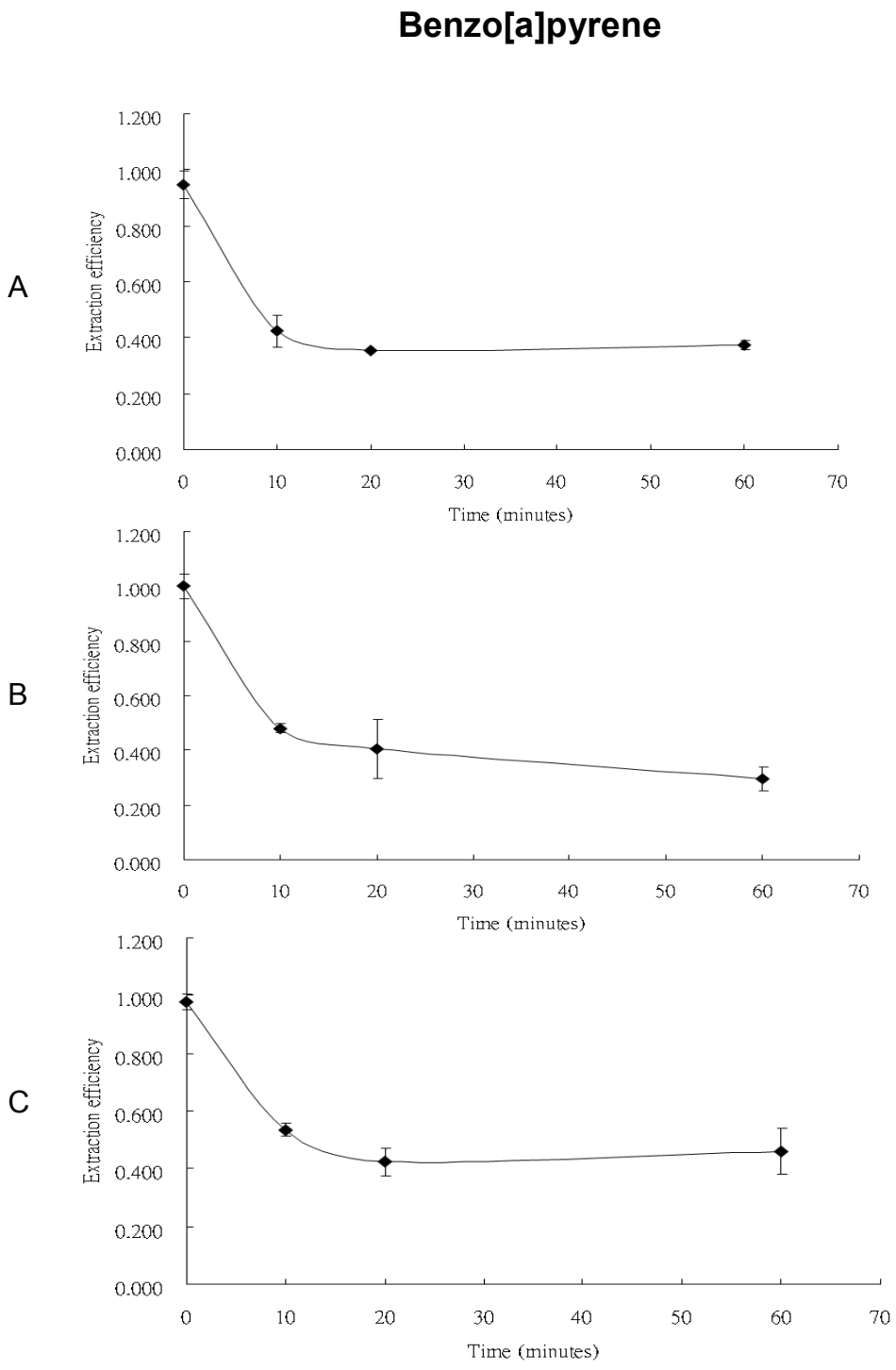

Figure 9. Extraction efficiency and standard deviation of benzo[a]pyrene from inactive control S9 liver homogenate as a function of the incubation time in replicate one (A), two (B), and three (C).

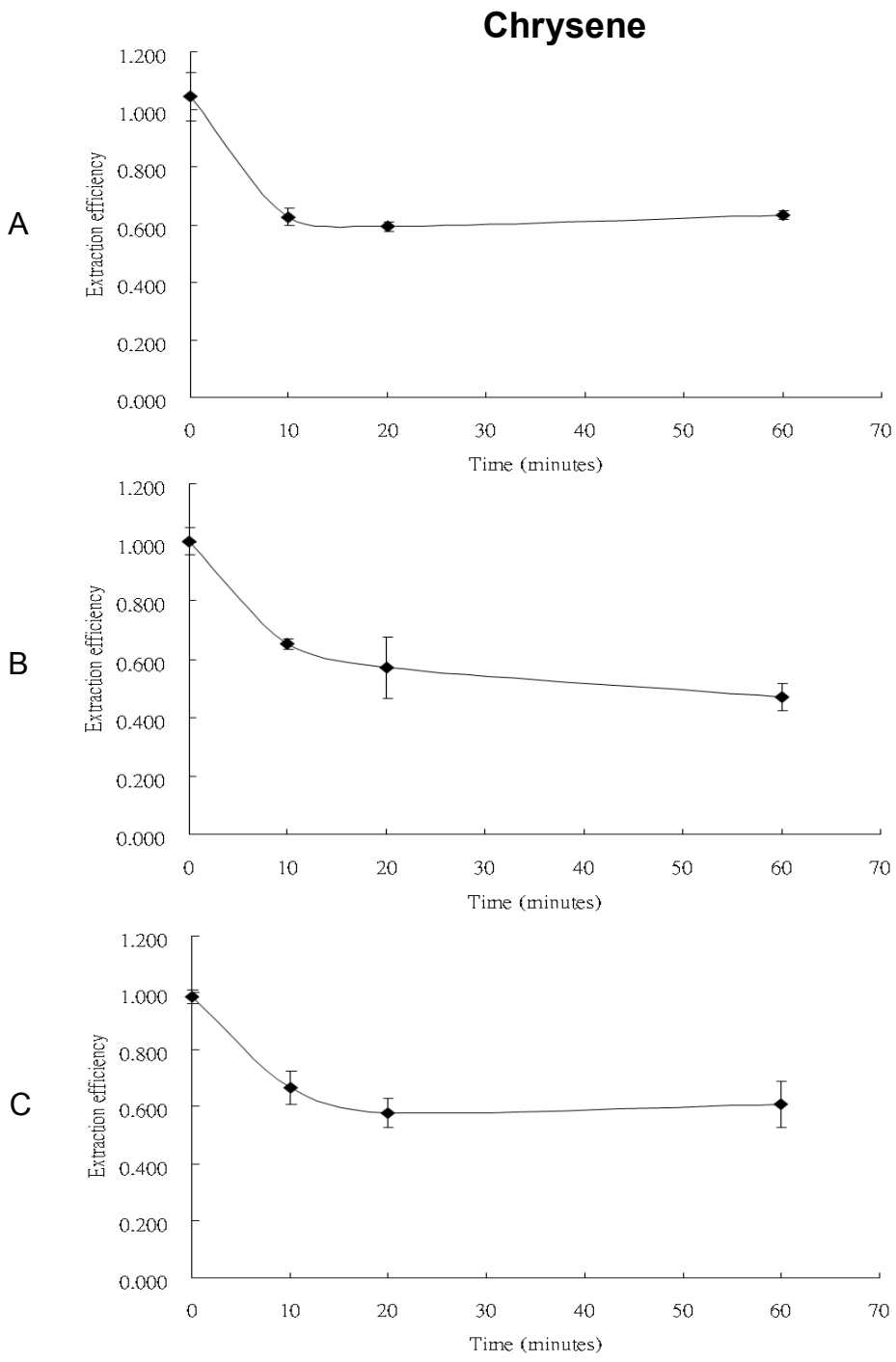

Figure 10. Extraction efficiency and standard deviation of chrysene from inactive control S9 liver homogenate as a function of the incubation time in replicate one (A), two (B), and three (C).

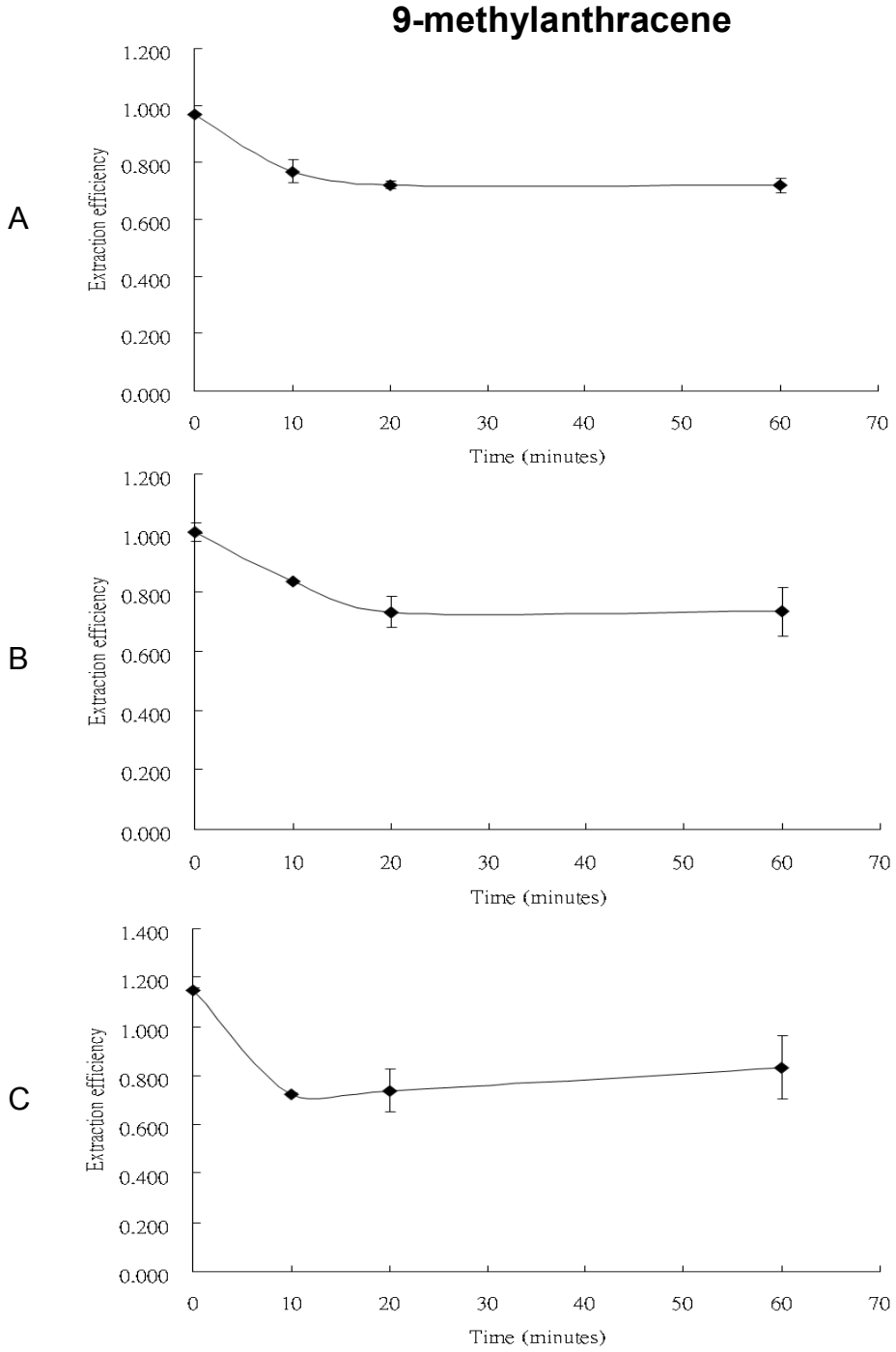

Figure 11. Extraction efficiency and standard deviation of 9-methylanthracene from inactive control S9 liver homogenate as a function of the incubation time in replicate one (A), two (B), and three (C).

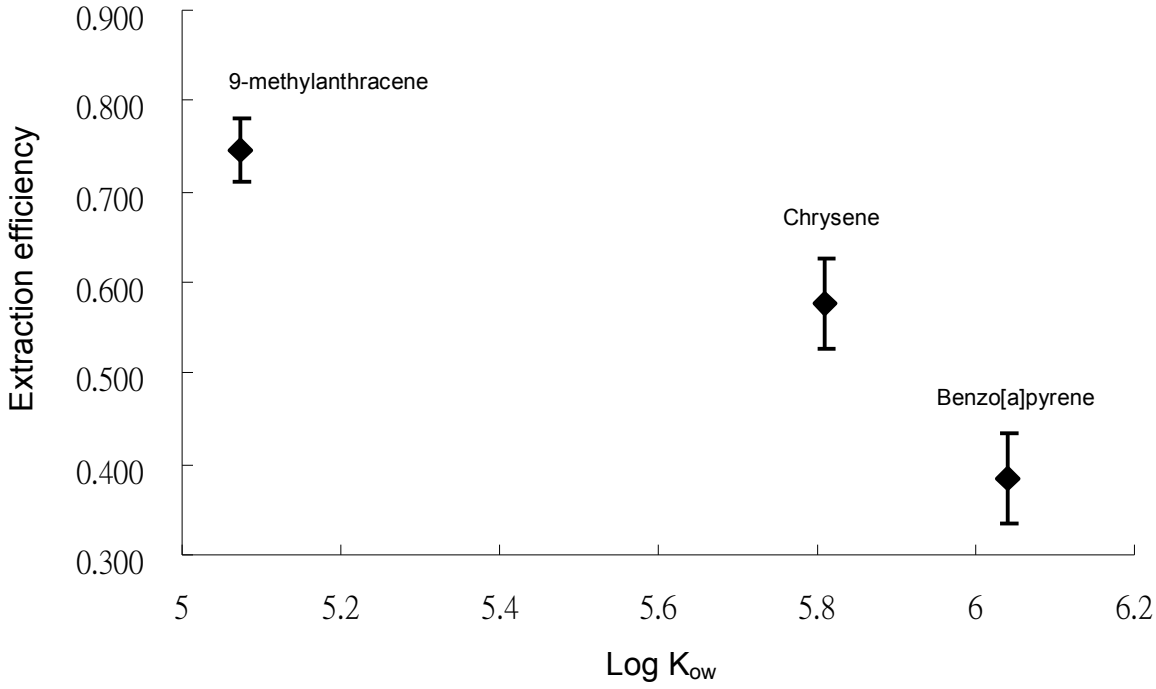

Figure 12. Extraction efficiency and standard deviation of 9-methylanthracene, chrysene, and benzo[a]pyrene from inactive S9 liver homogenate after 20 min incubation as a function of log K_{ow}.

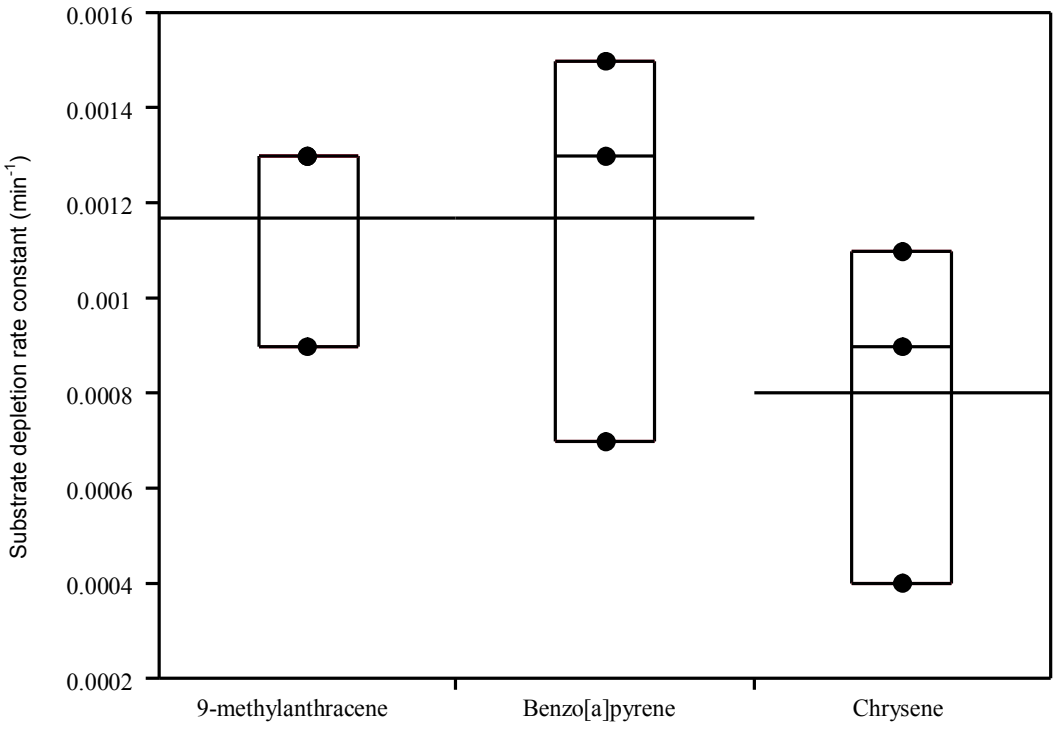

Figure 13. Box plots of the substrate depletion rate constants (k_ds) of benzo[a]pyrene, chrysene, and 9-methylanthracene obtained in heat-denatured trout live S9 homogenate using the solvent delivery method. The ends of the box are the 25th and 75th quantiles, the line within the middle region of the box is the median, and the line across the box identifies the mean value. ANOVA test revealed the mean k_ds of the three test chemicals were not significantly different among each other at 95% confidence level (p = 0.38).

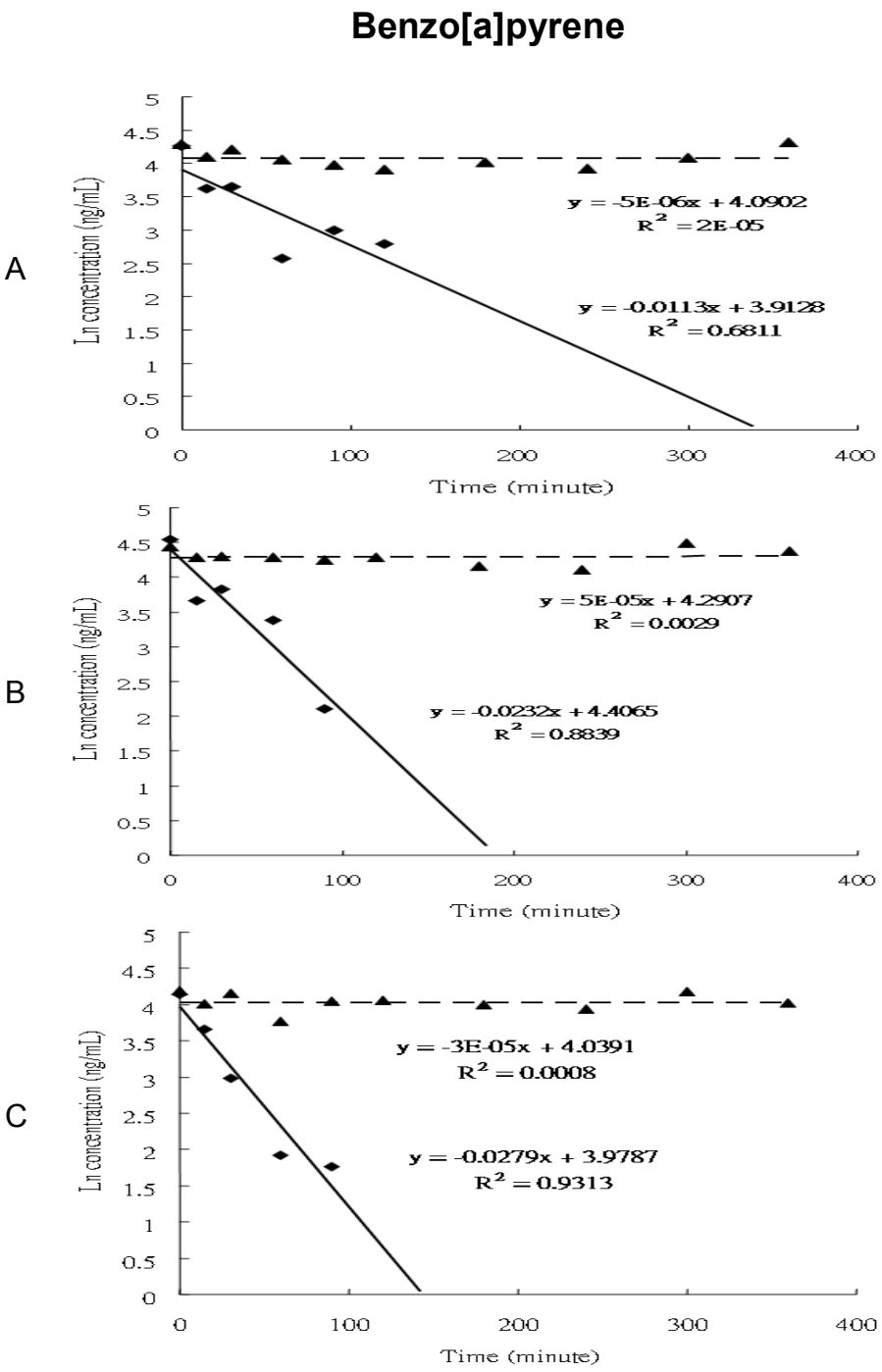

Figure 14. The natural logarithm of benzo[a]pyrene concentration in the incubation mixture as a function of the incubation time in assays using the solvent delivery method. (▲) are concentrations in inactive S9 trout liver homogenate. (♦) are concentration in active S9 trout liver homogenate. Data are collected from experimental replicate one (A), two (B), and three (C).

Chrysene

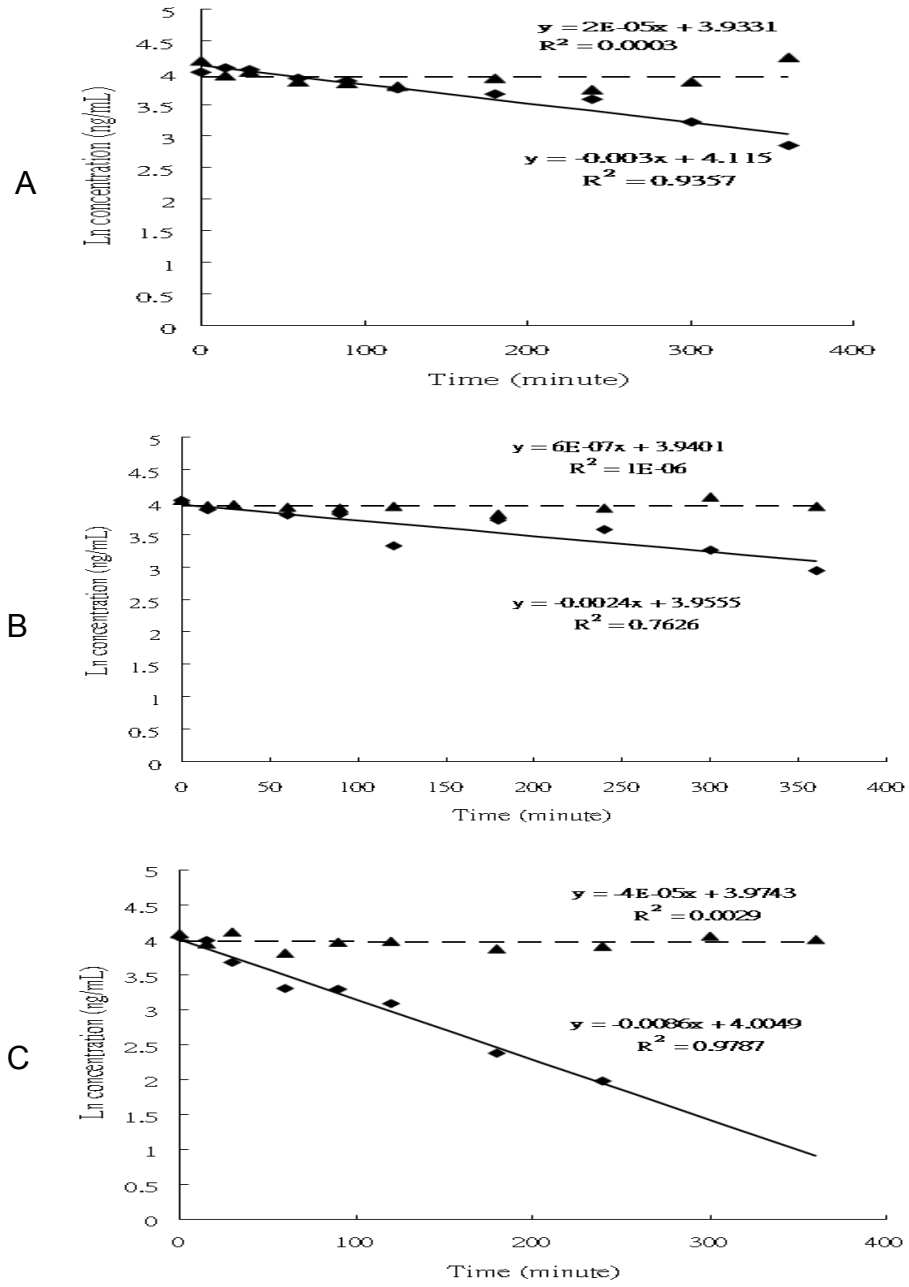

Figure 15. The natural logarithm of chrysene concentration in the incubation mixture as a function of the incubation time in assays using the solvent delivery method. (▲) are concentrations in inactive S9 trout liver homogenate. (♦) are concentration in active S9 trout liver homogenate. Data are collected from experimental replicate one (A), two (B), and three (C).

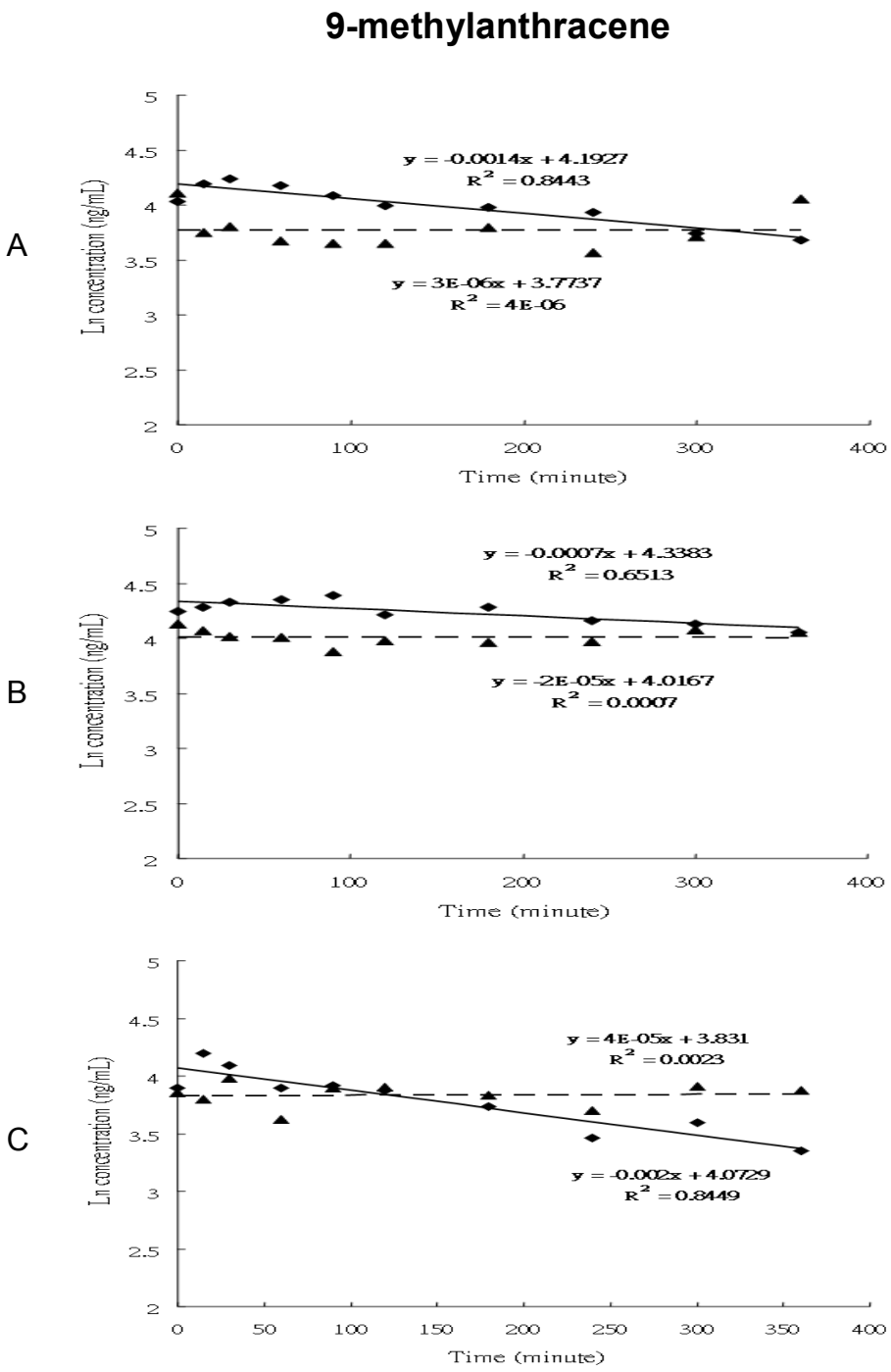

Figure 16. The natural logarithm of 9-methylanthracene concentration in the incubation mixture as a function of the incubation time in assays using the solvent delivery method. (▲) are concentrations in inactive S9 trout liver homogenate. (♦) are concentration in active S9 trout liver homogenate. Data are collected from experimental replicate one (A), two (B), and three (C).

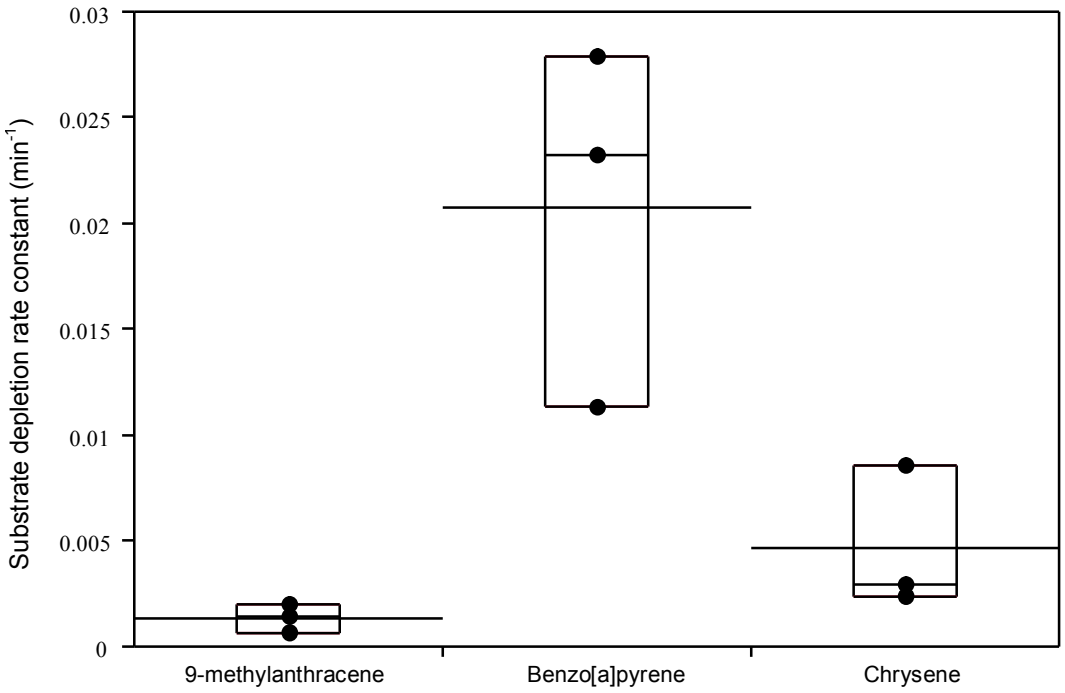

Figure 17. Box plots showing the substrate depletion rate constants (k_ds) of benzo[a]pyrene, chrysene, and 9-methylanthracene obtained in active trout liver S9 homogenate using the solvent delivery method. The ends of the box are the 25th and 75th quantiles, the line within the middle region of the box is the median, and the line across the box identifies the mean value. Welch ANOVA (p = 0.08) revealed the mean k_ds of the three test chemicals were not significantly different from one another at the 95% confidence level.

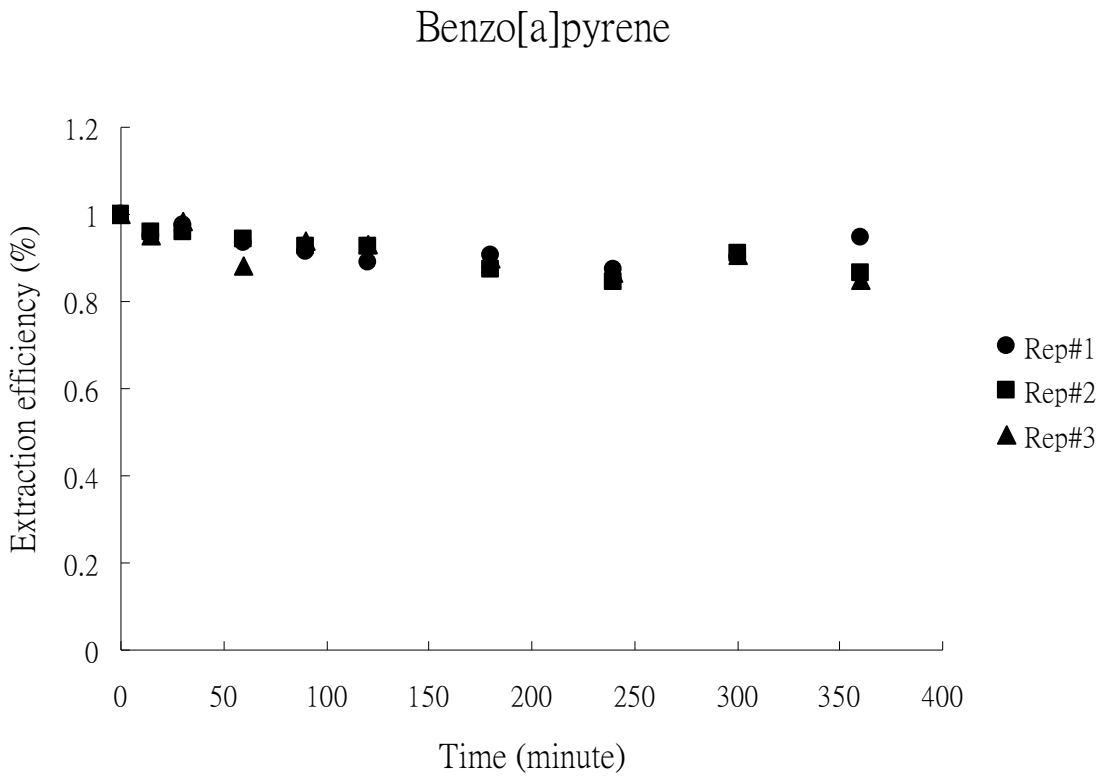

Figure 18. Extraction efficiencies of benzo[a]pyrene from heat-denatured S9 liver homogenates as a function of the incubation time.

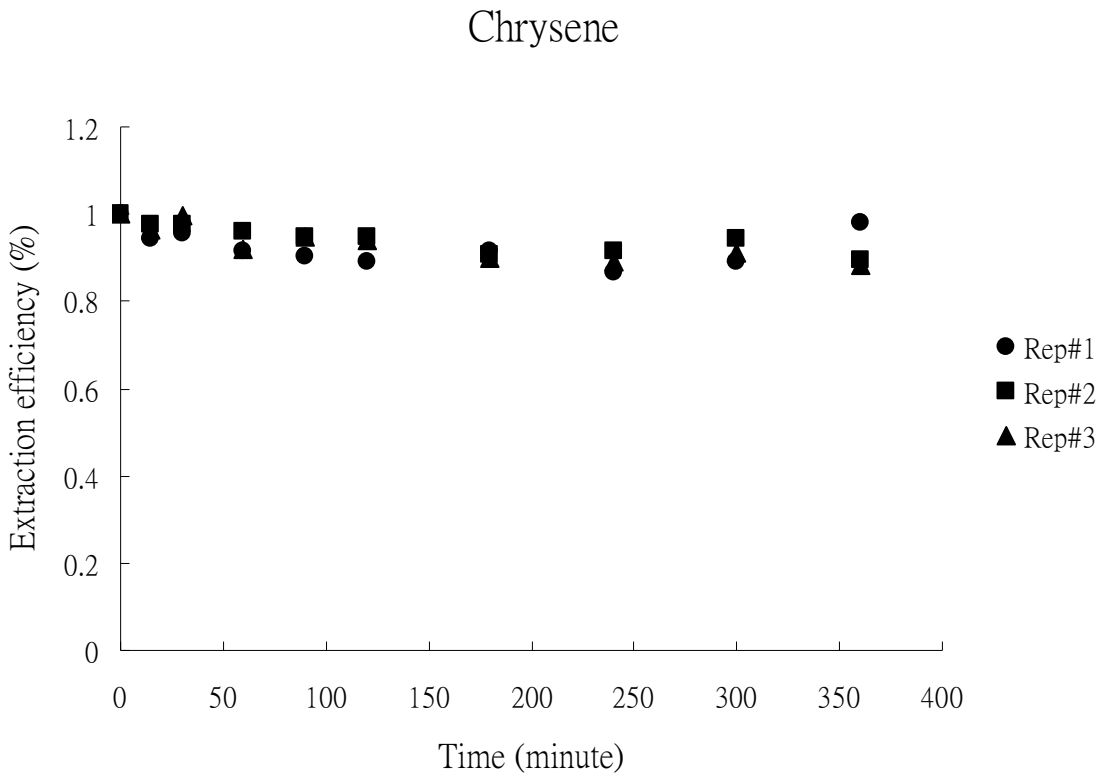

Figure 19. Extraction efficiencies of chrysene from heat-denatured S9 liver homogenates as a function of the incubation time.

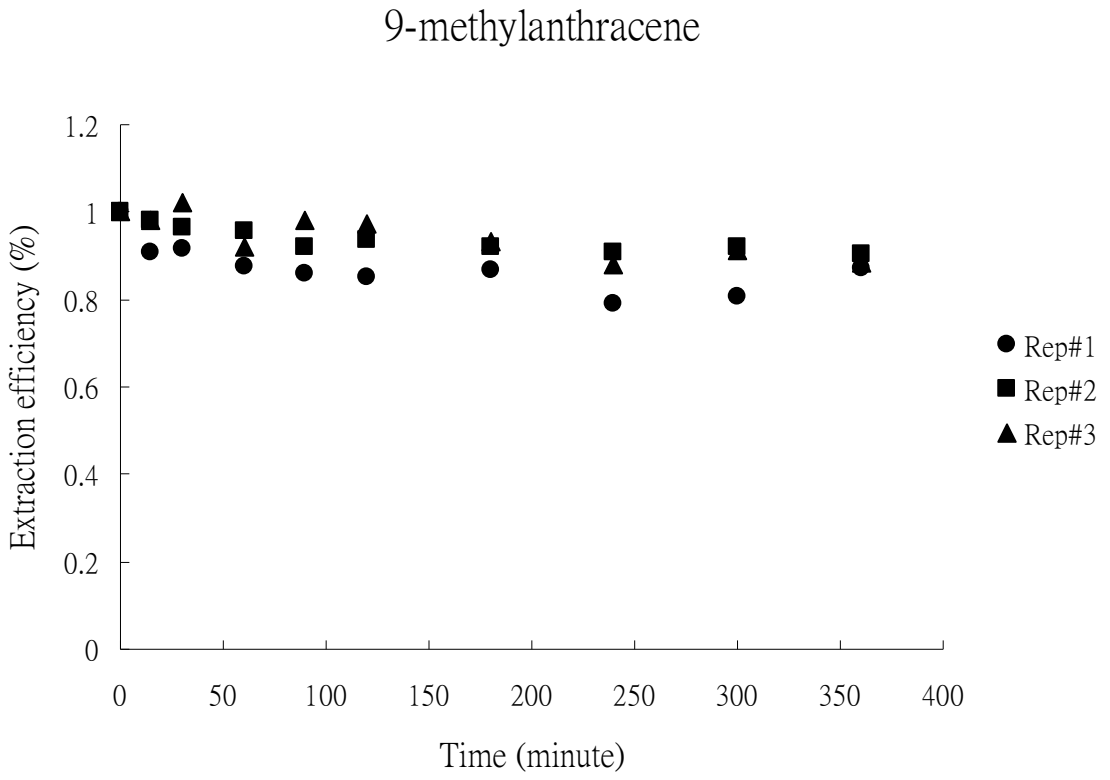

Figure 20. Extraction efficiencies of 9-methylanthracene from heat-denatured S9 liver homogenates as a function of the incubation time.

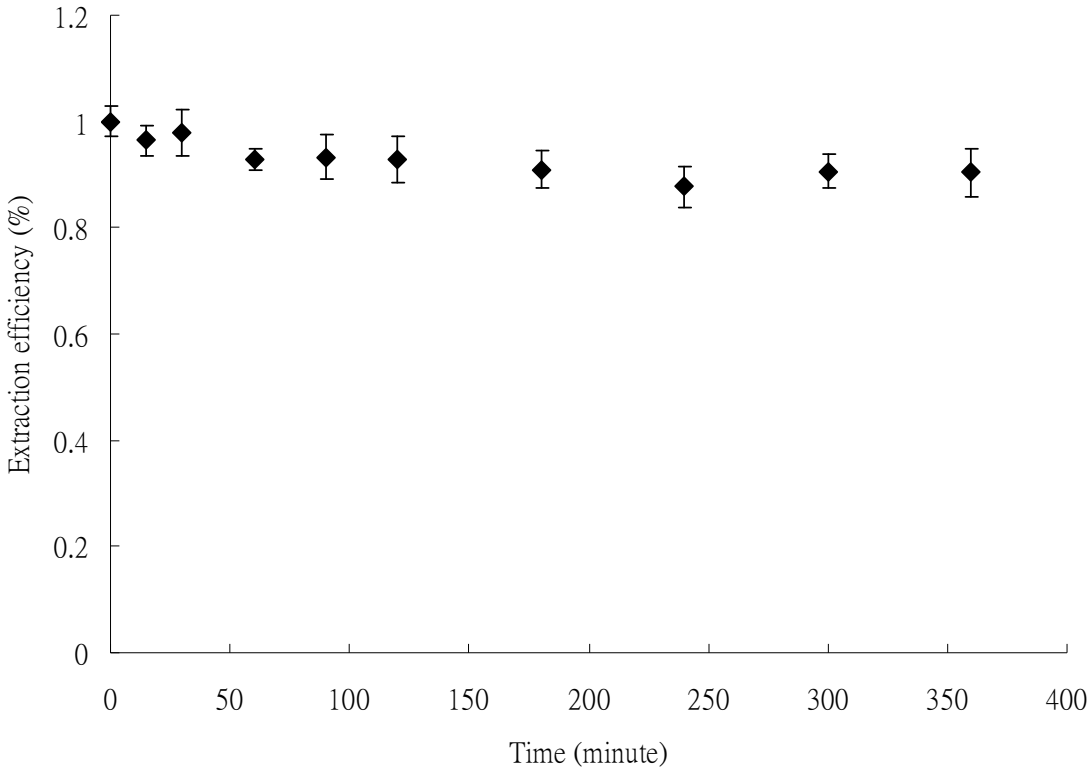

Figure 21. Combined extraction efficiencies and standard deviations (n = 9) of benzo[a]pyrene, chrysene, and 9-methylanthracene from heat-denatured S9 liver homogenates as a function of the incubation time.

Benzo[a]pyrene (EVA phase - no-cofactor control)

A

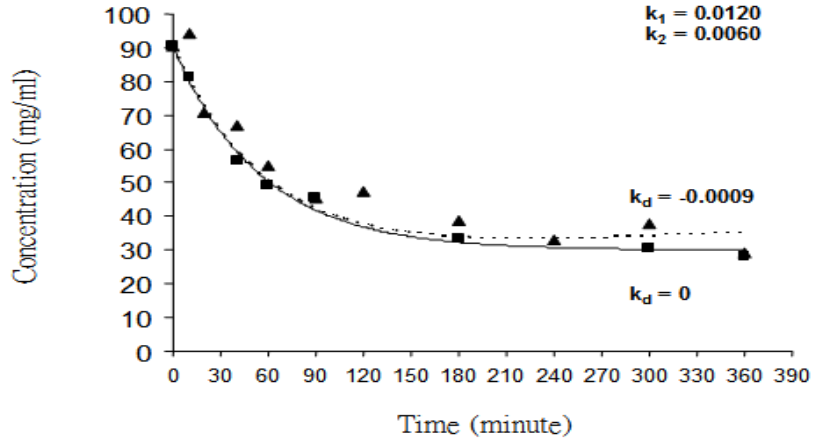

B

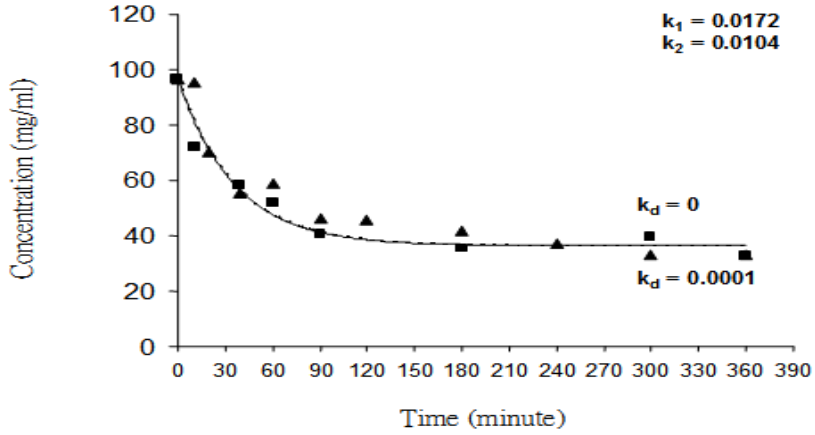

C

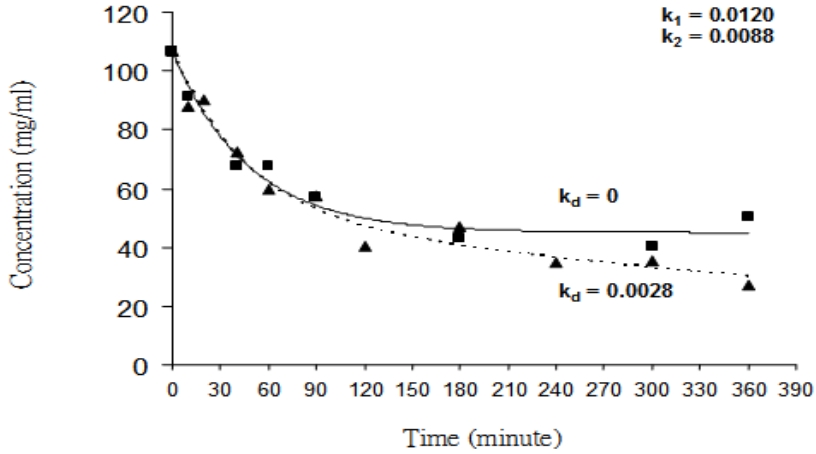

Figure 22. Concentration of benzo[a]pyrene in EVA in the test (i.e. active S9 liver homogenate) and in the no-cofactor control throughout the incubation period. (■) are concentrations in no-cofactor S9 liver homogenate. (▲) are concentrations in active S9 trout liver homogenate. Solid lines (—) and dotted lines (…) are chemical dynamics simulation curves for the control and test, respectively. Data are collected from replicate one (A), two (B), and three (C).

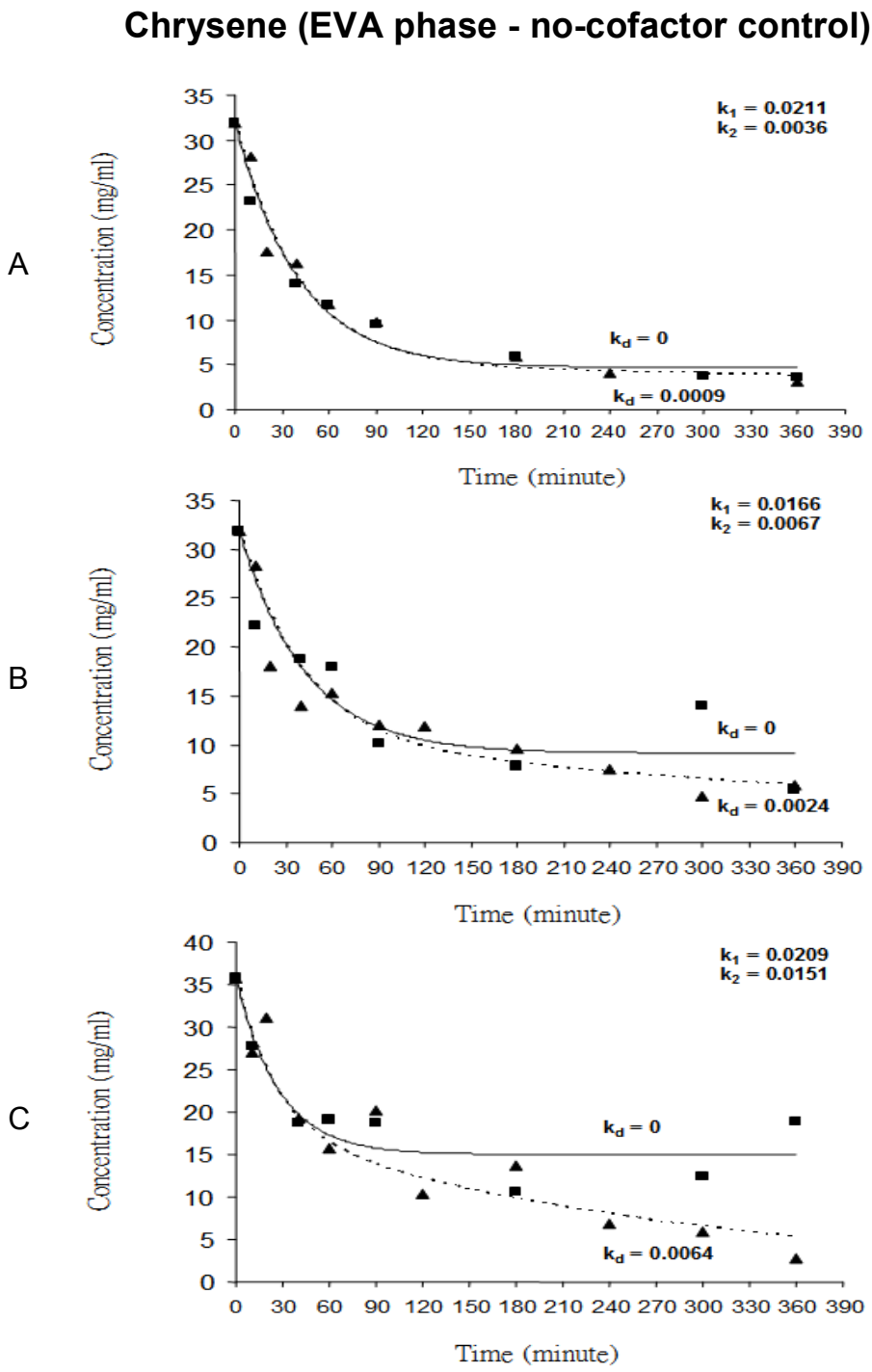

Figure 23. Concentration of chrysene in EVA in the test (i.e. active S9 liver homogenate) and in the no-cofactor control throughout the incubation period. (■) are concentrations in no-cofactor S9 liver homogenate. (▲) are concentrations in active S9 trout liver homogenate. Solid lines (—) and dotted lines (…) are chemical dynamics simulation curves for the control and test, respectively. Data are collected from replicate one (A), two (B), and three (C).

9-methylanthracene (EVA phase - no-cofactor control)

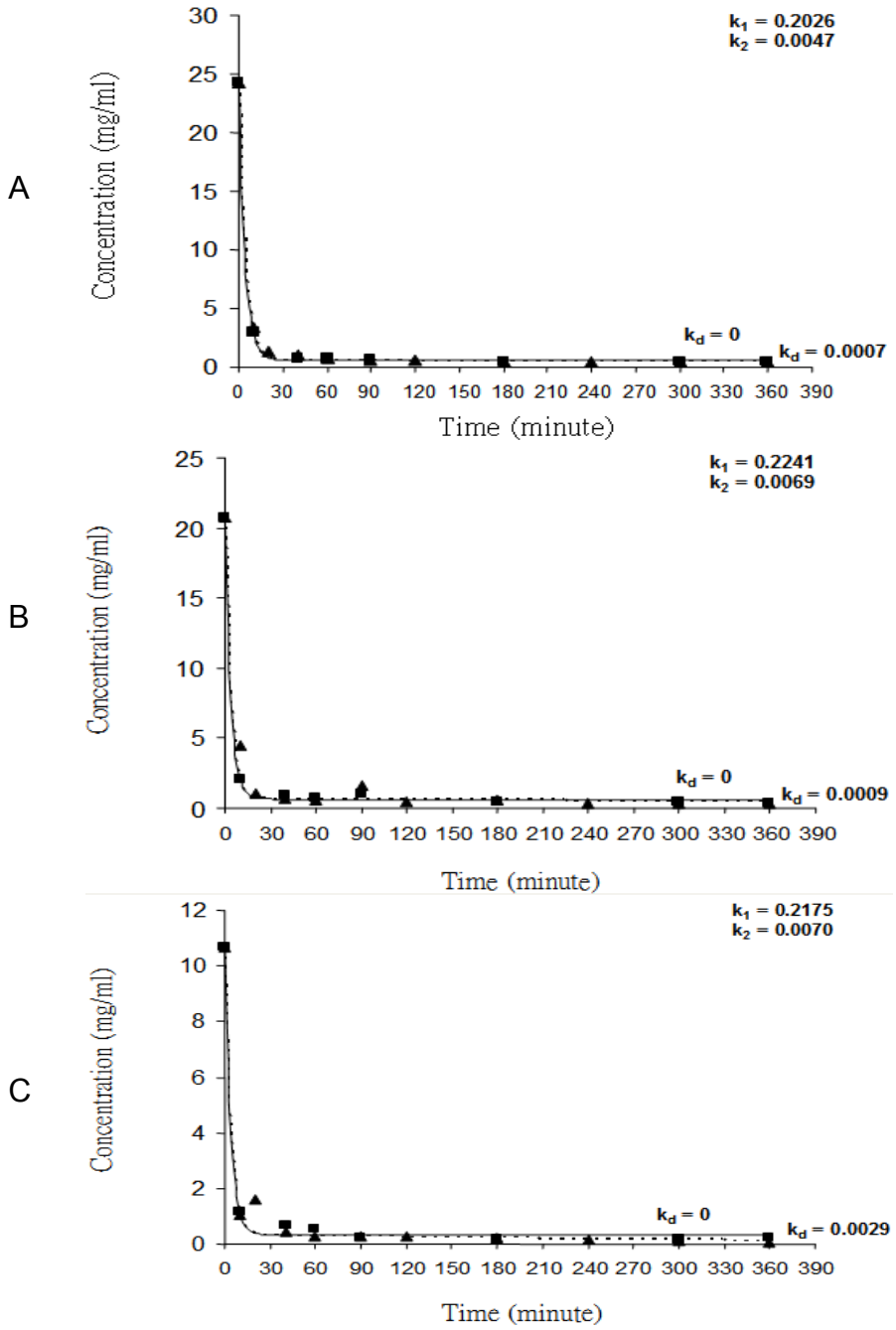

Figure 24. Concentration of 9-methylanthracene in EVA in the test (i.e. active S9 liver homogenate) and in the no-cofactor control throughout the incubation period. (■) are concentrations in no-cofactor S9 liver homogenate. (▲) are concentrations in active S9 trout liver homogenate. Solid lines (—) and dotted lines (…) are chemical dynamics simulation curves for the control and test, respectively. Data are collected from replicate one (A), two (B), and three (C).

Benzo[a]pyrene (medium phase - no-cofactor control)

A

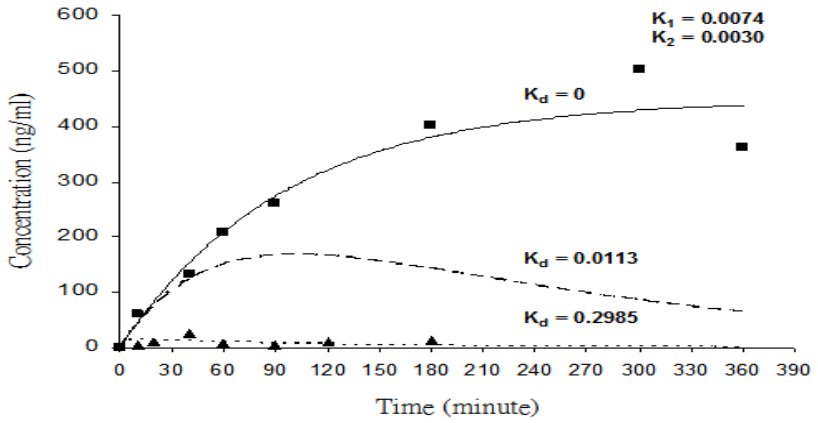

B

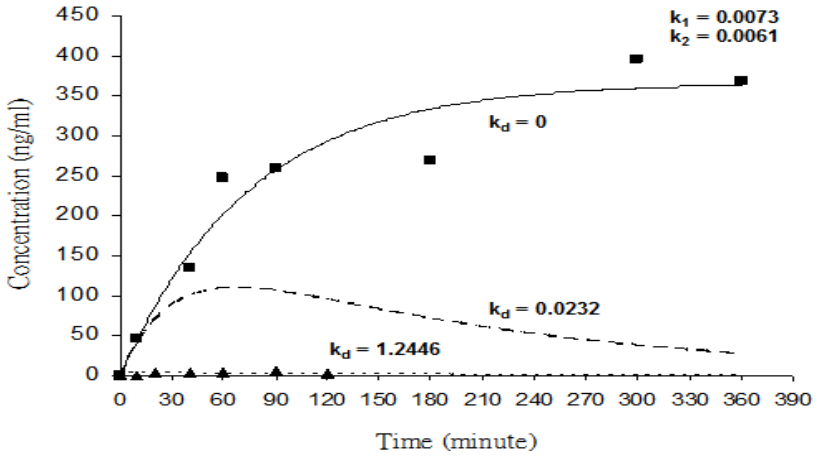

C

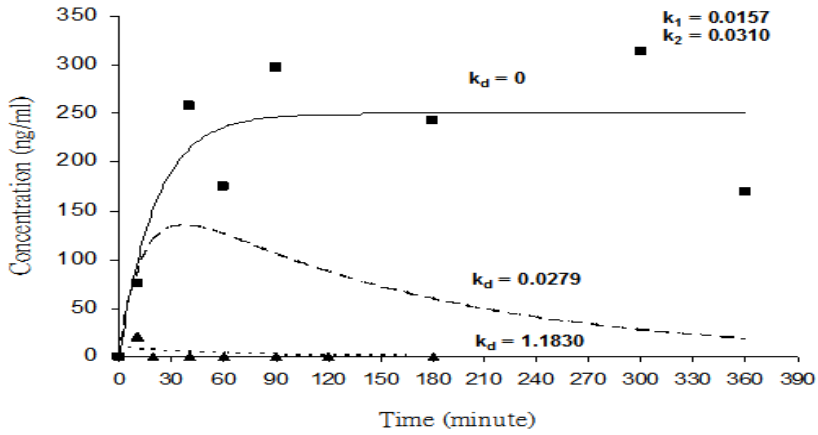

Figure 25. Concentration of benzo[a]pyrene in medium in the test (i.e. active S9 liver homogenate) and in the no-cofactor control throughout the incubation period. (■) are concentrations in no-cofactor S9 liver homogenate. (▲) are concentrations in active S9 trout liver homogenate. Solid lines (—) and dotted lines (…) are chemical dynamics simulation curves for the control and test, respectively. Dashed lines (---) are chemical dynamics simulation curves constructed using the substrate depletion rate constant, k_d, determined in the solvent delivery method. Data are collected from replicate one (A), two (B), and three (C).

Chrysene (medium phase - no-cofactor control)

A

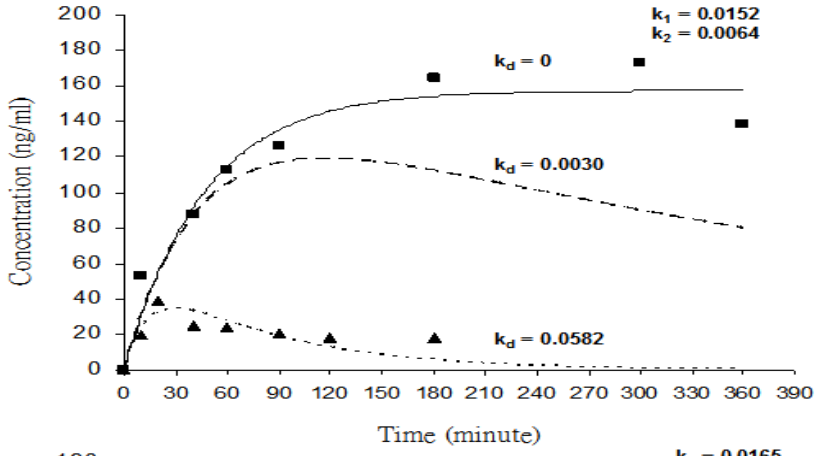

B

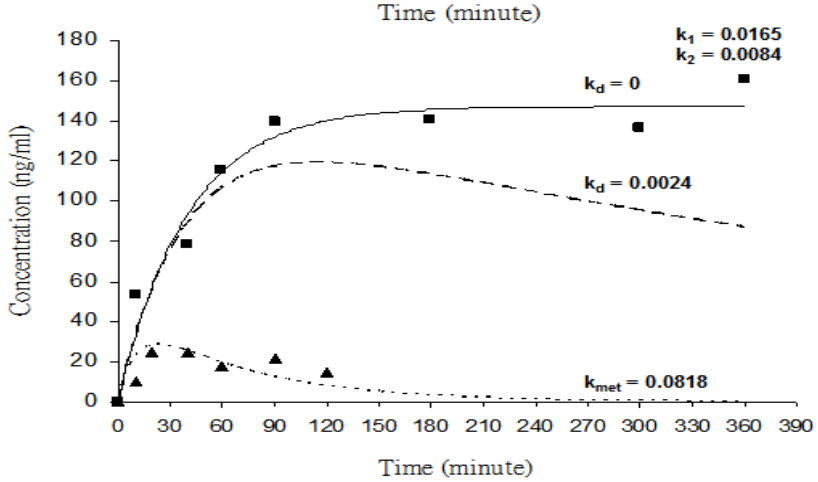

C

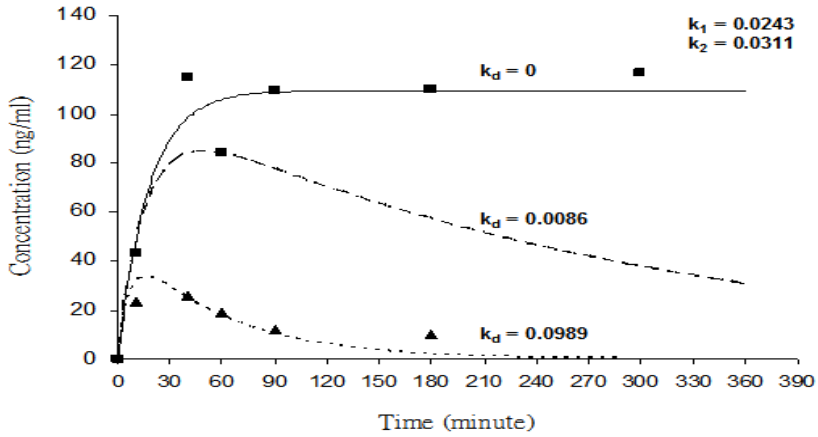

Figure 26. Concentration of chrysene in medium in the test (i.e. active S9 liver homogenate) and in the no-cofactor control throughout the incubation period. (■) are concentrations in no-cofactor S9 liver homogenate. (▲) are concentrations in active S9 trout liver homogenate. Solid lines (—) and dotted lines (…) are chemical dynamics simulation curves for the control and test, respectively. Dashed lines (---) are chemical dynamics simulation curves constructed using the substrate depletion rate constant, k_d, determined in the solvent delivery method. Data are collected from replicate one (A), two (B), and three (C).

9-methylanthracene (medium phase - no-cofactor control)

A

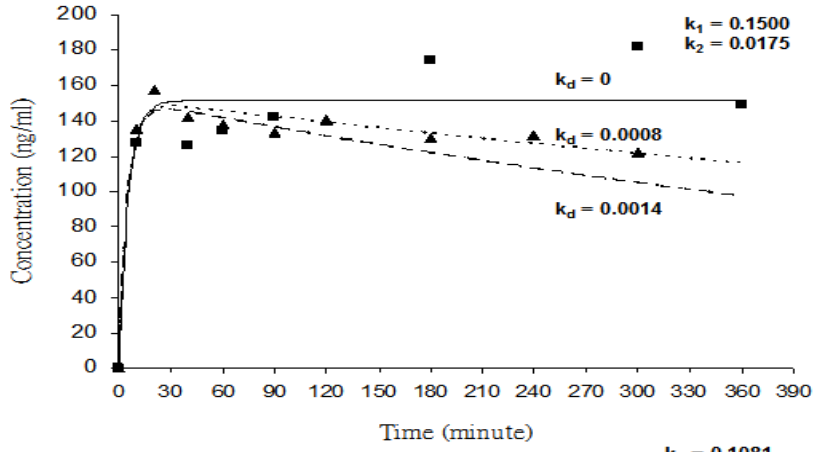

B

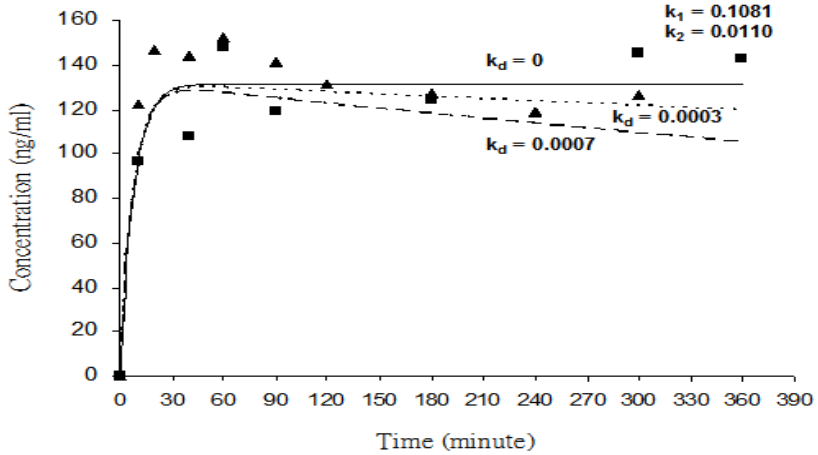

C

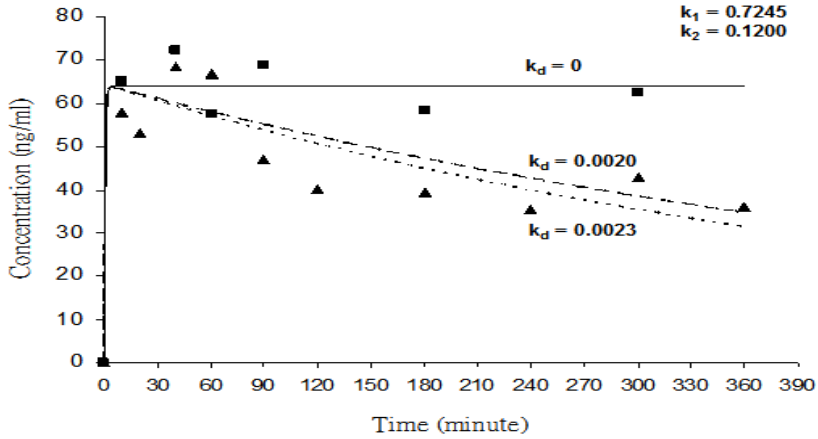

Figure 27. Concentration of 9-methylanthracene in medium in the test (i.e. active S9 liver homogenate) and in the no-cofactor control throughout the incubation period. (■) are concentrations in no-cofactor S9 liver homogenate. (▲) are concentrations in active S9 trout liver homogenate. Solid lines (—) and dotted lines (…) are chemical dynamics simulation curves for the control and test, respectively. Dashed lines (---) are chemical dynamics simulation curves constructed using the substrate depletion rate constant, k_d, determined in the solvent delivery method. Data are collected from replicate one (A), two (B), and three (C).

Benzo[a]pyrene (EVA and medium phase – heat-denatured control)

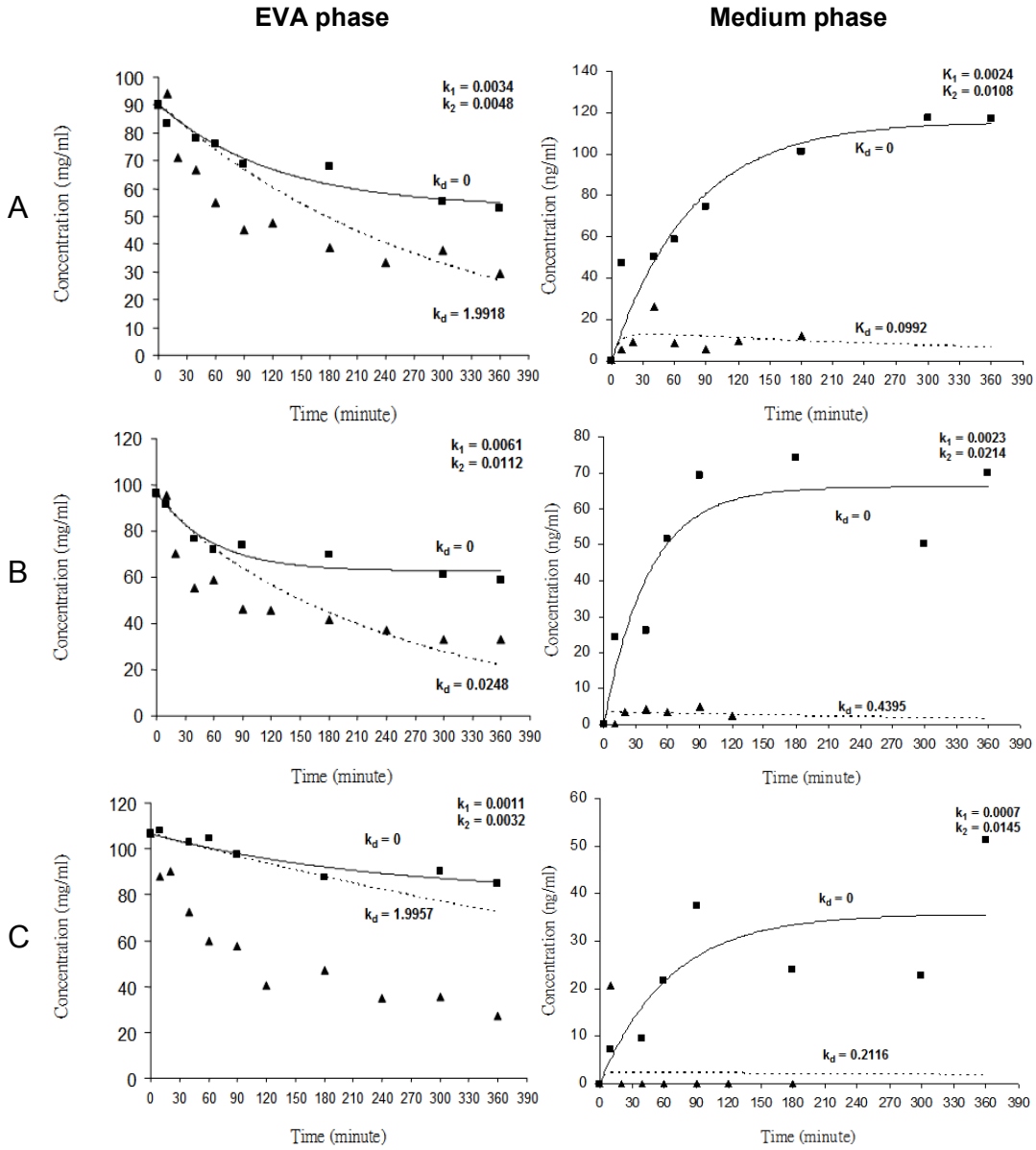

Figure 28. Concentration of benzo[a]pyrene in EVA and medium in the test (i.e. active S9 liver homogenate) and in the heat-denatured control throughout the incubation period. (■) are concentrations in heat-denatured S9 liver homogenate. (▲) are concentrations in active S9 trout liver homogenate. Solid lines (—) and dotted lines (…) are chemical dynamics simulation curves for the control and test, respective Data are collected from replicate one (A), two (B), and three (C).

Chrysene (EVA and medium phase – heat-denatured control)

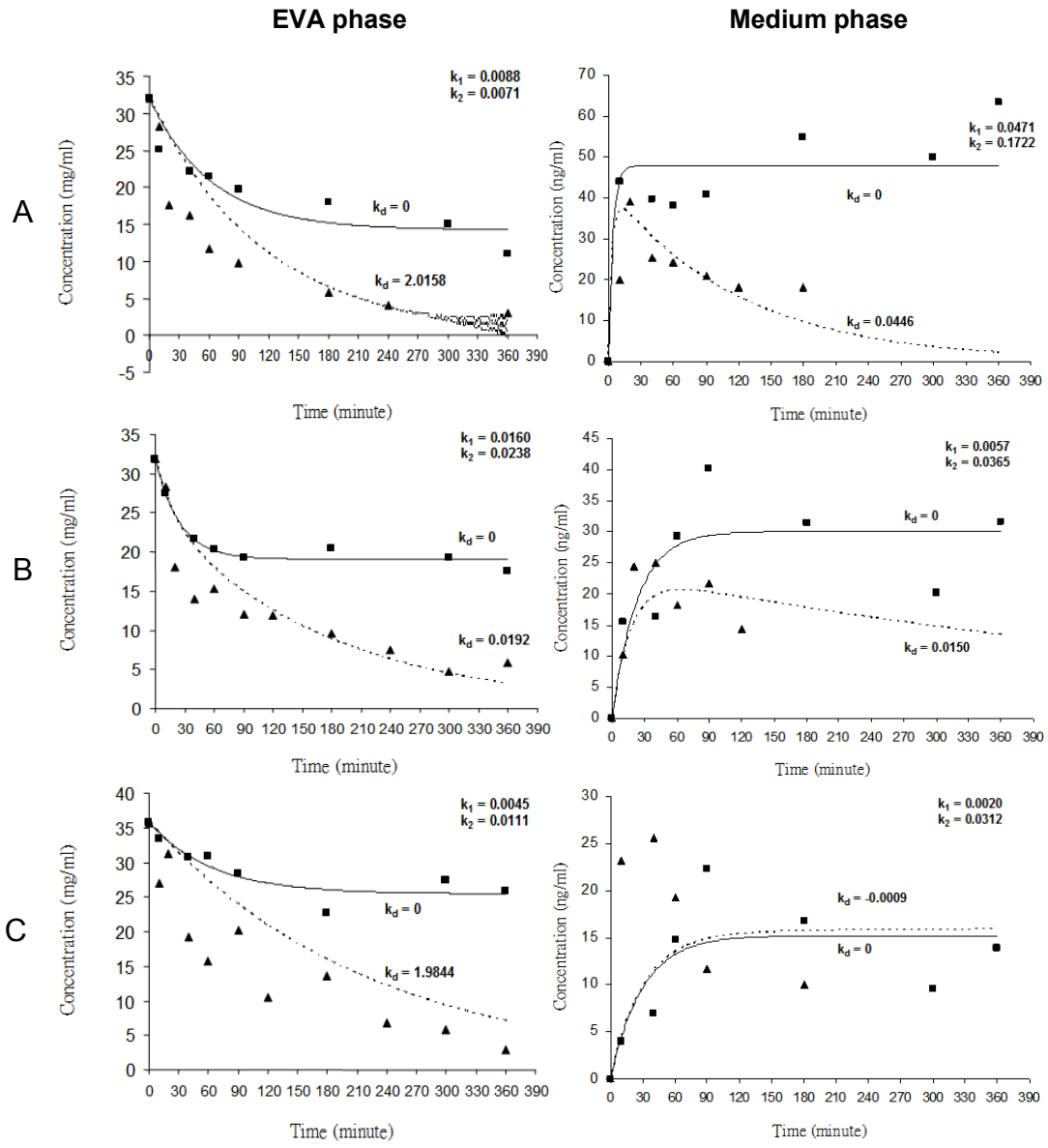

Figure 29. Concentration of chrysene in EVA and medium in the test (i.e. active S9 liver homogenate) and in the heat-denatured control throughout the incubation period. (■) are concentrations in heat-denatured S9 liver homogenate. (▲) are concentrations in active S9 trout liver homogenate. Solid lines (—) and dotted lines (…) are chemical dynamics simulation curves for the control and test, respective Data are collected from replicate one (A), two (B), and three (C).

9-methylanthracene (EVA and medium phase – heat-denatured control)

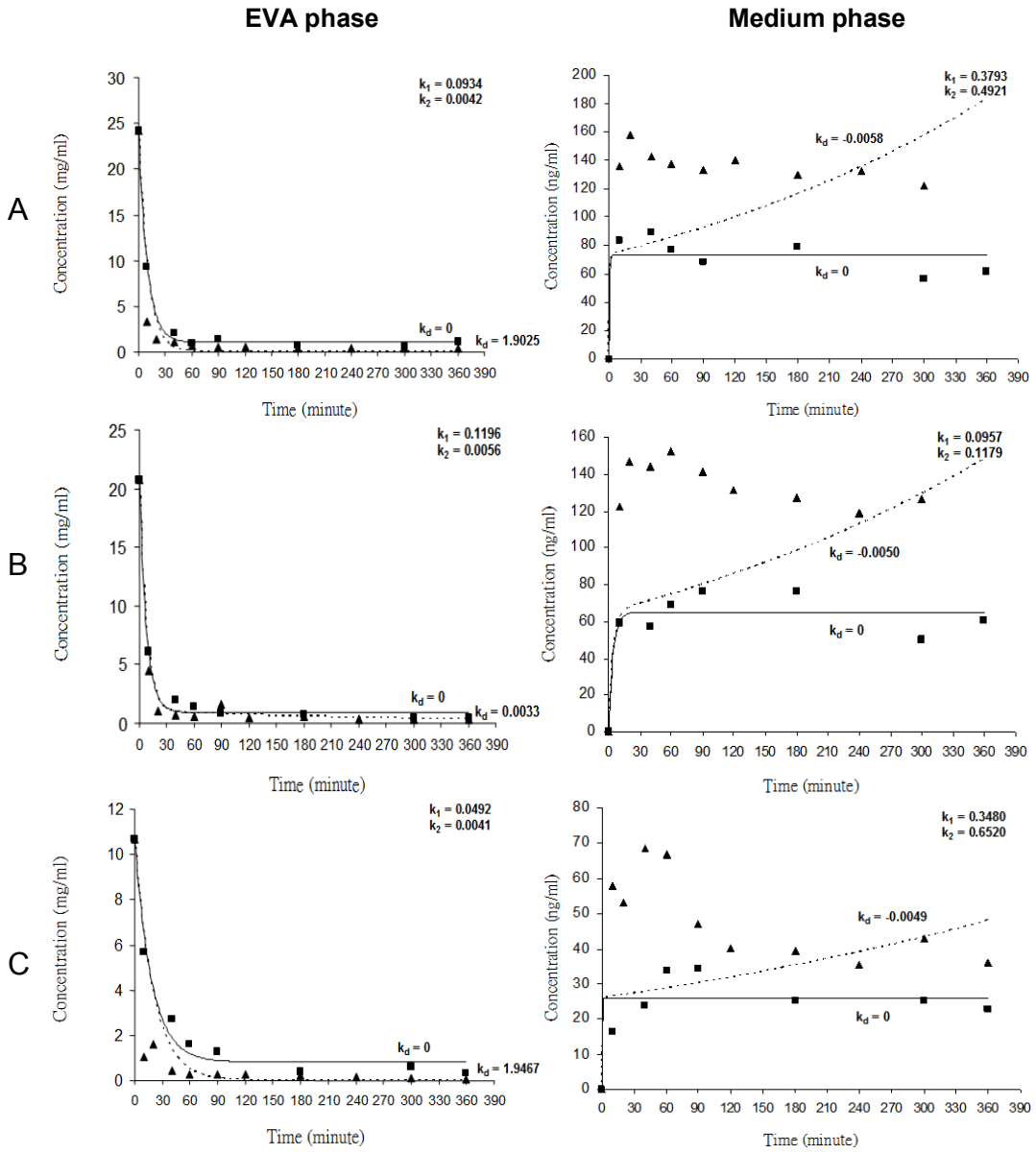

Figure 30. Concentration of 9-methylanthracene in EVA and medium in the test (i.e. active S9 liver homogenate) and in the heat-denatured control throughout the incubation period. (■) are concentrations in heat-denatured S9 liver homogenate. (▲) are concentrations in active S9 trout liver homogenate. Solid lines (—) and dotted lines (…) are chemical dynamics simulation curves for the control and test, respective Data are collected from replicate one (A), two (B), and three (C).

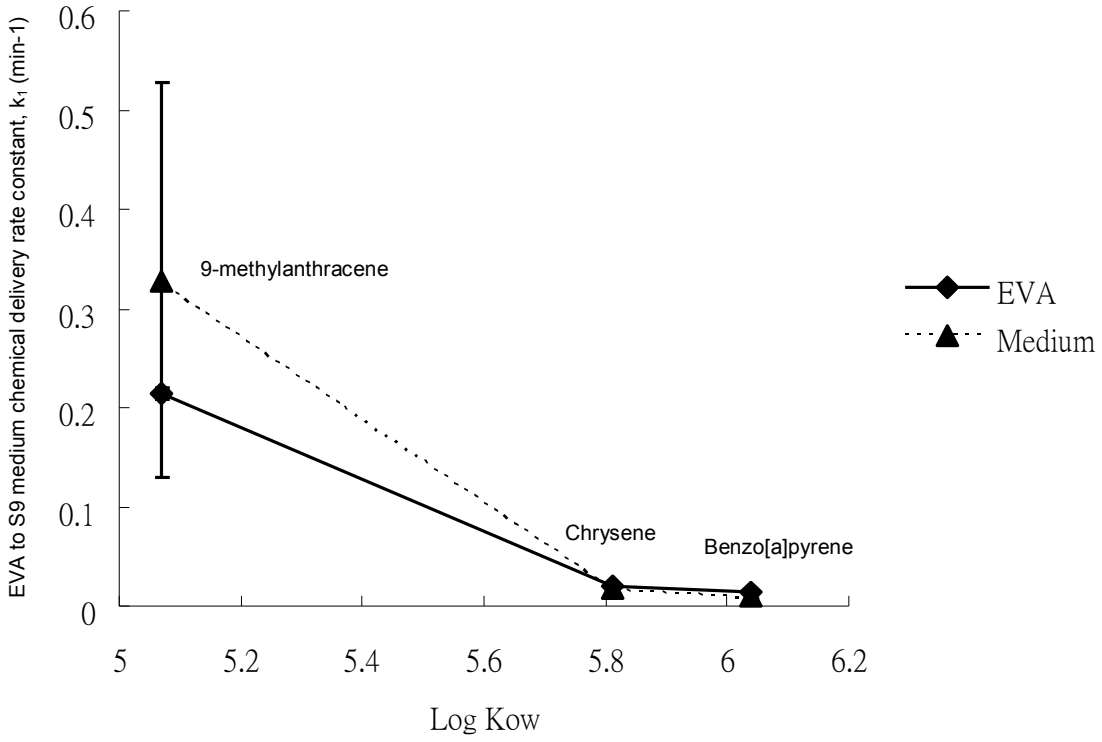

Figure 31. The mean ethylene vinyl acetate (EVA) to trout S9 medium chemical delivery rate constants, k_1 (± standard error), of the three test chemicals as a function of log K_{ow} in the EVA dosing experiments.

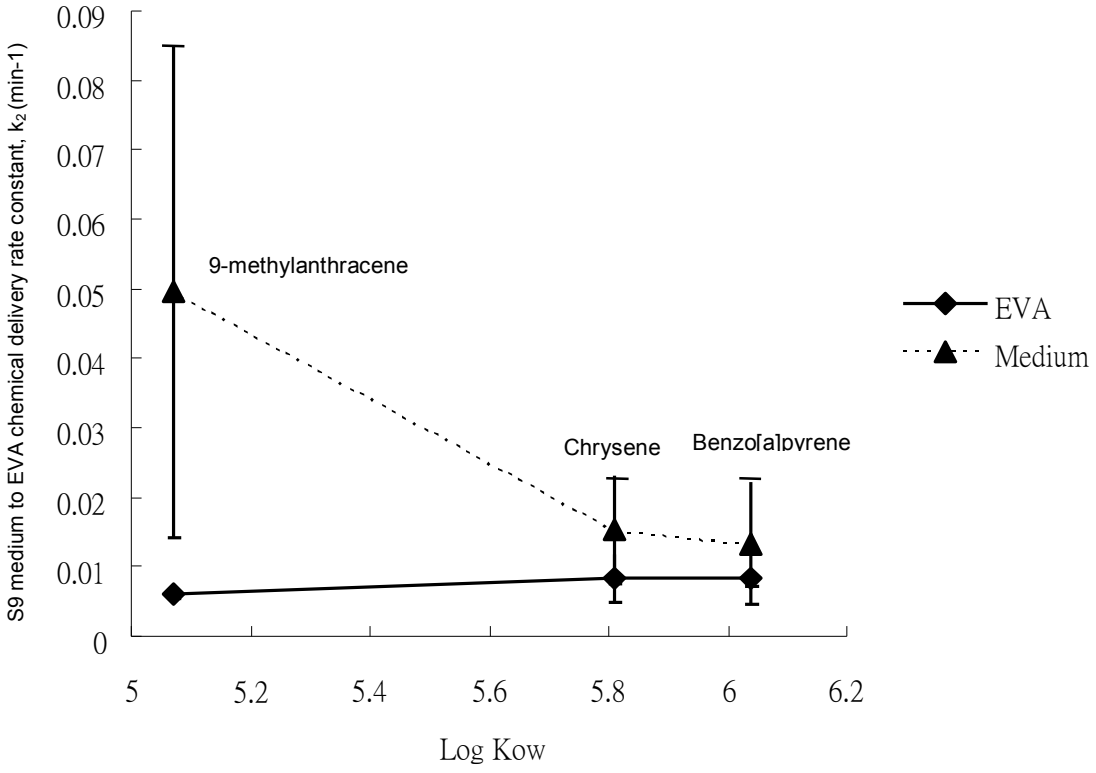

Figure 32. The mean trout S9 medium to ethylene vinyl acetate (EVA) chemical delivery rate constants, k_2 (± standard error), of the three test chemicals as a function of log K_{ow} in the EVA dosing experiments.

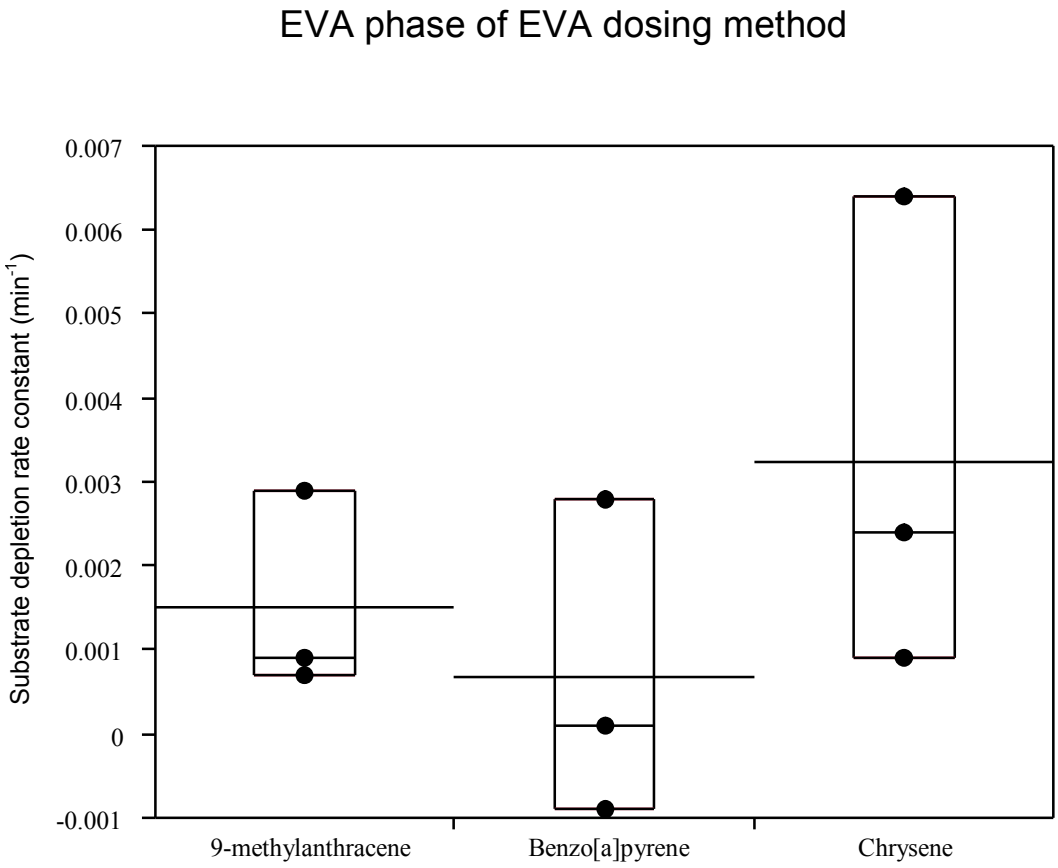

Figure 33. Box plots of the measured substrate depletion rate constants (k_ds) of benzo[a]pyrene, chrysene, and 9-methylanthracene derived from concentration in the EVA phase of a trout liver S9 incubation. The ends of the box are the 25th and 75th quantiles, the line within the middle region of the box is the median, and the line across the box identifies the mean value. ANOVA (p = 0.37) revealed the mean k_ds of the three test chemicals were not significantly different from one another.

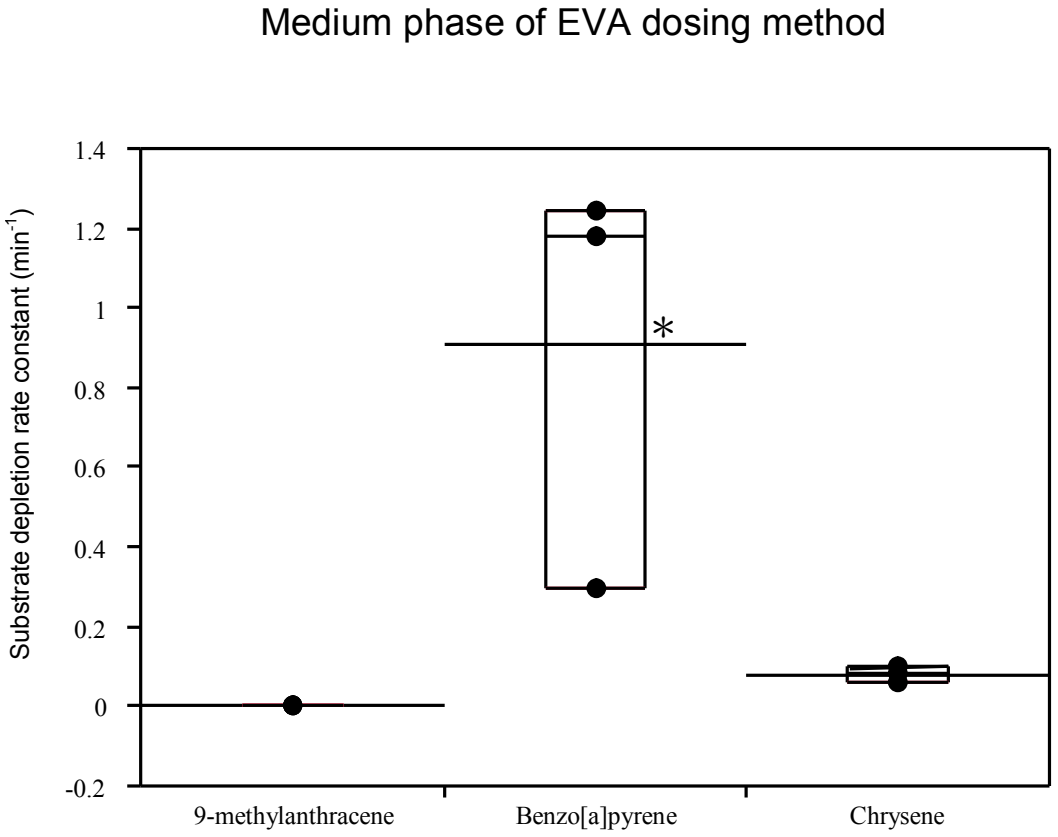

Figure 34. Box plots of the measured substrate depletion rate constants (k_ds) of benzo[a]pyrene, chrysene, and 9-methylanthracene derived from concentration in the medium phase of a trout liver S9 incubation. The ends of the box are the 25th and 75th quantiles, the line within the middle region of the box is the median, and the line across the box identifies the mean value. Welch ANOVA ($p = 0.023$) and Tukey's test ($p < 0.05$) revealed the mean k_d of benzo[a]pyrene was significantly different (*) from the other two chemicals.

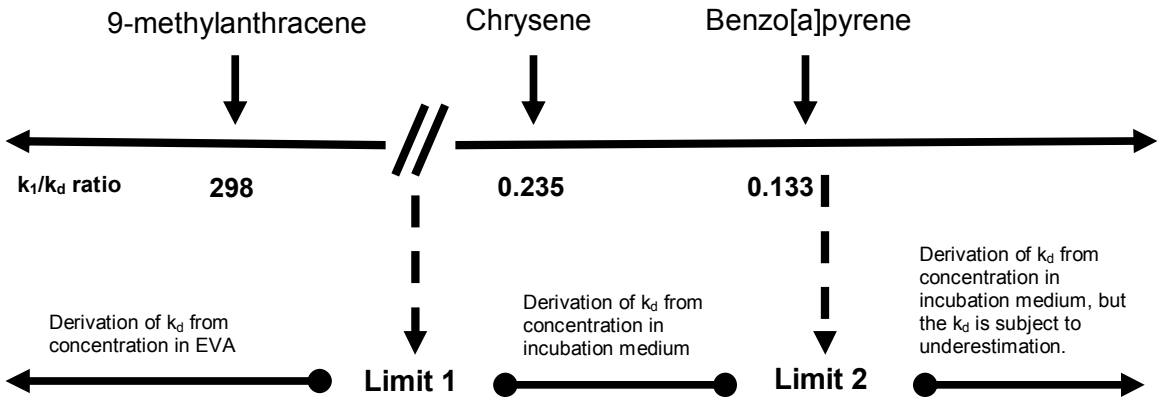

Figure 35. A conceptual diagram displaying the role of the ratio of EVA to incubation medium chemical delivery rate constant (min^{-1}) and substrate depletion rate constant (min^{-1}) of test chemical on the ability of measurements of concentration in the EVA or the incubation medium to determine substrate depletion rates.

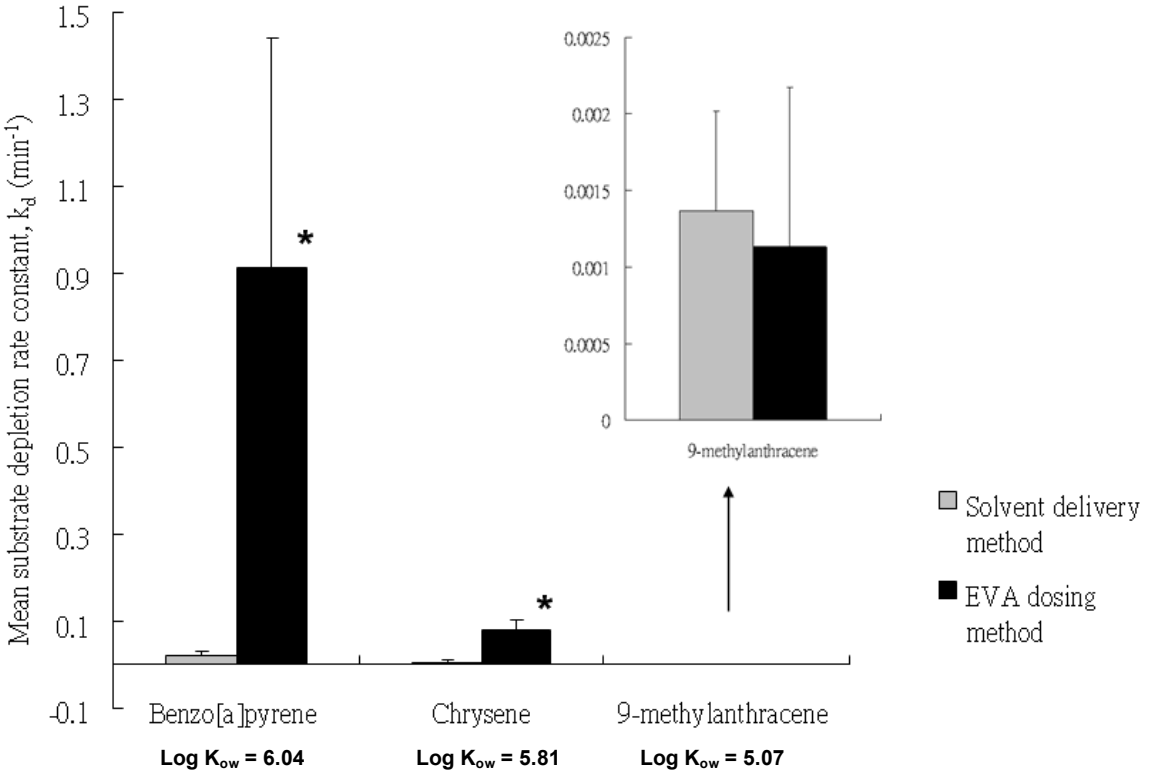

Figure 36. Mean substrate depletion rate constants, k_ds, of benzo[a]pyrene, chrysene, and 9-methylanthracene determined from the medium phase of the EVA dosing method and the solvent delivery method. Student's t-test revealed that the mean k_ds of benzo[a]pyrene (p = 0.050, α = 0.05) and chrysene (p = 0.011, α = 0.05) determined by the EVA dosing method were significantly different (*) from that by the solvent delivery method.

APPENDICES

APPENDIX A

Table 5. Numerical data showing chemical concentration-time profiles in the EVA and medium of the EVA dosing experiments. Data are collected from replicate number 1.

		Benzo[a]pyrene		Chrysene		9-methylanthracene	
	Time (min)	Conc. in **EVA** (millions ng/ml)	Conc. in **medium** (ng/ml)	Conc. in **EVA** (millions ng/ml)	Conc. in **medium** (ng/ml)	Conc. in **EVA** (millions ng/ml)	Conc. in **medium** (ng/ml)
	0 rep #1	88.38	0	31.33	0	23.87	0
	0 rep #2	92.17	0	32.62	0	24.65	0
	Average	90.27	0	31.97	0	24.26	0
Active liver S9	**10**	94.13	5.25	28.18	0.00	3.35	135.50
	20	70.99	8.88	17.57	19.99	1.39	158.12
	40	66.86	25.76	16.23	39.03	1.05	142.35
	60	55.00	8.22	11.71	25.40	0.70	137.94
	90	45.33	5.70	9.70	24.31	0.52	133.70
	120	47.60	9.70	12.79	20.87	0.57	140.20
	180	38.79	12.18	5.80	18.05	0.39	130.08
	240	33.25	⁄	4.07	⁄	0.43	132.11
	300	37.98	⁄	6.57	⁄	0.40	122.48
	360	29.33	⁄	3.08	⁄	0.43	⁄
Heat-denatured liver S9	**10**	83.13	47.25	25.15	43.88	9.24	83.63
	40	77.70	50.49	22.15	39.78	2.11	89.23
	60	75.95	58.75	21.48	38.23	0.96	77.14

	90	68.44	74.79	19.74	41.02	1.39	68.11
	180	67.60	101.19	18.03	54.85	0.68	79.65
	300	55.46	117.55	15.02	49.99	0.51	56.60
	360	52.78	116.98	10.96	63.42	1.11	61.24
No-cofactor liver S9	**10**	81.30	60.91	23.19	53.20	2.88	127.71
	40	56.36	134.06	14.02	87.52	0.76	126.22
	60	49.30	208.26	11.73	112.16	0.71	134.68
	90	45.30	259.95	9.41	126.83	0.58	142.63
	180	33.46	400.93	5.78	164.57	0.48	174.12
	300	30.45	502.61	3.70	173.37	0.41	181.66
	360	28.05	361.51	3.51	138.39	0.40	149.19

／= data omitted due to the possibility of enzyme attenuation.

APPENDIX B

Table 6. Numerical data showing chemical concentration-time profiles in the EVA and medium of the EVA dosing experiments. Data are collected from replicate number 2.

		Benzo[a]pyrene		Chrysene		9-methylanthracene	
	Time (min)	Conc. in **EVA** (millions ng/ml)	Conc. in **medium** (ng/ml)	Conc. in **EVA** (millions ng/ml)	Conc. in **medium** (ng/ml)	Conc. in **EVA** (millions ng/ml)	Conc. in **medium** (ng/ml)
	0 rep #1	98.15	0	32.04	0	20.40	0
	0 rep #2	95.19	0	31.62	0	21.22	0
	Average	96.68	0	31.83	0	20.81	0
Active liver S9	**10**	95.35	0.00	28.34	10.34	4.48	122.45
	20	70.14	3.48	18.03	24.44	1.07	146.79
	40	55.42	4.16	13.94	25.10	0.71	144.33
	60	58.76	3.40	15.26	18.22	0.52	152.32
	90	46.50	4.93	12.03	21.65	1.58	141.34
	120	45.97	2.53	11.84	14.36	0.47	131.47
	180	41.66	⁄	9.58	⁄	0.59	127.09
	240	36.89	⁄	7.46	⁄	0.36	118.84
	300	33.24	⁄	4.79	⁄	0.39	126.76
	360	33.12	⁄	5.92	⁄	0.33	107.32
Heat-denatured liver S9	**10**	91.50	24.24	27.44	15.57	6.08	59.14
	40	76.44	26.24	21.66	16.33	1.95	57.30
	60	71.98	51.33	20.28	29.31	1.38	69.12

	90	73.90	69.27	19.25	40.14	0.79	76.22
	180	69.80	74.09	20.50	31.47	0.68	76.54
	300	61.06	49.91	19.19	20.20	0.49	50.19
	360	59.08	69.77	17.59	31.65	0.45	60.61
No-cofactor liver S9	**10**	71.84	47.67	22.13	53.24	2.08	96.56
	40	58.51	135.26	18.78	78.02	0.86	107.63
	60	52.26	246.54	17.92	115.23	0.72	148.43
	90	40.54	258.97	10.14	140.03	1.01	119.29
	180	35.26	268.13	7.84	140.53	0.42	124.77
	300	39.43	395.32	14.03	136.41	0.40	145.24
	360	32.83	368.93	5.45	160.74	0.35	142.40

／= data omitted due to the possibility of enzyme attenuation.

APPENDIX C

Table 7. Numerical data showing chemical concentration-time profiles in the EVA and medium of the EVA dosing experiments. Data are collected from replicate number 3.

		Benzo[a]pyrene		Chrysene		9-methylanthracene	
	Time (min)	Conc. in **EVA** (millions ng/ml)	Conc. in **medium** (ng/ml)	Conc. in **EVA** (millions ng/ml)	Conc. in **medium** (ng/ml)	Conc. in **EVA** (millions ng/ml)	Conc. in **medium** (ng/ml)
	0 rep #1	110.73	0	35.75	0	10.77	0
	0 rep #2	102.32	0	35.85	0	10.63	0
	Average	106.56	0	35.80	0	10.70	0
Active liver S9	**10**	88.19	20.75	26.97	23.17	1.07	58.01
	20	90.08	0.00	31.17	5.69	1.62	53.04
	40	72.25	0.00	19.27	25.67	0.45	68.38
	60	59.54	0.00	15.67	19.26	0.29	66.62
	90	57.68	0.00	20.12	11.77	0.29	46.93
	120	40.13	0.00	10.44	⁄	0.25	40.19
	180	46.77	0.00	13.67	9.99	0.21	39.41
	240	35.01	⁄	6.89	⁄	0.15	35.44
	300	35.32	⁄	5.87	⁄	0.09	42.95
	360	27.25	⁄	2.85	⁄	0.07	36.25
Heat-denatured liver S9	**10**	107.88	7.31	33.47	4.05	5.72	16.34
	40	102.84	9.59	30.77	6.96	2.71	23.94
	60	104.31	21.71	30.81	14.83	1.62	33.84

	90	97.22	37.42	28.42	22.33	1.28	34.29
	180	87.58	24.16	22.70	16.73	0.41	25.34
	300	90.37	22.87	27.42	9.51	0.58	25.12
	360	84.35	51.26	25.82	13.87	0.33	22.93
No-cofactor liver S9	**10**	91.37	75.35	27.80	43.05	1.15	64.94
	40	67.28	258.63	18.78	115.00	0.68	72.19
	60	67.23	175.16	19.07	83.83	0.54	57.55
	90	56.76	297.34	18.77	109.31	0.24	68.87
	180	43.37	243.56	10.53	109.92	0.17	58.29
	300	40.25	314.04	12.46	116.77	0.19	62.36
	360	50.35	168.38	18.88	59.01	0.20	48.93

／= data omitted due to the possibility of enzyme attenuation.

REFERENCE LIST

Arnot J. A., and Gobas F. A. P. C.. 2003. A generic QSAR for assessing the bioaccumulation potential of organic chemicals in aquatic food webs. QSAR & Combinatorial Science **22**: 337-345.

Arnot J. A., and Gobas F. A. P. C.. 2004. A food web bioaccumulation model for organic chemicals in aquatic ecosystems. Environmental Toxicology and Chemistry **23**: 2316-2313

Arnot J. A., and Gobas F. A. P. C.. 2006. A review of bioconcentration factor (BCF) and bioaccumulation factor (BAF) assessments for organic chemicals in aquatic organisms. Environmental Reviews **14**: 257-297.

Bradford M. M.. 1976. A rapid and sensitive method for the quantitation of microgram quantities of protein utilizing the principle of protein-dye binding. Analytical Biochemistry **72**: 248-254.

Brandon E. F. A., Raap C. D., Meijerman I., Beijnen J. H., and Schellens J. H. M.. 2003. An update on *in vitro* test models in human hepatic drug biotransformation research: pros and cons. Toxicology and Applied Pharmacology **189**: 233-246.

Carpenter H. M., Fredrickson L. S., Williams D. E., Ruhler D. R., and Curtis L. R.. 1990. The effect of thermal acclimation on the activity of arylhydrocarbon hydroxylase in rainbow trout (*Oncorhynchus mykiss*). Comparative Biochemistry and Physiology **97C**: 127-132.

Dyer S. D., Bernhard M. J., and Cowan-Ellsberry C. E.. 2006. Determination of *In Vitro* Biotransformation of C16 Primary Amine in Fish Hepatocyte Suspension. Report to ERASM, pp. 23. Available from http://www.erasm.eu/Study/C16N-FINAL_REPORT-061205.pdf.

Ekins S., Ring B. J., Grace J., McRobie-Belle D. J., and Wrighton S. A.. 2000. Present and future *in vitro* approaches for drug metabolism. Journal of Pharmacological and Toxicological Methods **44**: 313-324.

Environment Canada. 2006. Preliminary Categorization Decisions for Organic Chemicals on the Canadian Domestic Substance List (CD-ROM). Ottawa, Ont., Canada. Existing Substances Program, Environment Canada.

European Commission. 2001. Strategy for a future chemicals policy. White Paper. European Commission, Brussels, BE. pp. 32.

Fitzsimmons P. N., Lien G. J., and Nichols J. W.. 2007. A compilation of *in vitro* rate and affinity values for xenobiotic biotransformation in fish, measured under

physiological conditions. Comparative Biochemistry and Physiology **145**: 485-506.

Giesy J. P., and Kannan K.. 2001. Global distribution of perfluorooctane sulfonate in wildlife. Environmental Science and Technology **35**: 1339-1342.

Golding C. J., Gobas F. A. P. C., and Birch G. F.. 2007. Characterization of polycyclic aromatic hydrocarbon bioavailability in estuarine sediments using thin-film extraction. Environmental Toxicology and Chemistry **26**: 829-836.

Gourley M. E., and Kennedy C. J.. 2009. Energy allocations to xenobiotic transport and biotransformation reactions in rainbow trout (*Oncorhynchus mykiss*) during energy intake restriction. Comparative Biochemistry and Physiology – Toxicology and Pharmacology **150**: 270-278.

Government of Canada. 1999. Canadian Environmental Protection Act, 1999. Canada Gazette Part III. 22. Public Works and Government Services, Canada, Ottawa, Ont., Canada. pp. 249.

Han X., Nabb D. L., Mingoia R. T., and Yang C. H.. 2007. Determination of xenobiotic intrinsic clearance in freshly isolated hepatocytes from rainbow trout (*Oncorhynchus mykiss*) and rat and its application in bioaccumulation assessment. Environmental Science and Technology **41**: 3269-3276.

Han X., Nabb D. L., Yang C. H., Snajdr S. I., and Mingoia R. T.. 2009. Liver microsomes and S9 from rainbow trout (*Oncorhynchus mykiss*): Comparison of basal-level enzyme activities with rat and determination of xenobiotic intrinsic clearance in support of bioaccumulation assessment. Environmental Toxicology and Chemistry **28**: 481-488.

Hankinson O.. 1995. The aryl hydrocarbon receptor complex. Annual Reviews of Pharmacology and Toxicology **35**: 307-340.

Hodson P. V., Kloepper-Sams P. J., Munkittrick K. R., Lockhart W. L., Metner D. A., Luxon L., Smith I. R., Gagnon M. M., Servos M., and Payne J. F.. 1991. Protocols for measuring mixed function oxygenases of fish liver. Canadian Technical Report of Fisheries and Aquatic Sciences **1829**: 49.

Houston J. B.. 1994. Utility of *in vitro* drug metabolism data in predicting *in vivo* metabolic clearance. Biochemical Pharmacology **47**: 1469-1479.

Houston J. B., and Carlile D. J.. 1997. Prediction of hepatic clearance from microsomes, hepatocytes and liver slices. Drug Metabolism Reviews **29**: 891-922.

Hu K., and Bunce N. J.. 1999. Metabolism of polychlorinated dibenzo-p-dioxins and related dioxin-like compounds. Journal of Toxicology and Environmental Health **2**: 183-210.

Ikonomou M. G., Rayne S., and Addison R. F.. 2002. Exponential increases of the brominated flame retardants, polybrominated diphenyl ethers, in the Canadian arctic from 1981 to 2000. Environmental Science and Technology **36**: 1886-1892.

Ito K., and Houston J. B.. 2004. Comparison of the use of liver models for predicting drug clearance using *in vitro* kinetic data from hepatic microsomes and isolated hepatocytes. Pharmaceutical Research **21**: 785-792.

Johnston B. D., Alexander G., and Kennedy C. J.. 1999. Thermal modulation of the toxicokinetics of benzo[a]pyrene in isolated hepatocytes of sablefish (*Anoplopoma fimbria*), black rockfish (*Sebastes melanops*), and chub mackerel (*Scomber japonicus*). Comparative Biochemistry and Physiology **124C**: 157-164.

Jones H. M., and Houston J. B.. 2004. Use of the substrate depletion approach for determining in vitro metabolic clearance: Time dependencies in hepatocytes and microsomal incubation. Drug Metabolism and Disposition **32**: 572-982.

Jones H. M., Nicholls G., and Houston J. B.. 2005. Impact of end-product inhibition on the determination of *in vitro* metabolic clearance. Xenobiotica **35**: 439-454.

Keller G. M., and Jefcoate C. R.. 1984. Benzo[a]pyrene activation to 7,8-dihydroldiol 9.10-oxide by rate liver microsomes control by selective product inhibition. The Journal of Biological Chemistry **259**: 13770-13776.

Keller G. M., Christou M., Pottenger L. H., Wilson N. M., and Jefcoate C. R.. 1987. Product inhibition of benzo[a]pyrene metabolism in uninduced rat liver microsomes: Effect of diol epoxide formation. Chemico-biological Interactions **61**: 159-175.

Kennedy C. J., and Tierney K. B.. 2008. Energy intake affects the biotransformation rate, scope for induction, and metabolic profile of benzo[a]pyrene in rainbow trout. Aquatic Toxicology **90**: 172-181.

Kennedy C. J., and Walsh P. J.. 1994. The effect of temperature on the uptake and metabolism of benzo[a]pyrene in isolated gill cells of the gulf toadfish, *Opsanus beta*. Fish Physiology and Biochemistry **13**: 93-103.

Kennedy C. J., Gill K. A., and Walsh P. J.. 1989. Thermal modulation of benzo-a-pyrene metabolism by the gulf toadfish *Opsanus beta*. Aquatic Toxicology **15**: 331-344.

Kennedy C J., Gill K. A., and Walsh P. J.. 1991. Temperature-acclimation of xenobiotic metabolizing enzymes in cultured-hepatocytes and whole liver of the gulf toadfish, *Opsanus beta*. Canadian Journal of Fisheries and Aquatic Sciences **48**: 1212-1219.

Kim C., Manning R. O., Brown R. P., and Bruckner J. V.. 1996. Use the vial equilibration technique for determination of metabolic rate constants for dichloromethane. Toxicology and Applied Pharmacology **139**: 243-251.

Laak T. L. T., Durjava M., Struijs J., and Hermens J. L. M.. 2005. Solid phase dosing and sampling technique to determine partition coefficients of hydrophobic chemicals in complex matrixes. Environmental Science and Technology **39**: 3736-3742.

Lafferrere L., Hoff C., and Veesler S.. 2004. Study of liquid-liquid demixing from drug solution. Journal of Crystal Growth **269**: 550-557.

Mackay D.. 1982. Correlation of bioconcentration factors. Environmental Science and Technology **16**: 274-278.

Maeda K., Hayashi A., Iimura K., Suzuki M., Hirota M., Asakuma Y., and Fukui K.. 2004. Generation of nanometer-scale crystals of hydrophobic compound from aqueous solution. Chemical Engineering and Processing **44**: 941-947.

Maria V. L., Correia A. C., and Santos M. A.. 2002. Benzo[a]pyrene and β-naphthoflavone mutagenic activation by European eel (*Anguilla anguilla L.*) S9 liver fraction. Ecotoxicology and Environmental Safety **53**: 81-85.

Minato K., Koizumi N., Honma S., Iwamura S., and Tsukamoto K.. 1999. Characterizations of mouse hepatic microsomal monooxygenase catalyzing 11 beta-hydroxylation of osaterone acetate. Biochemical Pharmacology **58**: 335-341.

Miranda C. L., Chung W. G., Wang-Buhler J. L., Musafia-Jeknic T., Naird W. M., and Buhler D. R.. 2006. Comparative *in vitro* metabolism of benzo[a]pyrene by recombinant zebrafish CYP1A and liver microsomes from β-naphthoflavone-treated rainbow trout. Aquatic Toxicology **80**: 101-108.

Nath A., and Atkins W. M.. 2006. A theoretical validation of the substrate depletion approach to determining kinetic parameters. Drug Metabolism and Disposition **34**: 1433-1435.

Nichols J., Erhardt S., Dyer S., James M., Moore M., Plotzke K., Segner H., Schultz. I., Thomas K., Vasiluk. L., and Weisbrod A.. 2007. Workshop report: use of *in vitro* absorption, distribution, metabolism, and excretion (ADME) data in bioaccumulation assessments for fish. Human and Ecological Risk Assessment **13**: 1164-1191.

Nichols J. W., Schultz I. R., and Fitzsimmons P. N.. 2006. In vitro-in vivo extrapolation of quantitative hepatic biotransformation data for fish. I. A review of methods, and strategies for incorporating intrinsic clearance estimates into chemical kinetic models. Aquatic Toxicology **78**: 74-90.

Obach R. S., and Reed-Hagen A. E.. 2002. Measurement of Michaelis constants for cytochrome P450-mediated biotransformation reactions using a substrate depletion approach. Drug Metabolism and Disposition **30**: 831-837.

OECD. 1996. OECD Guidelines for the Testing of Chemicals-Section 3- Degradation and Accumulation Test TG No 305 Bioconcentration: Static and Flow-through Fish Tests, A-E. Paris. Organisation for Economic Co-operation and Development.

Pangrekar J., Kole P. L., Honey S. A., Kumar S., and Sikka H. C.. 2003. Metabolism of chrysene by brown bullhead liver microsomes. Toxicological Sciences **71**: 67-73.

Pedersen M. G., Harshbarger W. K., Zachariah P. K., and Juchau M. R.. 1976. Hepatic biotransformation of environmental xenobiotics in six strains of rainbow trout (*Salmo gairdneri*). Journal of the Fisheries Research Board of Canada **33**: 666-675.

Rane A., Wilkinson G. R., and Shand D. G.. 1977. Prediction of hepatic extraction ratio from *in vitro* measurement of intrinsic clearance. The Journal of Pharmacology and Experimental Therapeutics **200**: 420-424.

Ryan D. E., Thomas P. E., Reik L. M., and Levin W.. 1982. Purification, characterization and regulation of five rat hepatic microsomal cytochrome P-450 isozymes. Xenobiotica **12**: 727-744.

Sandvik M., Horsberg T. E., Skaare J. U., and Ingebrigtsen K.. 1997. Hepatic CYP1A induction in rainbow trout (*Oncorhynchus mykiss*) after exposure to benzo[a]pyrene in water. Biomarkers **2**: 175-180.

Savas U., Christou M., and Jefcoate C. R.. 1993. Mouse endometrium stromal cells express a polycyclic aromatic hydrocarbon-inducible cytochrome P450 that closely resembles the novel P450 in mouse embryo fibroblasts (P450EF). Carcinogenesis **14**: 2013-2018.

Segel I. H. 1975. Enzyme kinetics. John Wiley and Sons, New York.

Seubert J. M., and Kennedy C. J.. 1997. The toxicokinetics of benzo[a]pyrene in juvenile coho salmon, *Oncorhynchus kisutch*, during smoltification. Fish Physiology and Biochemistry **16**: 437-447.

Shappell N. W., Carlino-MacDonald U., Amin S., Kumar S., and Sikka H.. 2003. Comparative metabolism of chrysene and 5-methylchrysene by rat and rainbow trout liver microsomes. Toxicological Sciences **72**: 260-266.

Shen A. L., Fahl W. E., Wrighton S. A., and Jefcoate C. R.. 1979. Inhibition of benzo[a]pyrene and benzo[a]pyrene 7,8-dihydrodiol metabolism by benzo[a]pyrene quinines. Cancer Research **39**: 4123-4129.

Sikka H. C., Rutkowski J. P., and Kandaswami C.. 1990. Comparative metabolism of benzo[a]pyrene by liver microsomes from brown bullhead and carp. Aquatic Toxicology **16**: 101-112.

UNEP. 2001. Final act of the conference of plenipotentiaries on the Stockholm convention on persistent organic pollutants. In Proceeding of the Conference of Plenipotentiaries on the Stockholm Convention on Persistent Organic Pollutants, Stockholm, Sweden, 22-23 May 2001. United Nations Environment Programme. Available from http://www.pops.int/documents/meetings/dipcon/25june2001/conf4_finalact/en/FINALACT-English.PDF.

USEPA. 1976. Toxic substances control act, 1976. US Environmental Protection Agency, Washington, DC., USA.

Varanasi U., Nishimoto M., Reichert W. L., and Egerhart B-T. L.. 1986. Comparative metabolism of benzo[a]pyrene and covalent binding to hepatic DNA in English sole, starry flounder, and rat. Cancer Research **46**: 3817-3824.

Vasiluk L., Pinto L. J., Walji Z. A., Tsang W. S., and Gobas F. A. P. C.. 2006. Benzo[a]pyrene bioavailability from pristine soil and contaminated sediment assessed using two *in vitro* models. Environmental Toxicology and Chemistry **26**: 387-393.

Veith G. D., Defoe D. L., and Bergstaedt B. V.. 1979. Measuring and estimating the bioconcentration factor of chemicals in fish. Journal of the Fisheries Research Board of Canada **36**:1040-1048.

Weisbrod A. V., Burkhard L. P., Arnot J., Mekenyan O., Howard P. H., Russom C., Boethling R., Sakuratani Y., Traas T., Bridges T., Lutz C., Bonnell M., Woodburn K., and Parkerton T.. 2007. Workshop report: review of fish bioaccumulation databases used to identify persistent, bioaccumulative, toxic substances. Environmental Health Perspectives **115**: 255-261.

Wills E. D.. 1983. Effects of dietary lipids on the metabolism of polycyclic hydrocarbons and the binding of their metabolites to DNA. Biochemical Society Transactions **11**: 258-261.

Wilcockson J. B., and Gobas F. A. P. C.. 2001. Thin-film solid-phase extraction to measure fugacities of organic chemicals with low volatility in biological samples. Environmental Science and Technology **35**: 1425-1431.

Wilson N. M., Christou M., Turner C. R., Wrighton S. A., and Jefcoate C. R.. 1984. Binding and metabolism of benzo[a]pyrene and 7,12-dimethylbenz[a]anthracene by seven purified forms of cytochrome P-450. Carcinogenesis **5**: 1475-1483.